

THE X-RAY STRUCTURE ANALYSES

OF THE NATURAL PRODUCTS

CEDRELONE and CHIMONANTHINE

BEING A THESIS FOR THE DEGREE OF

DOCTOR OF PHILOSOPHY

IN THE UNIVERSITY OF GLASGOW

SUBMITTED BY

IAN JAMES GRANT, B. Sc.

Chemistry Department

October, 1962.

ProQuest Number: 13849338

All rights reserved

INFORMATION TO ALL USERS

The quality of this reproduction is dependent upon the quality of the copy submitted.

In the unlikely event that the author did not send a complete manuscript and there are missing pages, these will be noted. Also, if material had to be removed, a note will indicate the deletion.



ProQuest 13849338

Published by ProQuest LLC (2019). Copyright of the Dissertation is held by the Author.

All rights reserved.

This work is protected against unauthorized copying under Title 17, United States Code
Microform Edition © ProQuest LLC.

ProQuest LLC.
789 East Eisenhower Parkway
P.O. Box 1346
Ann Arbor, MI 48106 – 1346

(1)

P R E F A C E

I particularly wish to thank Dr. G.A. Sim, Dr. T.A. Hamor and Professor J. Monteath Robertson for their instructive and informative supervision over my two years in the X-ray crystallography section of this department.

I am also indebted to Glasgow University Computing Laboratories for the use of their facilities and the large amounts of computer time made available to me. I would also like to thank Dr. J.S. Rollett and Dr. J.G. Sime for allowing me to use the many programmes they have written for the DEUCE computer.

I must also thank Dr. E. Gelles for his supervision of my kinetic studies in the period 1959 - 1960, and thank Dr. G. Nancollas for his helpful comments and guidance during the preparation of this work for thesis presentation.

Finally I wish to acknowledge the receipt of a Department of Scientific and Industrial Research maintenance grant throughout the period of my research work.

S U M M A R Y

X-ray studies have been carried out on crystals of heavy atom derivatives of naturally -occurring organic compounds. Two structures have been successfully determined in this fashion; the triterpene cedrelone ($C_{26} H_{30} O_5$) and the alkaloid chimonanthine ($C_{22} H_{26} N_4$).

Information on the structure of cedrelone was limited to spectral considerations alone, when a crystalline sample of the iodoacetate derivative was provided by Mr. S.G. McGeachin of Glasgow. The structure analysis was hindered initially by the iodine atom being close to a special position in the unit cell which gave rise to false symmetry in the initial Fourier syntheses. The fourth Fourier synthesis, however, resulted in most of the structure being determined and thereafter the complete structure was obtained and refined to give a discrepancy of, $R = 17.5\%$. The crystal and molecular dimensions were in agreement with accepted values although no attempt was made to locate atomic positions accurately.

Dr. G.F. Smith of Manchester University provided crystals of the dihydrobromide derivative of chimonanthine an alkaloid of the calycanthaceous variety. Chemical and spectral evidence had progressed to the stage where the structure was probably one of two possibilities. The first major problem in this

structure analysis was the determination of the position of the bromide ions in the unit cell of the crystal. There were two bromide ions per asymmetric unit and the derivative crystallised in the tetragonal system; these two facts resulted in a very complex Patterson map which required much study before a solution was found. Thereafter the major problem was minimising the extremely large amounts of computer time required for this analysis. The structure and relative stereochemistry of chimonanthine have been determined and the structure was in fact one of the two structures proposed by the organic chemists. The crystal and molecular dimensions agree with accepted values within the limits of experimental accuracy and refinement of this structure has been carried out to give an average discrepancy between observed and calculated structure amplitudes of 14.9%.

The final section of this thesis describes the work carried out under the supervision of Dr. E. Gelles lately of this Department. The copper ion catalysed hydrolysis of glycylglycine has been studied over a range of pH values and cupric ion concentrations. It has been established that the first complex formed between glycylglycine and cupric ions (Cu GG^+) is the one responsible for catalysed hydrolysis and that subsequently formed complexes inhibit hydrolysis. These results are in agreement with other workers theoretical predictions.

The structure analysis of cedrelone was carried in conjunction with Dr. J.A. Hamilton of this department and the kinetic studies were a continuation of experiments first started by Mr. J.M. Wilson lately of this department.

C O N T E N T S

Preface	...	(i)
Summary	...	(ii)

PART I

SOME METHODS OF CRYSTAL STRUCTURE ANALYSIS.

1.1	Introduction	...	Page 1.
1.2	Derivation of Laue and Bragg Equations	...	2.
1.3	The Structure Factor Expression	...	5.
1.4	The atomic scattering factor	...	7.
1.5	Fourier Series	...	8.
1.6	The Patterson Series	...	10.
1.7	The Heavy Atom Method	...	11.
1.8	Fourier Refinement	...	13.
1.9	Least Squares Refinement	...	15.
1.10	The Accuracy of Crystal Structure Determination.	...	18.

PART II.

THE STRUCTURE OF CEDRELONE: X-RAY ANALYSIS OF CEDRELONE

IODOACETATE.

2.1	Introduction	...	20.
2.2	Crystal data	...	21.
2.3	Intensity data	...	22.
2.4	Determination of the Heavy Atom Position	...	23.
2.5	Structure Determination	...	26.
2.6	Refinement of the Structure	...	29.

2.7	Results.	...	30
2.8	Discussion	...	31

PART III.

THE STRUCTURE OF CHIMONANTHINE: X RAY ANALYSIS OF CHIMONANTHINE DIHYDROBROMIDE.

3.1	Introduction	...	53.
3.2	Crystal Data	...	54.
3.3	Intensity Data	...	55.
3.4	Determination of the heavy atoms' positions	...	56.
3.5	Structure Determination	...	63.
3.6	Refinement of the Structure	...	66.
3.7	Results	...	68.
3.8	Discussion	...	69.

<u>REFERENCES: PARTS I, II, and III.</u>	...	93.
--	-----	-----

PART IV.

THE CUPRIC ION CATALYSED HYDROLYSIS OF GLYCYLGLYCINE.

4.1	Introduction	...	97.
4.2	Experimental	...	104.
4.3	Results	...	108.
4.4	Discussion	...	119.

<u>REFERENCES: PART IV.</u>	...	128.
-----------------------------	-----	------

PART I.

SOME METHODS OF CRYSTAL STRUCTURE ANALYSIS.

1. (1) INTRODUCTION

Von Laue's discovery in 1912 of the diffraction of X-rays by crystals provided a new, powerful technique for investigating the structure of matter on an atomic scale. This discovery was quickly given a sound theoretical basis and the determination of the structures of simple compounds soon followed. The quantity of calculations required for the determination of even a relatively simple compound is very great and prior to the 1950's most of the structure determinations carried out were two-dimensional. With the advent of fast digital computers, three-dimensional structure determinations are now possible. Further, natural products containing upwards of twenty atoms, other than hydrogen, can now be successfully tackled with little prior knowledge of their structures. The largest chemical substances to date whose structures have been determined by X-ray crystal analysis are the proteins haemoglobin and myoglobin.

One major problem remains, namely, that no method has yet been devised for measuring the relative phases of the diffracted spectra. Although the magnitudes of the spectra can be measured either photographically or by counter techniques the phases must be obtained by other means. In the determination of the structures of cedrelone and chimonanthine the "heavy atom" method was employed to give an initial set of approximate phases which were used in a Fourier synthesis. Successive cycles of structure-factor calculations and Fourier maps were computed, including

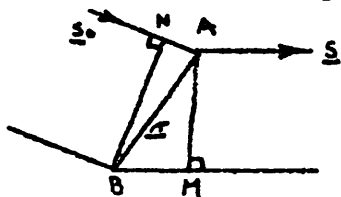
more atomic coordinates as they became available, until the complete structure had been determined. Thereafter, refinement by Fourier and least-squares methods was employed.

1. (2) DERIVATION OF THE BRAGG AND LAUE EQUATIONS.

Crystals consist of a three-dimensional periodic repetition of a basic geometric unit called a unit cell. Alternatively, crystals may be considered as being made up of a large number of identical assemblages of atoms repeating regularly in three dimensions. It is convenient to replace each such group of atoms by a point, and the three-dimensional pattern of such points forms the space lattice of the crystal. If it is assumed that each lattice point is replaced by an electron then the positions of these electrons can be defined by the ends of a vector \underline{r} such that

$$\underline{r} = u\underline{a} + v\underline{b} + w\underline{c}$$

where \underline{a} , \underline{b} , \underline{c} are the primitive translations of the lattice and u , v , w are integers. On irradiation by an X-ray beam these electrons vibrate and act as sources of secondary radiation. In (I), A and B are two lattice points and the incident radiation's direction is denoted by the vector \underline{s}_0 , of length λ , where λ is the wavelength of the radiation used.



(I)

The path difference between the scattered waves from the two lattice points in the direction defined by the vector \underline{a} , equal in magnitude to \underline{s}_0 , is given by,

$$\begin{aligned} BM - AN &= (\underline{r} \cdot \underline{a} - \underline{r} \cdot \underline{s}_0) \\ &= \underline{r} \cdot \underline{S} \dots\dots\dots (1) \end{aligned}$$

$$\text{where } \underline{S} = (\underline{a} - \underline{s}_0)$$

For the waves scattered by A and B to be in phase this path difference must be a whole number of wave-lengths, i.e. $\underline{r} \cdot \underline{S}$ must be an integer. Hence, $(u \underline{a} + v \underline{b} + w \underline{c}) \cdot \underline{S}$ must be integral and since u, v, w are integers, each of the products

$$\begin{aligned} \underline{a} \cdot \underline{S} &= h \\ \underline{b} \cdot \underline{S} &= k \dots\dots\dots (ii) \\ \underline{c} \cdot \underline{S} &= l \end{aligned}$$

in turn must be integral, where h, k and l are integers. These equations, (ii), are known as the Laue equations.

The Laue equations are unsuitable for direct application to diffraction problems but W.L.Bragg showed their physical significance by relating the integers h, k, l to the Miller indices of the lattice planes. Bragg's law is related to the Laue equations and this can be shown as follows;

$$\left. \begin{aligned} \underline{a}/h \cdot \underline{S} &= 1 \\ \underline{b}/k \cdot \underline{S} &= 1 \\ \underline{c}/l \cdot \underline{S} &= 1 \end{aligned} \right\} \text{Laue equations.}$$

4.

Subtraction of the first two equations gives

$$\left(\frac{a}{h} - \frac{b}{k} \right) \cdot \underline{S} = 0$$

which means the vector \underline{S} is perpendicular to $\left(\frac{a}{h} - \frac{b}{k} \right)$.

Similarly \underline{S} is perpendicular to $\left(\frac{a}{h} - \frac{c}{l} \right)$. Thus \underline{S} is perpendicular to the plane defined by the intercepts $\frac{a}{h}$, $\frac{b}{k}$, $\frac{c}{l}$, i.e. the plane with Miller indices (h, k, l) . Since by definition the vector \underline{S} bisects the incident and diffracted beams and is perpendicular to the lattice plane (h, k, l) a similarity to reflection exists.

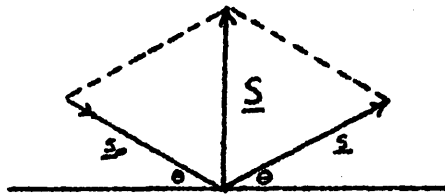
If d is the spacing of the planes $(h k l)$ then d is the projection of $\frac{a}{h}$, $\frac{b}{k}$, $\frac{c}{l}$ on the vector \underline{S} .

$$\text{i.e. } d(h k l) = \frac{\frac{a}{h} \cdot \underline{S}}{|\underline{S}|}$$

But $\frac{a}{h} \cdot \underline{S} = 1$, (from the Laue equations)

$$\text{and } |\underline{S}| = \frac{2 \sin \theta}{\lambda} \quad \text{from (II)}$$

where θ is the angle of incidence of the radiation.



II

$$\therefore d(h k l) = \frac{\lambda}{2 \sin \theta}$$

$$\therefore \lambda = 2 d \sin \theta \quad \dots\dots\dots (111)$$

This is Bragg's law and it indicates that a reflection from a lattice plane can only take place when the angle of incidence of the X-ray beam satisfies the condition given by the equation.

1. (3) THE STRUCTURE FACTOR EXPRESSION.

If the unit cell of a crystal contains N atoms, the n^{th} of which has coordinates (x_n, y_n, z_n) the position of the n^{th} can be defined by the vector \underline{r}_n where

$$\underline{r}_n = (x_n \underline{a} + y_n \underline{b} + z_n \underline{c}) \dots\dots\dots (iv)$$

The path difference of the wave scattered by this atom relative to an atom at the origin of the unit cell is by (i), $\underline{r}_n \cdot \underline{S}$, and the phase change is,

$$\frac{2\pi}{\lambda} \cdot \lambda \cdot \underline{r}_n \cdot \underline{S} = 2\pi \cdot \underline{r}_n \cdot \underline{S}$$

Thus the expression for the wave scattered by the n^{th} atom contains the term,

$$f_n \exp. (2\pi \cdot i \cdot \underline{r}_n \cdot \underline{S})$$

where f_n is the atomic scattering factor of the n^{th} atom. The complete wave scattered by the N atoms in the unit cell will thus contain the term

$$F = \sum_{n=1}^N f_n \cdot \exp. (2\pi i \underline{r}_n \cdot \underline{S}) \dots\dots\dots (v)$$

Substituting (iv) in (v),

$$F = \sum_{n=1}^N f_n \exp. 2\pi i (x_n \underline{a} \cdot \underline{S} + y_n \underline{b} \cdot \underline{S} + z_n \underline{c} \cdot \underline{S})$$

Hence by (ii)

$$F(h k \ell) = \sum_{n=1}^N f_n \exp_{\rho} 2\pi i (h x_n + k y_n + \ell z_n)$$

The quantity F is known as the structure factor and it is a complex quantity which can be represented by a modulus $|F(h k \ell)|$, known as the structure amplitude and a phase $\alpha_{\lambda}^{\text{angle}}(h k \ell)$. The structure amplitude can be obtained from the measured intensities, but the phase is not an observable quantity.

It is often convenient to separate the real and imaginary parts of $F(h k \ell)$, so that

$$F(h k \ell) = A(h k \ell) + i B(h k \ell)$$

$$\text{and } \alpha(h k \ell) = \tan^{-1} \frac{B(h k \ell)}{A(h k \ell)}$$

where,

$$A(h k \ell) = \sum_{n=1}^N f_n \cos 2\pi (h x_n + k y_n + \ell z_n)$$

$$\text{and } B(h k \ell) = \sum_{n=1}^N f_n \sin 2\pi (h x_n + k y_n + \ell z_n)$$

These are the equations used in practice and if the space group is known these summations can be carried out over the coordinates of the equivalent positions resulting in a simplified expression.

Instead of introducing point atoms, the structure factor may be expressed in terms of electron density at a point $\rho(x y z)$, thus

$$F(h k \ell) = V \int \int \int \rho(x y z) \exp 2\pi i (hx + ky + \ell z) \cdot dx \cdot dy \cdot dz$$

1. (4). THE ATOMIC SCATTERING FACTOR.

In 1.(2) it was implied that the scattering unit in the crystal was an electron which in turn implies that to calculate structure factors the positions of all the electrons in the unit cell must be known. Since each atom has a number of electrons associated with it, the difficulties associated with the location of the electrons can be avoided. As these electrons are assumed to be loosely held in the atom any change of phase on scattering is the same for all of them and so the amplitude scattered in the forward direction is Z times that due to a single electron, where Z is the atomic number. In a direction making a finite angle with the direction of incident radiation, there will be path differences between waves scattered from electrons in different parts of the atom. These waves will interfere and produce a resultant amplitude less than Z times that due to a single electron. The phase differences depend upon the angle of scattering, the wavelength of the radiation and the volume throughout which the electrons are distributed. The scattering factor, f , will approach Z for small angles of scattering and will fall away with increasing angle at a rate that, for a given wavelength, is determined by the distribution of electrons in the atom. Atomic scattering factors have been calculated by several workers including James and Brindley (2), Thomas (3), Fermi (4), McWeeny (5), Tomie

and Stam (6), Berghuis et al (7), etc.

The atomic scattering factors available in the literature make no allowance for the atom undergoing thermal motion. As this is never the case in practice, some modification of the atomic scattering factor must be made to allow for this thermal vibration. If $\bar{\mu}$ is the mean displacement of the atom from its mean position, then it can be shown that for simple isotropic motion the scattering factor f_0 should be modified by a factor,

$$\exp. (- 8\pi^2 \bar{\mu}^2 \sin^2 \theta / \lambda^2)$$

$$\text{i.e. } f = f_0 \exp. (- B \sin^2 \theta / \lambda^2)$$

where $B = 8\pi^2 \bar{\mu}^2$ and is known as the Debye (8) temperature factor.

The approximate overall value of B can be found by the method described by Wilson (9).

However, if the thermal vibration of the atom is anisotropic, the scattering factor, f_0 , must be modified by a factor such as

$$\exp. - (b_{11}h^2 + b_{22}k^2 + b_{33}l^2 + b_{12}hk + b_{23}kl + b_{31}lh)$$

(Cruiokshahk (10)) where the b_{11} and b_{1j} terms characterise the time averaged ellipsoidal volume through which the electron density is distributed.

1. (5) FOURIER SERIES.

Since a crystal is periodic in three dimensions its electron density $\rho(x y z)$ at any point with fractional coordinates $(x y z)$

can be represented by a triple Fourier series.

$$\rho(x y z) = \sum_{-\infty}^{+\infty} \sum_{-\infty}^{+\infty} \sum_{-\infty}^{+\infty} A(pqr) \exp - 2\pi i(px + qy + rz) \dots\dots\dots (vii)$$

The number of electrons in the volume element $dx dy dz$ is given by

$\rho(xyz).dx dy dz$. When the unit cell has a volume V , it may be shown that

$$F(h k \ell) = V \int \int \int \rho(x y z) \exp. 2\pi i(hx + ky + \ell z) dx dy dz \dots\dots\dots(viii)$$

The values of the coefficients $A(pqr)$ in (vii) are obtained by substituting for $\rho(xyz)$ in (viii) and obtaining,

$$F(hk\ell) = V \int \int \int \left[\sum_{-\infty}^{+\infty} \sum_{-\infty}^{+\infty} \sum_{-\infty}^{+\infty} A(pqr) \exp - 2\pi i(px + qy + rz) \right] \exp. 2\pi i(hx + ky + \ell z) dx dy dz \dots\dots\dots (ix)$$

On integrating, all terms in (ix) vanish except those for which

$p = h, q = k$ and $r = \ell$. Thus,

$$F(hk\ell) = V \int \int \int A(pqr) dx dy dz = VA(pqr) \dots\dots\dots (x)$$

The electron-density distribution at every point in the crystal

can be represented by the Fourier series;

$$\rho(xyz) = \frac{1}{V} \sum_{-\infty}^{+\infty} \sum_{-\infty}^{+\infty} \sum_{-\infty}^{+\infty} F(hk\ell) \exp (-2\pi i[hx + ky + \ell z]) \dots\dots\dots (xi)$$

The constant term in the series in $F(000)$ and is defined as

$$F(000) = V \int \int \int \rho(xyz) dx dy dz = Z$$

Since the value of f_n the scattering factor falls off with $\sin \theta$, the values of terms in this series will decrease and consequently the series will converge if sufficient data are available. Equation (xi) is not suitable for summation of a Fourier series so it is

more convenient to express (xi) in the form,

$$\rho(xyz) = \frac{1}{V} \sum_{- \infty}^{+ \infty} \sum_{- \infty}^{+ \infty} \sum_{- \infty}^{+ \infty} |F(hk\ell)| \cos 2\pi[hx + ky + \ell z - \alpha(hk\ell)] \dots\dots\dots (xii)$$

where $\alpha(hk\ell)$ represents the phase constant associated with the amplitude $|F(hk\ell)|$. From the observed intensities of the diffracted spectra, $|F(hk\ell)|$ can be calculated but no information concerning the relative value of $\alpha(hk\ell)$ can be obtained. This limitation precludes direct or immediate application of the series (xii) to the solution of crystal structures (except in special cases).

1. (6) THE PATTERSON SERIES.

In the last section it was stated that the course of a crystal structure analysis cannot in general be direct, because, in the process of recording the diffraction pattern, knowledge of the phases of the various spectra are lost. Trial and error methods may be used provided one can postulate a trial structure for use in phasing calculations and Fourier summations.

A.L. Patterson (11), (12) devised the series, which bears his name, as a method of obtaining information about crystal structures using the data available, viz; the structure amplitudes $|F(hk\ell)|$. The Patterson function of an electron-density distribution.

$$\rho(xyz) = \frac{1}{V} \sum_{-\infty}^{+\infty} \sum_{-\infty}^{+\infty} \sum_{-\infty}^{+\infty} F(hkl) \exp[-2\pi i(hx + ky + lz)]$$

is defined as

$$P(uvw) = V \iiint \rho(xyz) \rho(x+u, y+v, z+w) dx dy dz \dots\dots\dots (xiii)$$

which can be defined as the Fourier series,

$$P(uvw) = \frac{1}{V} \sum_{-\infty}^{+\infty} \sum_{-\infty}^{+\infty} \sum_{-\infty}^{+\infty} |F(hkl)|^2 \exp[-2\pi i(hu + kv + lw)] \dots\dots\dots (xiv)$$

This expression can be directly computed unambiguously since the coefficients, $|F(hkl)|^2$, are proportional to the observed intensities.

The function $P(uvw)$ in equation (xiii) can only have a large value when both $\rho(xyz)$ and $\rho(x+u, y+v, z+w)$ are large. A peak in the function $P(uvw)$ at (u_1, v_1, w_1) corresponds to an interatomic distance in the crystal defined by a vector with components u_1, v_1, w_1 and the height of the peak is proportional to the product of the scattering factors of the two atoms concerned.

If the asymmetric unit of a structure contains N atoms, $N(N-1)/2$ distinct vector peaks will occur. If N is large the vector map will contain very many peaks. Many of these peaks will overlap forming diffuse peaks making the vector map difficult to interpret. However, the structures of simple molecules containing relatively few atoms have been successfully determined by the Patterson method.

1. (7) THE HEAVY ATOM METHOD.

In section 1. (5) it was demonstrated that the electron density

in a crystal can be evaluated by Fourier methods provided the structure amplitudes can be measured, leaving the relative phases unknown. The determination of these phases constitutes the basic problem of X-ray structure analysis. No general method of evaluating the phases exists and the method used in any specific analysis will depend upon the circumstances.

In organic molecules containing upwards of twenty atoms other than hydrogen, the "heavy atom" method has been found to be a powerful method of solving the phase problem (13). In organic molecules with many carbon, oxygen and nitrogen atoms the Patterson method is seldom of use on account of the large number of peaks of approximately equal weight. If, however, a chemical derivative of the compound under study can be prepared which contains one or two atoms with an atomic number much greater than those of the other atoms, the positions of the heavy atoms in the unit cell can generally be found by using the Patterson summation. The vector peaks in the vector map due to these heavy atoms will be readily located on account of their high value of $P(UVW)$ leading to the coordinates of the heavy atoms. If these coordinates are used in a cycle of structure-factor calculations a set of approximate phase constants will be obtained. These phases are then used in a Fourier series and an electron-density distribution approximating to the correct distribution results. At this stage some or all of the light atoms may be distinguished. These additional atoms

are now included in the next cycle of structure-factor calculations which provides an improved set of phase constants. Successive rounds of Fourier summation and structure-factor calculations serving to reveal the positions of all the atoms in the structure. Complications in the above method may arise if the heavy atom's position is close to or on a special position in the unit cell. This usually results in false symmetry in the electron-density distribution making the choice of atomic positions ambiguous.

The effectiveness of a heavy atom in determining the phases in a particular structure can be roughly indicated by the ratio of the square of the atomic number of the heavy atom to the sum of the squares of the atomic numbers of the light atoms. This ratio should be about unity for maximum effectiveness (14). Calculations of the number of phases that should be determined within acceptable limits for various ratios of scattering factors of heavy and light atoms have been carried out by Sim (15). If the atom is so heavy that the square of the atomic number is very much greater than the sum of the squares of the atomic numbers of the light atoms undesirable effects could arise such as, diffraction 'ripples', which might obliterate genuine detail, or errors in the measured structure amplitudes due to high absorption of the X-rays.

1. (8) FOURIER REFINEMENT.

After a structure has been solved it is usual to refine the

structure to obtain good agreement between observed and calculated structure amplitudes and to approximate the calculated phases to the true phases. If $|F_0|$ Fourier maps are computed and the new atomic coordinates used in a new cycle of phasing calculations only a limited amount of refinement can be achieved. This arises from the fact that a Fourier series requires an infinite number of terms and collecting data with copper K α radiation limits the number of data that can be collected. It is quite reasonable to expect that for any postulated structure there will be structure factors outwith the recording limit of the radiation having quite large amplitudes. The omission of such terms from the observed data causes termination of series effects.

These effects cause the atoms to be shifted from their true positions and allowance for this effect can be made by a method due to Booth (16). The final $|F_0|$ synthesis is known to have its atomic peaks displaced by unknown amounts from their true positions due to termination of series effects. Another Fourier synthesis is calculated using $|F_c|$ data as coefficients but the same phases as the $|F_0|$ synthesis. If there were no errors due to termination of series effects, the position of any peak in the $|F_0|$ map should be identical to that in the $|F_c|$ map, calculated from a model containing all the atoms in the structure. Hence, the deviations of the peaks from these sites ($\Delta x, \Delta y, \Delta z$) represent the correction, with change of sign, to be applied

to the positions of the peaks in the $|F_o|$ map. This correction is known as the back-shift correction and is based on the assumption that no errors exist in the postulated structure, except those due to termination of series effects. These corrections should not be applied until straight-forward Fourier refinement ceases to be effective.

1. (9) LEAST-SQUARES REFINEMENT.

The use of least-squares procedures was first introduced by Hughes (17) in the structure analysis of melamine. It is a method of refinement which overcomes the effects due to termination of series and also provides a method of decreasing the influence of inaccurate coefficients on the results.

The best values of the atomic parameters are those which minimise the function;

$$R = \sum_q w(h k \ell) [|F_o| - |F_o|]^2$$

where q is the number of independent observations and $w(h k \ell)$ is the weight of the plane $(h k \ell)$ and should be taken as inversely proportional to the square of the probable error in the corresponding $|F_o|$. The value of R is influenced by the atomic coordinates and the temperature factor. When R is near to its minimum, a small change Δx_n in the x -coordinate of the n^{th} atom changes F_o by an amount,

$$\Delta F_0 = \frac{\partial F_0}{\partial x_n} \cdot \Delta x_n$$

If simultaneous changes to all the coordinates occur the change in F_0 is,

$$\Delta F_0 = \sum_{n=1}^N \left[\frac{\partial F_0}{\partial x_n} \cdot \Delta x_n + \frac{\partial F_0}{\partial y_n} \cdot \Delta y_n + \frac{\partial F_0}{\partial z_n} \cdot \Delta z_n \right] \dots \dots \dots (xv)$$

The best values of Δx_n etc. are therefore those which most nearly equate ΔF_0 to $(F_0 - F_c)$ for the q possible equations which can be set up. In order to provide accurate results, the number of observational equations must ^{be} much greater than the number of unknowns. The unknowns are generally three positional and six thermal parameters per atom plus an overall scale factor or $(9N + 1)$ unknowns where N is the number of atoms in the structure.

If only positional parameters are being refined, ΔF_0 has the form of equation (xv). To obtain the values of Δx_n etc., the q observational equations are reduced to $3N$ normal equations. This is achieved by multiplying each of the q equations of ΔF_0 by the weighted coefficient of each of the unknowns in turn. This results in $3N$ sets of q equations, each set is then summed to produce one normal equation. The n^{th} of these normal equations is obtained by multiplying the q equations of the type,

$$\sum_{n=1}^N \left[\frac{\partial F_0}{\partial x_n} \cdot \Delta x_n + \frac{\partial F_0}{\partial y_n} \cdot \Delta y_n + \frac{\partial F_0}{\partial z_n} \cdot \Delta z_n \right] = (F_0 - F_c)$$

by $w \cdot \frac{\partial F_0}{\partial x_n}$ and adding to produce the equation;

$$\begin{aligned} \sum_m w \left[\left(\frac{\partial F_0}{\partial x_n} \right)^2 \cdot \Delta x_n + \frac{\partial F_0}{\partial x_n} \cdot \frac{\partial F_0}{\partial y_n} \cdot \Delta y_n + \frac{\partial F_0}{\partial x_n} \cdot \frac{\partial F_0}{\partial z_n} \cdot \Delta z_n \right. \\ \left. + \sum_m \frac{\partial F_0}{\partial x_n} \left\{ \frac{\partial F_0}{\partial x_m} \cdot \Delta x_m + \frac{\partial F_0}{\partial y_m} \cdot \Delta y_m + \frac{\partial F_0}{\partial z_m} \cdot \Delta z_m \right\} \right] \\ = \sum_q w (F_0 - F_0) \frac{\partial F_0}{\partial x_n} \dots \dots \dots (xvi) \end{aligned}$$

where \sum_m denotes the sum over all the atoms except the n^{th} . The $3N$ normal equations have then to be solved for the $3N$ unknowns. This equation is too complicated for convenient use thus simplifications must be made. If the atoms are well resolved it can be shown that quantities such as $\sum_q w \frac{\partial F_0}{\partial x_n} \cdot \frac{\partial F_0}{\partial x_m}$ are likely to be small compared with $\sum_q w \left(\frac{\partial F_0}{\partial x_n} \right)^2$ and may be neglected. Further if the axes are orthogonal or nearly so, quantities of the form, $\sum_q w \cdot \frac{\partial F_0}{\partial x_n} \cdot \frac{\partial F_0}{\partial y_n}$ can also be neglected

and equation (xvi) reduces to

$$\Delta x_n \sum_q w \left(\frac{\partial F_0}{\partial x_n} \right)^2 = \sum_q w (F_0 - F_0) \cdot \frac{\partial F_0}{\partial x_n}$$

which can be more readily evaluated than (xvi). Similar equations can be obtained for changes in temperature factors, the variables x_n being replaced by each of six thermal parameters, $b_{11} b_{22} b_{33} b_{23} b_{31} b_{12}$ to give $6N$ normal equations. The scale factor can also be refined by least-squares methods.

1. (10) THE ACCURACY OF A CRYSTAL STRUCTURE DETERMINATION.

The final results of the two structure determinations described in this thesis were subjected to certain tests of accuracy. The accuracy to which the positional parameters had been found was estimated from the values of the least-squares totals in the final cycle of refinement. The formula used was,

$$\sigma(x) = a / \left\{ \frac{n\Delta^2}{(n-s)} \left[\sum w \frac{\partial \Delta}{\partial x/a} \right]^2 \right\}^{\frac{1}{2}}$$

where n is the number of reflections used in the refinement and s is the number of parameters refined or $s = (9N + 1)$ where N is the number of atoms. The standard deviation, $\sigma(A - B)$, of a bond between atoms A and B was found from the formula,

$$\sigma(A - B) = \sqrt{[\sigma^2(A) + \sigma^2(B)]}$$

where $\sigma(A)$ and $\sigma(B)$ are the standard deviations of atoms A and B respectively. The standard deviation, $\sigma(\theta)$ in radians, for an angle (θ) is given by the formula

$$\sigma^2(\theta) = \frac{\sigma^2(A)}{(AB)^2} + \sigma^2(B) \left[\frac{1}{(AB)^2} - \frac{2 \cos \theta}{AB \cdot BC} + \frac{1}{(BC)^2} \right] + \frac{\sigma^2(C)}{(BC)^2}$$

where (θ) is formed at atom (B) by atoms (A) and (C). This formula is the one due to Cruickshank and Robertson (18).

The significance of the mean plane calculations was tested using the χ^2 distribution which has been calculated and is available in tabular form. These tables give the frequency with which different values of χ^2 are exceeded and also the value of χ^2 corresponding to these particular frequencies (19). The value

of χ^2 was obtained from the formula,

$$\chi^2 = \sum \frac{\Delta^2}{\sigma^2}$$

where Δ is the deviation in $\overset{\circ}{A}$ of an atom from the calculated plane and σ is the mean standard deviation in $\overset{\circ}{A}$ in the positional parameters. The probability that no atoms deviate significantly from the calculated plane can be found from tables knowing the value of χ^2 and the number of degrees of freedom ($n - 3$).

Throughout the course of each analysis the validity of the proposed structure (or partial structure) was gauged by the average discrepancy R . This is a rough measure of accuracy and is defined as,

$$R = \frac{\sum [|F_o| - |F_c|]}{\sum |F_o|}$$

Whilst it does not contain any of the functions normally minimised during refinement it is nonetheless a useful guide.

PART II.

THE STRUCTURE OF CEDRELONE: X-RAY
ANALYSIS OF CEDRELONE IODOACETATE.

2. (1) INTRODUCTION

Cedrelone, was first isolated from Cedrela Toona a tree belonging to the natural order Meliacea. This tree grows to a height of some 50 feet and is found near the Himalayas to the east of the Indus. The reddish-brown, aromatic smelling heartwood of this tree has long been used for medicinal purposes and as a source of a dyestuff. The tree's medicinal importance prompted Parikar and Dutt (20) to attempt to find the active principle. The main crystalline product obtained by these workers was assigned the formula $C_{25}H_{30}O_5$ and was stated to contain a lactone ring, a phenolic hydroxyl group, a ketone function and an ethylenic double bond, further these workers called it Cedrelone. However, more recently chemical and spectral evidence by workers in Glasgow (21), Zurich (22) and Madras (22) has led to the molecular formula $C_{26}H_{30}O_5$ being assigned. The molecule was stated to contain an α/β - unsaturated ketone, β - substituted furan ring and an enolised α - diketone function similar in environment to that of diosphenols in the limonin series (23).

This then was the information available to us when we undertook the analysis of the iodoacetate derivative of cedrelone.

2. (2) CRYSTAL DATACedrelone Iodoacetate $C_{28}H_{31}O_6I$

Molecular Weight = 590.44

Melting Point = 149 - 150°C

Density Calculated = 1.490 gm/cm³Density Measured = 1.498 gm/cm³

(By flotation using carbon tetrachloride and petroleum ether).

The crystal is orthorhombic with

$$a = 6.97 \pm 0.02 \text{ \AA}$$

$$b = 27.44 \pm 0.03 \text{ \AA}$$

$$c = 13.74 \pm 0.04 \text{ \AA}$$

Volume of the unit cell = 2628 Å³

Number of Molecules per unit cell = 4

Absent spectra; hoo when h is odd

oko when k is odd

ool when l is odd

Space group $P2_1^2 2_1^2 2_1^2$ (D_2^4)Linear absorption coefficient for X-rays (Copper K α radiation)

$$\mu = 108 \text{ cm}^{-1}$$

Total number of electrons per unit cell = F(000) = 1200

$$\sum f^2 \text{ (light atoms)} = 1423 \quad (\sin\theta = 0)$$

$$\sum f^2 \text{ (heavy atoms)} = 2809 \quad (\quad \quad)$$

2. (3) INTENSITY DATA

The crystals of cedrelone iodoacetate used in this analysis were in the form of small hexagonal plates and were obtained from Mr. S.G. McGeachin, a member of the Organic Chemistry Research Laboratory at Glasgow University. Rotation, oscillation and moving-film photographs were taken with copper $K\alpha$ ($\lambda = 1.542\text{\AA}$) radiation. The unit cell dimensions were obtained from rotation and equatorial layer-line Weissenberg photographs. The space group was uniquely determined, from the systematic halvings in the X-ray spectra, to be $P2_12_12_1$ (D_2^4).

Small crystals were used for the intensity measurements and no absorption corrections were made. Using a Weissenberg equi-inclination camera the $0\ k\ l \dots 5\ k\ l$ and $h\ k\ 0 \dots h\ k\ 6$ spectra were collected photographically using the multiple film technique (24). The intensities were estimated visually using a calibrated step-wedge and were corrected for the usual Lorentz, polarisation and rotation (25) factors. The various layers were put on the same relative scale by comparison of common reflections in the two series of photographs, and the absolute scale was found at a later stage by comparison with the calculated structure factors, $|F_0|$. In all 1163 independent structure amplitudes, $|F_0|$, were measured and 122 unobserved reflections were included, which were included at half the minimum $|F_0|$ value locally observed. The small amount of data available was a consequence of the non-appearance of spectra beyond moderate values

of $\sin \Theta$ indicating a high temperature factor, B. Further the crystals slowly decomposed during the period of photography.

2. (4) DETERMINATION OF THE HEAVY ATOM POSITION

For a crystal belonging to the orthorhombic system, the expression for the Patterson function $P(U, V, W)$ is

$$P(U, V, W) = \frac{8}{V_c} \sum_0^{\infty} \sum_0^{\infty} \sum_0^{\infty} |F(hkl)|^2 \cos 2\pi hu \cos 2\pi kv \cos 2\pi lw.$$

This expression can be simply reduced to that for the Patterson projections $P(U, V)$ and $P(V, W)$ down the c and a - axes respectively

The vectors to be expected between iodine atoms in the space group $P2_12_12_1$ with one molecule in the asymmetric unit are

	x, y, z	$\frac{1}{2}-x, \bar{y}, \frac{1}{2}+z$	$\frac{1}{2}+x, \frac{1}{2}-y, \bar{z}$	$\bar{x}, \frac{1}{2}+y, \frac{1}{2}-z$
x, y, z	-	$\frac{1}{2}-2x, -2y, \frac{1}{2}$	$\frac{1}{2}, \frac{1}{2}-2y, -2z$	$-2x, \frac{1}{2}, \frac{1}{2}-2z$
$\frac{1}{2}-x, \bar{y}, \frac{1}{2}+z$	$\frac{1}{2}+2x, +2y, \frac{1}{2}$	-	$+2x, \frac{1}{2}, \frac{1}{2}-2z$	$\frac{1}{2}, \frac{1}{2}+2y, -2z$
$\frac{1}{2}+x, \frac{1}{2}-y, \bar{z}$	$\frac{1}{2}, \frac{1}{2}+2y, +2z$	$-2x, \frac{1}{2}, \frac{1}{2}+2z$	-	$\frac{1}{2}-2x, +2y, \frac{1}{2}$
$\bar{x}, \frac{1}{2}+y, \frac{1}{2}-z$	$+2x, \frac{1}{2}, \frac{1}{2}+2z$	$\frac{1}{2}, \frac{1}{2}-2y, +2z$	$\frac{1}{2}+2x, -2y, \frac{1}{2}$	-

The two-dimensional Patterson projections $P(U, V)$ and $P(V, W)$ were computed using 259 and 218 terms respectively and the maps are shown in Figures II and I respectively. In the part of the $P(V, W)$ projection shown there should be double weight peaks at $(2y, \frac{1}{2})$ on the line, $P(\frac{1}{2}, \frac{1}{2})$ and at $(\frac{1}{2}, \frac{1}{2} - 2z)$ on the line $P(\frac{1}{2}, W)$ with a single weight peak at $(\frac{1}{2} - 2y, 2z)$ in a general position. Clearly the concentration of vectors at A in Fig. I is $(2y, \frac{1}{2})$ and those at B in

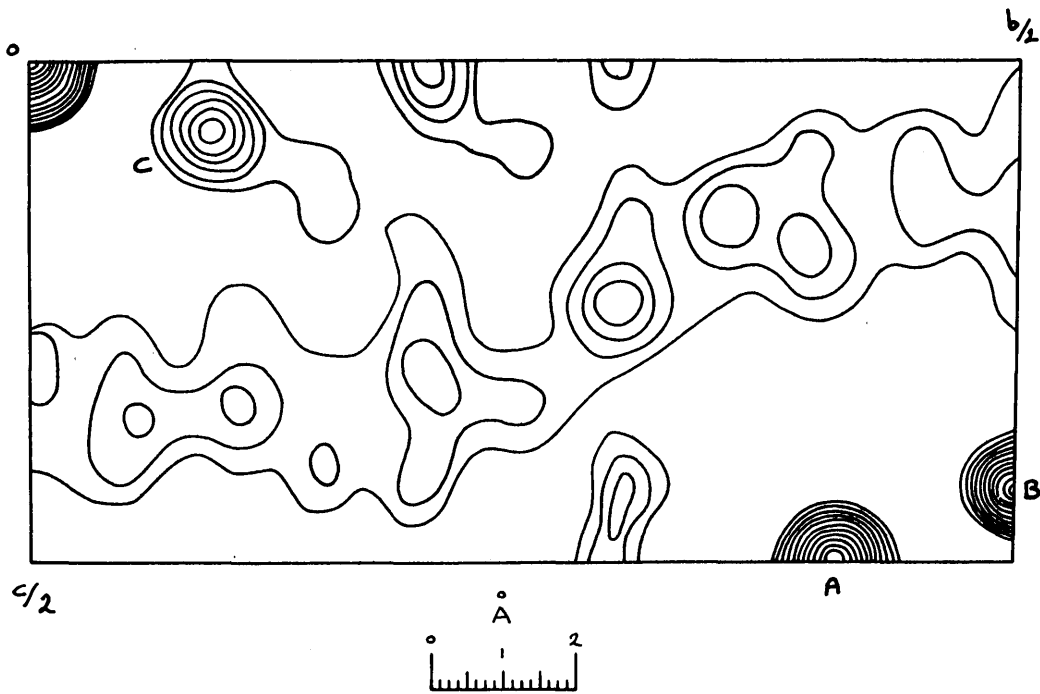


Fig. I. Projection $P(V,W)$ of the Patterson function. Contour scale arbitrary. The iodine-iodine vector peaks are marked A, B and C.

in Fig. I, $(\frac{1}{2}, \frac{1}{2} - 2z)$. Finally the vector peak marked C in Fig. I is the general peak $(\frac{1}{2} - 2y, 2z)$.

In the part of the P (U,V) projection shown there should be peaks of double weight at $(2x, \frac{1}{2})$ on the line P $(U, \frac{1}{2})$ and at $(\frac{1}{2}, \frac{1}{2} - 2y)$ on the line P $(\frac{1}{2}, v)$ with a single weight peak at $(\frac{1}{2} - 2x, 2y)$ in a general position. In Fig. II, the three largest vector peaks (with the exception of the origin peak) all lie on the mirror planes which bound the part of the projection shown. It was found that if we assume an iodine atom \underline{x} - coordinate = 0.25 that peak D, Fig. II, must be the peak $(2x, \frac{1}{2})$. Following on this peak E is the vector $(\frac{1}{2}, \frac{1}{2} - 2y)$ and the general peak is F, $(\frac{1}{2} - 2x, 2y)$.

The coordinates obtained for the heavy atom in this way are $\frac{x}{a} = 0.250$, $\frac{y}{b} = 0.205$, $\frac{z}{c} = 0.039$ expressed as fractions of the cell edges. As the iodine atoms have an \underline{x} - coordinate = $0.25a$ a centrosymmetrical arrangement of the iodine atoms in the unit cell results which will lead to spurious planes of symmetry in electron-density distributions which in turn will render location of real atomic positions difficult. However, inspection of Fig. II reveals that peaks D and F are elliptical. If the \underline{x} - coordinate was not exactly $0.25a$ but displaced slightly from this value, peak D would be elliptical due to fusion of the two actual peaks, mirrored about the line $\frac{a}{2}$, into a single peak. The same considerations make F elliptical also. Accordingly it was decided to calculate the displacement, Δ , from the observed \underline{x} - coordinate.

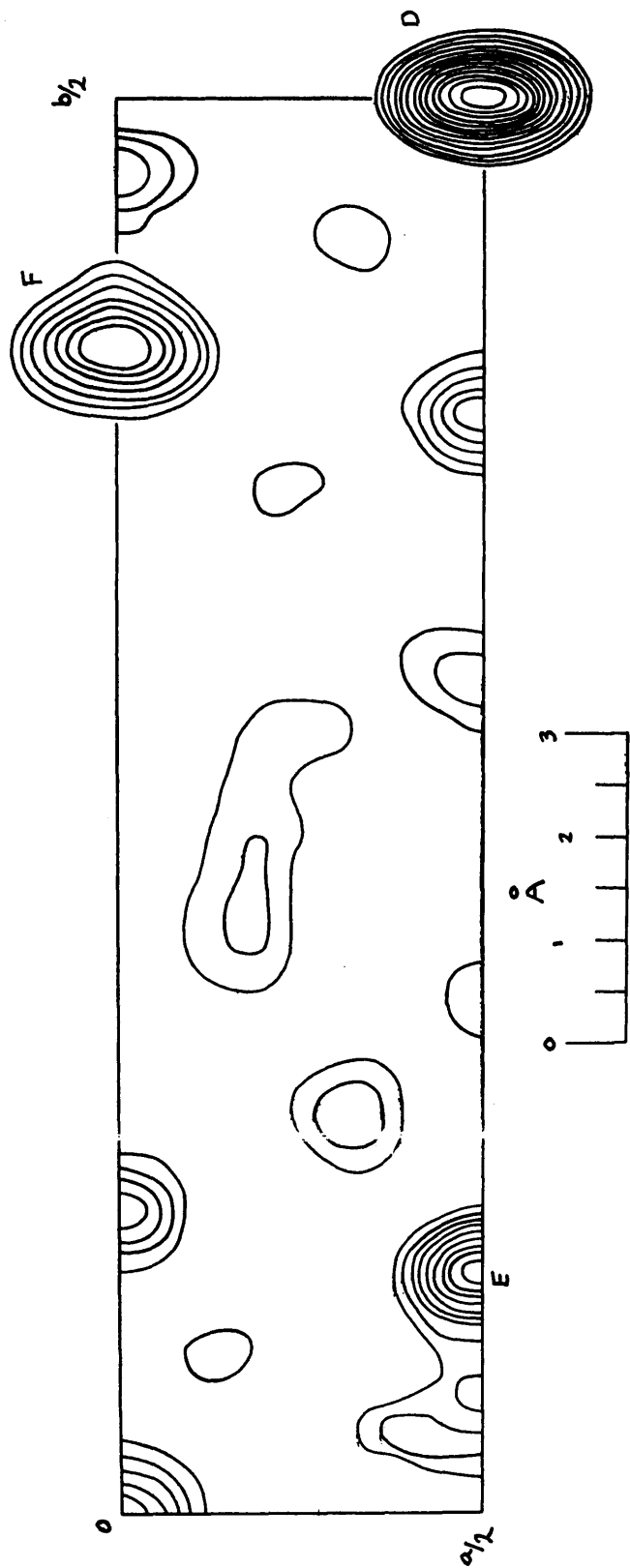


Fig. II. Projection $P(U, V)$ of the Patterson function. Contour scale is arbitrary. The iodine-iodine vector peaks are marked D, E and F.

It is possible, by using the method of Burns (26), to calculate the peak separation, 2Δ , of the two peaks on either side of the mirror plane which merge due to lack of resolution. The value of Δ is found from,

$$\epsilon = \sqrt{2\beta\Delta}$$

where ϵ is the eccentricity of the elliptical peak and the value of β is derived from the Gaussian function,

$$P(r) = P_0 \exp[-\beta r^2]$$

The term P_0 is the electron density at the peak centre and $P(r)$ is the electron density at a distance r from the peak centre.

A plot of $\log P(r)$ against r^2 gives a straight line of negative gradient $\beta/2.303$ and intercept P_0 .

Two methods are available for finding the eccentricity ϵ . If the peak is drawn out accurately and the major and minor axes, a and b respectively, are measured the eccentricity is given by

$$\epsilon = \sqrt{1 - b^2/a^2}$$

The second method is analytical and is due to Ladell and Katz (27).

In this method it is assumed that the peak resembles an elliptic paraboloid near its maximum. Both methods were used to determine the eccentricity of peak D in Fig. II and this was used to

calculate Δ . From this process, a value of $\frac{x}{a} = 0.23$, for the iodine, was found. Trial sets of structure-factor calculations $|F_0|$, were computed using the (hko) zone of data and iodine

x - coordinates; $\frac{x}{a} = 0.24$ and 0.23 respectively. The average discrepancies were 61% and 55% respectively for these x coordinate

values. In this way the final set of iodine coordinates;

$$\frac{x}{a} = 0.230, \quad \frac{y}{b} = 0.205, \quad \frac{z}{c} = 0.039$$

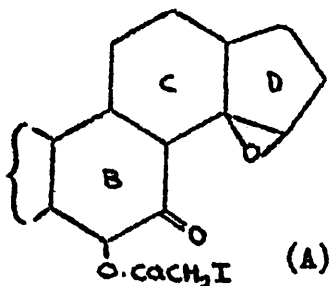
was found and was used in the first set of phasing calculations.

2. (5). STRUCTURE DETERMINATION

The first set of structure factor calculations using only the iodine coordinates gave an approximate set of phase constants. Using these phases and the observed structure amplitudes as coefficients, a Fourier synthesis was computed. The results were mapped out on glass sheets (and contoured at 1e^{-3} intervals) and stacked up parallel to (100) to give a three dimensional effect. A great number of areas of positive electron density were present but all were diffuse and could not with any degree of certainty be ascribed to atoms. The improved iodine coordinates obtained from this map were used to calculate a better set of phase constants and these in turn used in a second Fourier synthesis. This synthesis was drawn out as before but this time as sections parallel to (001) because in the first map it was believed that a six-membered ring was located near the iodine atom but perpendicular to the glass sheets. Again no great detail was observable and this was ascribed to the spurious symmetry and the high temperature factor which tended to make the atom peaks indistinct.

Nine of the most prominent peaks from the second Fourier map reached a height above $2 e \text{ \AA}^{-3}$ and were ascribed to atomic positions. The coordinates of these peaks were determined by the method of Booth (28) and weighted as carbon atoms were included in a third cycle of structure-factor calculations. All atoms had the same isotropic temperature factor of $B = 4.5 \text{ \AA}^2$. The average discrepancy R fell from 43% to 35.7%. On drawing up the results of the third Fourier synthesis, not much extra detail was observed although a general decrease in the background of small spurious peaks had occurred. A further ten prominent peaks were selected as probably being atoms and assigned coordinates. Apart from iodine, nineteen atoms weighted as carbon were included in the next cycle of phasing ($|F_c|$) calculations. The value of R, the average discrepancy between calculated and observed structure amplitudes, fell from the previous value of 35.7% to 34.9%. The improvement was disappointingly small and it seemed that some of the peaks selected could not represent genuine atoms. The coordinates of these nineteen atoms were then plotted on the (okl) Fourier projection and those that did not fall on positive regions or low value negative regions were omitted from the next cycle of phasing calculations. In all four atoms were omitted and inclusion of the remaining fifteen atoms (as carbon) plus iodine in a cycle of structure factor calculations resulted in R being lowered to 33.9%. The subsequent three-dimensional Fourier map on initial examination showed that apart from a further decrease

in small spurious peaks and better resolution of the iodoacetate group, little improvement had taken place. However, a more detailed examination of this map revealed that a distorted six-membered ring was not of the cyclo-hexane type but was actually a cyclopentane ring bearing a 1:2 - epoxide. Joined to this ring, a decalin-type ring system was observed and joined to one of these six-membered rings was the iodoacetate group. Further, a large peak was observed to be near to the ring atom adjacent to that to which the iodoacetate was joined. From stereochemical and bond-length considerations this atom was deduced to be a carbonyl oxygen atom. The relationship of this partial structure (A) to limonin (23), (29) was immediately apparent and the location



of the remaining atoms was straightforward.

The iodine atom, twenty-three carbon atoms and five oxygen atoms were employed in the next calculation of structure factors and phase constants and the value of R fell to 29.6%. In the subsequent three dimensional electron density distribution all the remaining atoms were clearly resolved. The correct chemical type was now assigned to each atom with the exception of the

oxygen in the furan ring where the choice was not unique. The next cycle of structure factors calculated over all the atoms gave a R value of 27.4%.

The course of the analysis is given in Table I. Atomic scattering values due to Berghuis et al (30) were used for the carbon and oxygen atoms and those due to Thomas and Fermi (31) for the iodine atom. An average isotropic temperature factor of $B = 4.9 \text{ \AA}^2$ was assumed.

2. (6) STRUCTURE REFINEMENT.

Initial refinement of the atomic coordinates was achieved by means of both $|F_o|$ and $|F_c|$ maps. Comparison of the peak height of an atom in each map enabled individual isotropic temperature factors to be assigned. In all two cycles of $|F_o|$ and $|F_c|$ maps were computed to correct errors due to termination of series and the value of R fell to 20.5%. At this stage it was still impossible to distinguish the furan ring oxygen atom on the basis of the peak heights alone.

Refinement was continued and completed by four cycles of least-squares calculations, using the program for DEUCE devised by Dr. J.S. Rollett (32). This program refines three positional and six thermal parameters for each atom and the following weighting scheme was used;

$$\sqrt{W} = |F_0|/|F^*| \text{ if } |F_0| < |F^*| ; \quad \sqrt{W} = |F^*|/|F_0| \text{ if } |F_0| > |F^*|$$

where $|F^*|$ is a constant. It was taken equal to the average value of $|F_0|$ (about 30).

After the fourth cycle the shifts in the atomic parameters were negligible and a final cycle of structure-factor calculations with anisotropic temperature factors completed the analysis. The final value for the discrepancy, R, was 17.5% over all the observed structure amplitudes.

2. (7) RESULTS.

The final atomic coordinates are listed in Table II and the corresponding anisotropic thermal parameters in Table III, they are the values of b_{ij} in the equation,

$$\exp(-B \sin^2 \theta / \lambda^2) = 2^{-1} (b_{11} h^2 + b_{22} k^2 + b_{33} l^2 + b_{12} hk + b_{23} kl + b_{13} hl)$$

The final values of $|F_0|$, $|F_c|$ and α are given in Table IV. Table V contains the interatomic distances and Table VI the interbond angles. Table VII lists the intra-molecular non-bonded distances $< 4.0 \text{ \AA}$, while Table VIII gives some of the inter-molecular distances $< 4.0 \text{ \AA}$. Table IX gives the standard deviations of the final atomic coordinates. They were derived from the least-squares residuals by application of the equation;

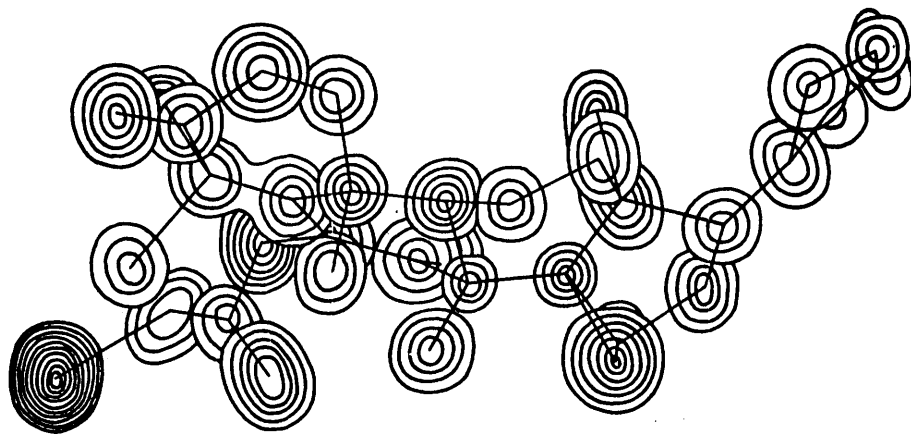
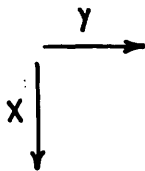


Fig.III. The final three dimensional electron density distribution for cedrelone iodoacetate. The superimposed contour sections are drawn parallel to (001). Contour level 1_e \AA^{-3} except around the iodine atom where it is 5_e \AA^{-3} . The first contour level is omitted in both cases.

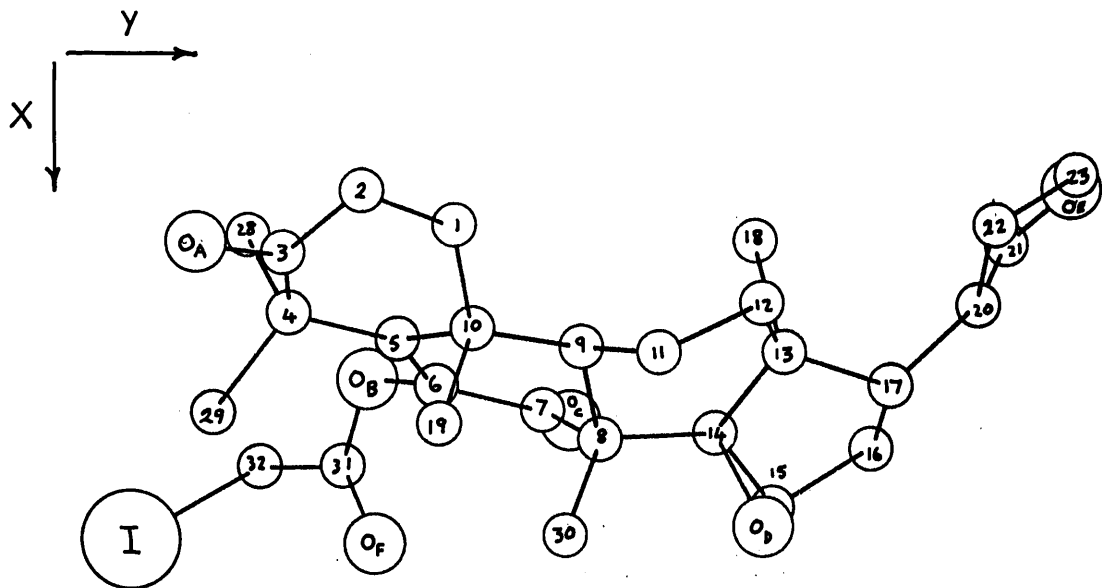


Fig.IV. The atomic arrangement corresponding to Fig.III.

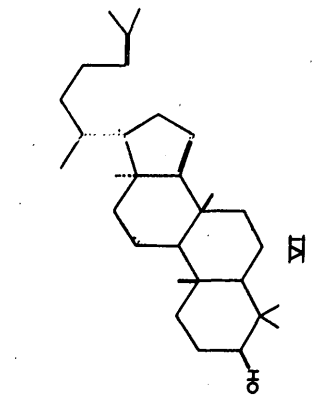
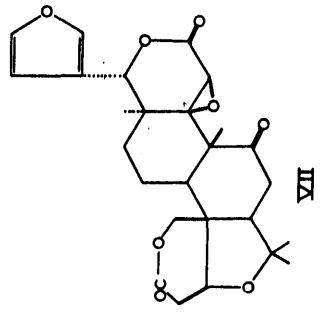
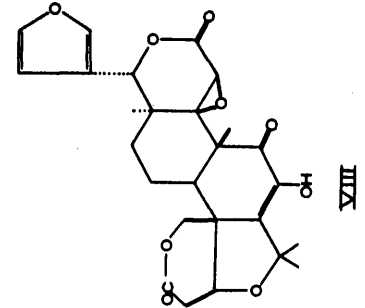
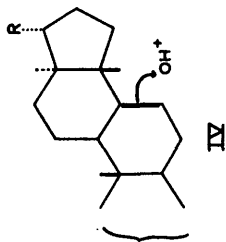
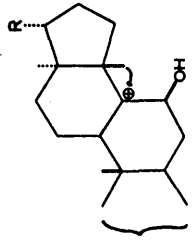
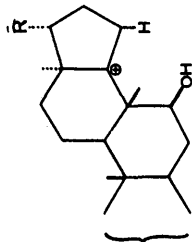
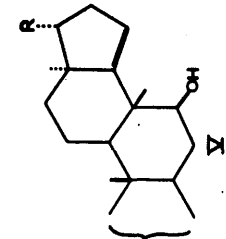
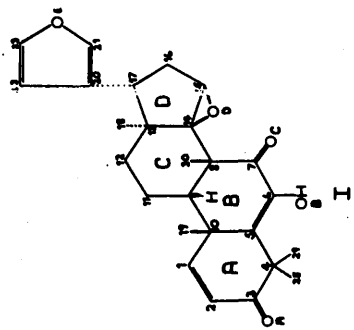
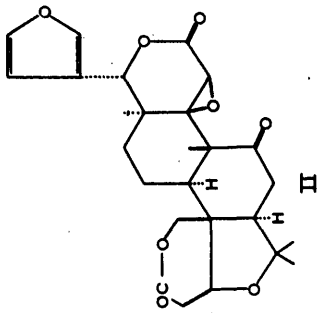
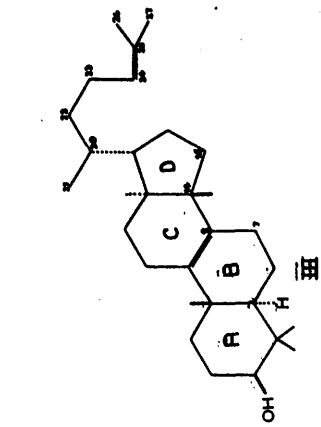
$$\sigma^2(x_i) = \sum_j w_j (\Delta F_j)^2 / \left[(n-s) \sum_j w_j \left(\frac{\partial F_j}{\partial x_i} \right)^2 \right]$$

The average standard deviation of a C - C bond is 0.09Å, that of a C - O bond is 0.07 Å, and of the C - I bond 0.06 Å. The average standard deviation in a bond angle is 4°.

The final electron-density distribution over the region of one molecule is shown as superimposed contour sections drawn parallel to (001) in Figure III. The corresponding atomic arrangement is shown in Figure IV and the atomic arrangement as viewed in projection along the a - axis is shown in Figure V. Figures VI and VII show the crystal structure of cedrelone iodoacetate as viewed in projection down the c - and a - axes respectively.

2. (8) DISCUSSION

The final results of this analysis have established the constitution and stereochemistry (apart from absolute configuration) of cedrelone to be as in (I), the iodoacetate grouping in the derivative used for this analysis being linked to carbon 6 of ring B. Independent chemical studies at Glasgow (21), (23); Madras and Zurich (22) are in complete agreement with this structure. From structural and stereochemical considerations, cedrelone like limonin (II) is clearly a triterpenoid of the euphol (34) (III) type and its biogenesis presumably follows the route proposed for limonin (35). This class of triterpenoids is characterised by the presence of a carbonyl function at C7, a methyl group at C 8 and an epoxide ring between C14 and C15.



O_3 / KO^tBu

By means of a prototropic shift of a hydrogen atom from C7 in a precursor of the euphol type, a $\Delta^{7,8}$ unsaturated intermediate is formed which undergoes oxygenation at C7 by means of attack on the double bond by (OH^+) or its equivalent. A Wagner-Meerwein migration of the methyl group from C14 to C8 followed by loss of a proton from C15 leads as shown (IV) - (V) to a structure of the apoeuphol type (VI). Reactions have been carried out (36) which provide support for this hypothesis. The furan ring is formed by loss of four carbon atoms from the side chain (VI) and cyclisation of the remainder C20 - C23. Further oxidation in rings A and D give rise to the remaining oxygen functions of limonin. In cedrelone ring D is not oxidised to a δ -lactone unlike the other members of this class of compounds. Cedrelone is also unusual in being a diosphenol of which relatively few examples occur naturally. It has been observed, however, (36) that oxidation of limonin and its derivatives to diosphenols of this type is easily carried out by means of oxygen in the presence of potassium t-butoxide (VII) - (VIII) .

In the cedrelone molecule, ring C (I) is locked in a boat conformation by the β - orientated epoxide group. The steric interaction between the 28 and 29 methyl groups and the oxygen substituent at position 6 is presumably the reason for ring A adopting a half-boat conformation. Strong steric interaction occurs between the 1 : 3 - diaxial methyl groups and is reflected in the non-bonded distance of 3.04 Å between C19 and C30. Measure-

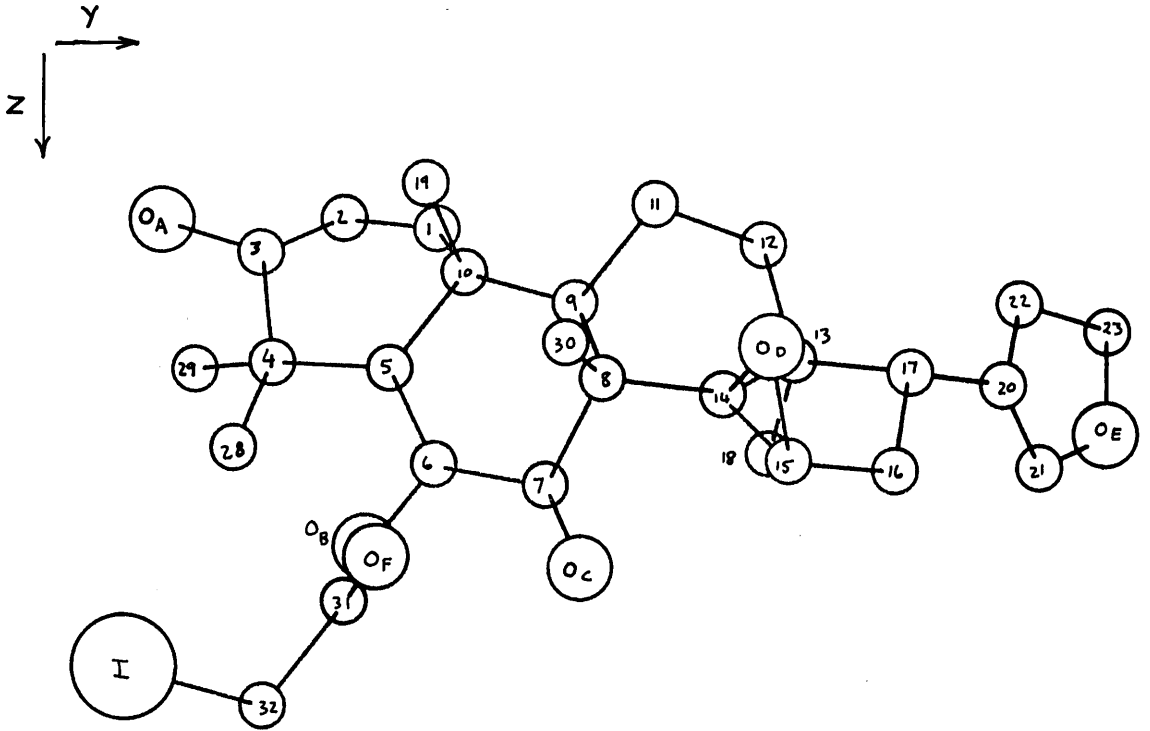


Fig. V. The arrangement of atoms in the molecule as viewed in projection along the a - axis.

-ment of this distance on a standard Dreiding model gives a distance between these atoms of 2.54 \AA .

During the refinement, it was impossible at any stage to distinguish the oxygen atom in the furan ring. Consideration of the bond lengths in the ring, the intermolecular contacts involving the ring, the temperature factors of the ring atoms obtained by the least squares program, and the peak heights from electron-density distributions led to the oxygen being assigned as in Table II and Figure IV. The alternative assignment of C23 as the oxygen and the oxygen as a carbon atom is also possible. In the crystal there is possibly some disorder, the furan ring adopting at random one or other of the two configurations by 180° rotation about the C17 - C20 single bond.

The average carbon-carbon single bond length is 1.55 \AA in favourable agreement with the value of 1.545 \AA in diamond. The average length of a similar bond in two other compounds of this type, epilimonol iodoacetate (29) and guarigayl iodoacetate (37), is 1.52 \AA and 1.55 \AA respectively. The carbon (sp^3) - carbon (sp^2) average bond length of 1.55 \AA is also in agreement with the accepted value of 1.525 \AA . The average carbon-carbon double-bond length is 1.35 \AA and does not differ significantly from the value of 1.334 \AA in ethylene (38). The average carbonyl carbon-oxygen bond length of 1.20 \AA agrees with the values of 1.212 \AA in parabanic acid

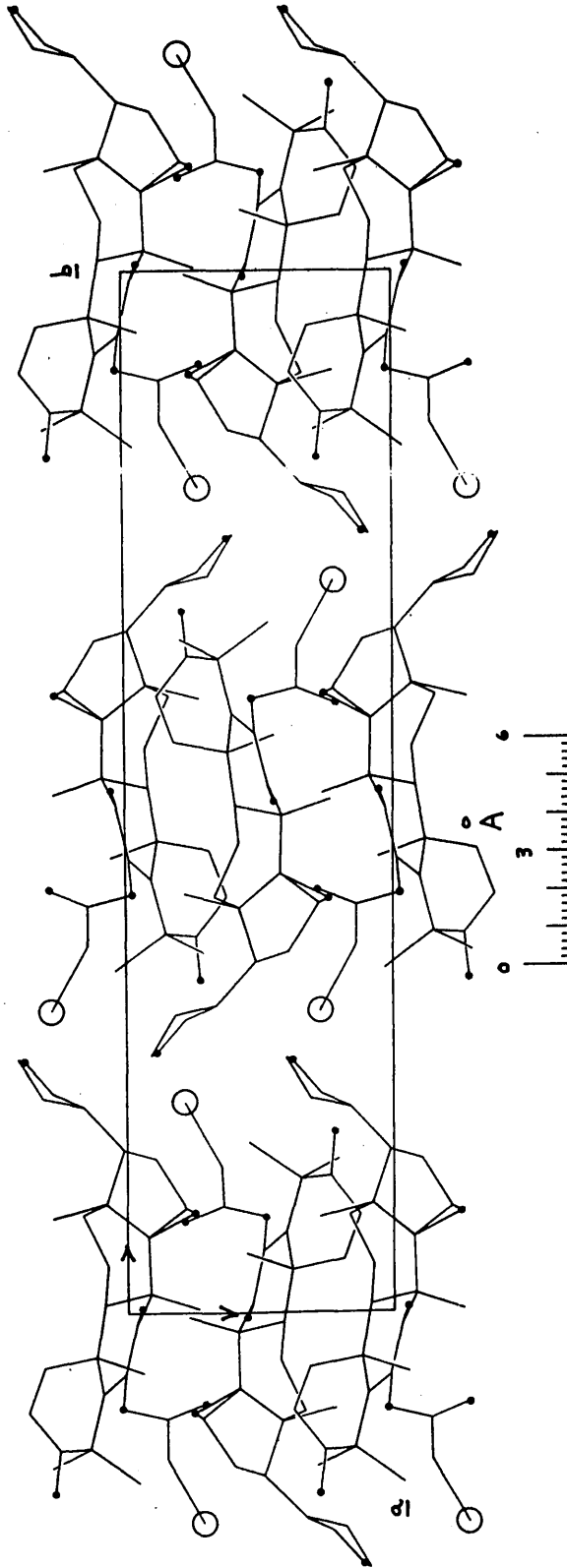
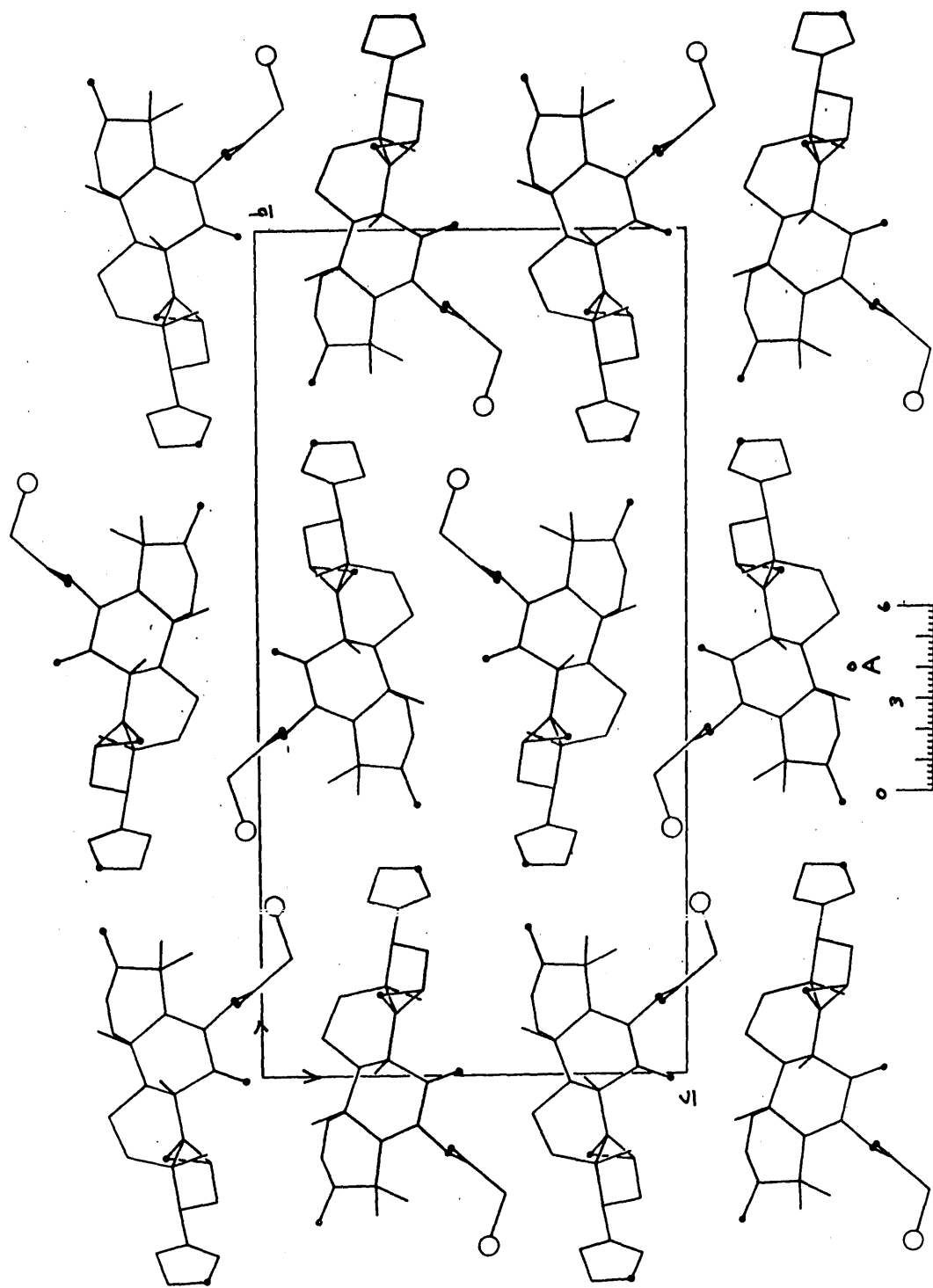


Fig. VI. The crystal structure of cedrelone iodoacetate as viewed in projection along the c - axis

(39) and 1.222 Å in *p* - benzoquinone (40). Further the carbon-oxygen bond length of 1.30 Å compares favourably with the value of 1.32 Å in limonin (29). The average carbon-oxygen distance of 1.47 Å in the epoxide ring agrees with the values of 1.44 Å in ethylene oxide (41), 1.47 Å in cyclopentene oxide (42) and 1.49 Å in clerodin bromo-lactone (43). Table X gives a comparison of the bond lengths in the furan ring with those obtained by Bak *et al* for furan (44) and the comparable distances found in limonin (29) and guariganyl iodoacetate (37). There is no significant disagreement in values except that the carbon-oxygen distance of 1.22 Å in cedrelone iodoacetate is rather short. Finally inspection of the bond lengths in the iodoacetate group reveals no great disagreement with accepted values. The carbon-iodine bond length is 2.15 Å and compares well with the value of 2.14 Å quoted for alkyl iodides (45), (46). Therefore all the bond lengths agree within the estimated standard deviations with accepted values of comparable bonds. Further the non-bonded inter-molecular (Table VIII) distances are normal. The average angle about a sp^2 carbon is 120.3° compared to the expected value of 120° . The average angle about sp^3 carbon atoms is 109° compared with the accepted tetrahedral value of $109^\circ 28'$. Only one tetrahedral angle, C8 - C9 - C10 = 119° , is at great variance with the expected value. This angle reflects the steric repulsion between the 1 : 3

Fig. VII. The crystal structure of cedrelone iodoacetate as viewed in projection along the \underline{a} - axis.



- diaxial methyl groups C19 and C30 in ring B.

The equation of the mean plane through the furan ring calculated by the method of Schomaker et al (47) is,

$$0.651X + 0.750Y - 0.115Z - 7.238 = 0$$

The deviations of the atoms from the plane are shown in Table XI. Application of the χ^2 test to these deviations suggested that they are probably significant. No reason can be put forward to explain this either chemically or sterically. In the crystal, as can be seen from the intermolecular contacts (Table VIII), normal van der Waals interactions hold the molecules together.

TABLE I.

COURSE OF ANALYSIS

<u>Operation</u>	<u>Date used</u>	<u>Atoms included</u>	<u>R (%)</u>	<u>$\sum v\Delta^2$</u>
2D Patterson syntheses	ok ℓ and hko reflections.	-	-	-
1st 3DF _o synthesis	1158F _o	1I	49	-
2nd " "	1164F _o	1I	43	-
3rd " "	1205F _o	1I + 9C	35.7	-
4th " "	1227F _o	1I + 15C	33.9	-
5th " "	1285F _o	1I + 23C + 50	29.6	-
6th " "	"	"	"	"
1st 3DF _o	1285	1I + 29C + 50	27.4	-
7th 3DF _o	"	"	"	"
and	"	"	"	"
2nd 3DF _o	1285	1I + 29C + 50	24.2	-
1st Least-squares cycle	1285F _o	1I + 29C + 50	20.5	10800

TABLE I. (continued)

<u>Operation</u>	<u>Data used</u>	<u>Atoms included</u>	<u>R (%)</u>	<u>$\sum w\Delta^2$</u>
2nd Least-squares cycle	1285F _o	1I + 29c + 50	19.1	9800
3rd " "	1285F _o	1I + 29c + 50	18.4	8300
4th " "	1285F _o	1I + 29c + 50	18.0	7700
8th 3DF _o synthesis	1285F _o	1I + 29c + 50	17.5	-

1285 structure amplitudes were used in the phasing calculations.
 In fact 122 of these were unobserved.

TABLE II.ATOMIC CO-ORDINATES

(Origin of co-ordinates as in "International Tables")

<u>Atom</u>	<u>x/a</u>	<u>y/b</u>	<u>z/c</u>
C ₁	- 0.3157	- 0.0520	0.1550
C ₂	- 0.3783	- 0.0957	0.1406
C ₃	- 0.2634	- 0.1337	0.1687
C ₄	- 0.1512	- 0.1311	0.2654
C ₅	- 0.0985	- 0.0781	0.2787
C ₆	- 0.0131	- 0.0596	0.3679
C ₇	0.0318	- 0.0086	0.3925
C ₈	0.0840	0.0185	0.2986
C ₉	- 0.0851	0.0093	0.2311
C ₁₀	- 0.1186	- 0.0424	0.1949
C ₁₁	- 0.0764	0.0460	0.1412
C ₁₂	- 0.1651	0.0958	0.1854
C ₁₃	- 0.0779	0.1067	0.2925
C ₁₄	0.0798	0.0744	0.3175
C ₁₅	0.0235	0.1024	0.3824
C ₁₆	0.1063	0.1495	0.3960
C ₁₇	- 0.0109	0.1585	0.3085
C ₁₈	- 0.2785	0.0931	0.3694
C ₁₉	0.0544	- 0.0578	0.1154

TABLE II (Continued)

<u>Atom</u>	<u>x/a</u>	<u>y/b</u>	<u>z/c</u>
C ₂₀	- 0.1626	0.2006	0.3251
C ₂₁	- 0.2756	0.2147	0.4005
C ₂₂	- 0.3139	0.2093	0.2532
C ₂₃	- 0.4079	0.2487	0.2789
C ₂₈	- 0.2911	- 0.1504	0.3437
C ₂₉	0.0410	- 0.1661	0.2702
C ₃₀	0.2710	0.0030	0.2637
C ₃₁	0.1412	- 0.1035	0.4855
C ₃₂	0.1435	- 0.1425	0.5768
O _A	- 0.2808	- 0.1767	0.1316
O _B	- 0.0223	- 0.0932	0.4444
O _C	0.0597	0.0047	0.4678
O _D	0.2559	0.0974	0.2779
O _E	- 0.3849	0.2467	0.3740
O _F	0.2847	- 0.0888	0.4452
I	0.2808	- 0.2054	0.5353

TABLE IIIANISOTROPIC TEMPERATURE - FACTOR PARAMETERS ($b_{ij} \times 10^5$)

	b_{11}	b_{22}	b_{33}	b_{12}	b_{23}	b_{13}
C_1	3743	243	642	597	124	- 2186
C_2	5176	238	558	- 282	461	0
C_3	8289	213	768	-1498	177	3246
C_4	3464	188	729	- 166	82	- 1779
C_5	3791	138	730	1007	178	- 1821
C_6	4980	163	523	249	359	0
C_7	5221	386	426	-1494	678	- 2774
C_8	3979	134	389	502	567	0
C_9	1678	103	955	- 211	58	- 2396
C_{10}	5893	315	658	- 243	381	1248
C_{11}	7183	240	1047	201	241	0
C_{12}	5452	140	1301	432	158	1120
C_{13}	3849	277	514	652	- 196	3074
C_{14}	2400	277	439	761	-51	0
C_{15}	6076	164	562	312	-82	- 1924
C_{16}	6744	142	829	595	265	- 1385
C_{17}	3669	170	1017	- 702	-98	1171
C_{18}	411	181	1113	204	132	- 280
C_{19}	2492	324	528	0	- 153	3237
C_{20}	7048	298	274	1308	749	2656

TABLE III (Continued)

	b_{11}	b_{22}	b_{33}	b_{12}	b_{23}	b_{13}
c_{21}	6734	550	850	658	87	1876
c_{22}	4880	257	1400	-328	- 404	- 4043
c_{23}	11336	186	1440	0	381	0
c_{28}	5574	250	1065	- 440	- 102	0
c_{29}	8943	266	928	379	- 443	0
c_{30}	1576	284	1012	649	304	3046
c_{31}	3786	239	1319	- 254	- 431	979
c_{32}	2258	424	925	- 350	- 25	0
o_A	9457	283	901	14	-498	660
o_B	4094	247	855	-575	65	- 2712
o_C	6168	216	402	- 297	236	2189
o_D	2497	179	941	- 419	- 64	2861
o_E	11733	143	1192	1981	367	1894
o_F	6717	210	790	513	186	0
I	6717	183	983	356	- 34	- 438

Table IV. Measured and calculated values of the structure factors and phase angles.

h	k	l	F _o		F _c		Δ	φ _o	φ _c
			meas.	calc.	meas.	calc.			
0	0	0	100	100	100	100	0	0	0
0	0	1	100	100	100	100	0	0	0
0	0	2	100	100	100	100	0	0	0
0	0	3	100	100	100	100	0	0	0
0	0	4	100	100	100	100	0	0	0
0	0	5	100	100	100	100	0	0	0
0	0	6	100	100	100	100	0	0	0
0	0	7	100	100	100	100	0	0	0
0	0	8	100	100	100	100	0	0	0
0	0	9	100	100	100	100	0	0	0
0	0	10	100	100	100	100	0	0	0
0	0	11	100	100	100	100	0	0	0
0	0	12	100	100	100	100	0	0	0
0	0	13	100	100	100	100	0	0	0
0	0	14	100	100	100	100	0	0	0
0	0	15	100	100	100	100	0	0	0
0	0	16	100	100	100	100	0	0	0
0	0	17	100	100	100	100	0	0	0
0	0	18	100	100	100	100	0	0	0
0	0	19	100	100	100	100	0	0	0
0	0	20	100	100	100	100	0	0	0
0	0	21	100	100	100	100	0	0	0
0	0	22	100	100	100	100	0	0	0
0	0	23	100	100	100	100	0	0	0
0	0	24	100	100	100	100	0	0	0
0	0	25	100	100	100	100	0	0	0
0	0	26	100	100	100	100	0	0	0
0	0	27	100	100	100	100	0	0	0
0	0	28	100	100	100	100	0	0	0
0	0	29	100	100	100	100	0	0	0
0	0	30	100	100	100	100	0	0	0
0	0	31	100	100	100	100	0	0	0
0	0	32	100	100	100	100	0	0	0
0	0	33	100	100	100	100	0	0	0
0	0	34	100	100	100	100	0	0	0
0	0	35	100	100	100	100	0	0	0
0	0	36	100	100	100	100	0	0	0
0	0	37	100	100	100	100	0	0	0
0	0	38	100	100	100	100	0	0	0
0	0	39	100	100	100	100	0	0	0
0	0	40	100	100	100	100	0	0	0
0	0	41	100	100	100	100	0	0	0
0	0	42	100	100	100	100	0	0	0
0	0	43	100	100	100	100	0	0	0
0	0	44	100	100	100	100	0	0	0
0	0	45	100	100	100	100	0	0	0
0	0	46	100	100	100	100	0	0	0
0	0	47	100	100	100	100	0	0	0
0	0	48	100	100	100	100	0	0	0
0	0	49	100	100	100	100	0	0	0
0	0	50	100	100	100	100	0	0	0
0	0	51	100	100	100	100	0	0	0
0	0	52	100	100	100	100	0	0	0
0	0	53	100	100	100	100	0	0	0
0	0	54	100	100	100	100	0	0	0
0	0	55	100	100	100	100	0	0	0
0	0	56	100	100	100	100	0	0	0
0	0	57	100	100	100	100	0	0	0
0	0	58	100	100	100	100	0	0	0
0	0	59	100	100	100	100	0	0	0
0	0	60	100	100	100	100	0	0	0
0	0	61	100	100	100	100	0	0	0
0	0	62	100	100	100	100	0	0	0
0	0	63	100	100	100	100	0	0	0
0	0	64	100	100	100	100	0	0	0
0	0	65	100	100	100	100	0	0	0
0	0	66	100	100	100	100	0	0	0
0	0	67	100	100	100	100	0	0	0
0	0	68	100	100	100	100	0	0	0
0	0	69	100	100	100	100	0	0	0
0	0	70	100	100	100	100	0	0	0
0	0	71	100	100	100	100	0	0	0
0	0	72	100	100	100	100	0	0	0
0	0	73	100	100	100	100	0	0	0
0	0	74	100	100	100	100	0	0	0
0	0	75	100	100	100	100	0	0	0
0	0	76	100	100	100	100	0	0	0
0	0	77	100	100	100	100	0	0	0
0	0	78	100	100	100	100	0	0	0
0	0	79	100	100	100	100	0	0	0
0	0	80	100	100	100	100	0	0	0
0	0	81	100	100	100	100	0	0	0
0	0	82	100	100	100	100	0	0	0
0	0	83	100	100	100	100	0	0	0
0	0	84	100	100	100	100	0	0	0
0	0	85	100	100	100	100	0	0	0
0	0	86	100	100	100	100	0	0	0
0	0	87	100	100	100	100	0	0	0
0	0	88	100	100	100	100	0	0	0
0	0	89	100	100	100	100	0	0	0
0	0	90	100	100	100	100	0	0	0
0	0	91	100	100	100	100	0	0	0
0	0	92	100	100	100	100	0	0	0
0	0	93	100	100	100	100	0	0	0
0	0	94	100	100	100	100	0	0	0
0	0	95	100	100	100	100	0	0	0
0	0	96	100	100	100	100	0	0	0
0	0	97	100	100	100	100	0	0	0
0	0	98	100	100	100	100	0	0	0
0	0	99	100	100	100	100	0	0	0
0	0	100	100	100	100	100	0	0	0

MOLECULAR DIMENSIONSINTERATOMIC DISTANCES (Å) AND ANGLESTABLE VINTRAMOLECULAR BONDED DISTANCES

C ₁ - C ₂	1.29	C ₈ - C ₃₀	1.45
C ₁ - C ₁₀	1.50	C ₉ - C ₁₀	1.52
C ₂ - C ₃	1.37	C ₉ - C ₁₁	1.59
C ₃ - C ₄	1.54	C ₁₀ - C ₁₉	1.68
C ₃ - O _A	1.29	C ₁₁ - C ₁₂	1.62
C ₄ - C ₅	1.51	C ₁₂ - C ₁₃	1.62
C ₄ - C ₂₈	1.55	C ₁₃ - C ₁₄	1.45
C ₄ - C ₂₉	1.65	C ₁₃ - C ₁₇	1.51
C ₅ - C ₆	1.45	C ₁₃ - C ₁₈	1.79
C ₅ - C ₁₀	1.52	C ₁₄ - C ₁₅	1.55
C ₆ - C ₇	1.48	C ₁₄ - O _D	1.48
C ₆ - O _B	1.40	C ₁₅ - C ₁₆	1.54
C ₇ - C ₈	1.53	C ₁₅ - O _D	1.46
C ₇ - O _C	1.11	C ₁₆ - C ₁₇	1.47
C ₈ - C ₉	1.52	C ₁₇ - C ₂₀	1.58
C ₈ - C ₁₄	1.56	C ₂₀ - C ₂₁	1.36

TABLE V. (Continued)

$C_{20} - C_{22}$	1.47	$C_{31} - C_{32}$	1.65
$C_{21} - C_E$	1.22	$C_{31} - O_B$	1.30
$C_{22} - C_{23}$	1.31	$C_{31} - O_F$	1.21
$C_{23} - O_E$	1.32	$I - C_{32}$	2.05

TABLE VIINTERBOND ANGLES

C ₂ C ₁ C ₁₀	122	C ₇ C ₈ C ₉	104
C ₁ C ₂ C ₃	118	C ₇ C ₈ C ₁₄	110
C ₂ C ₃ C ₄	120	C ₇ C ₈ C ₃₀	110
C ₂ C ₃ O _A	122	C ₉ C ₈ C ₁₄	105
C ₄ C ₃ O _A	115	C ₉ C ₈ C ₃₀	117
C ₃ C ₄ C ₅	106	C ₁₄ C ₈ C ₃₀	111
C ₃ C ₄ C ₂₈	105	C ₈ C ₉ C ₁₀	118
C ₃ C ₄ C ₂₉	115	C ₈ C ₉ C ₁₁	110
C ₅ C ₄ C ₂₈	114	C ₁₀ C ₉ C ₁₁	110
C ₅ C ₄ C ₂₉	111	C ₁ C ₁₀ C ₅	104
C ₂₈ C ₄ C ₂₉	107	C ₁ C ₁₀ C ₉	115
C ₄ C ₅ C ₆	123	C ₁ C ₁₀ C ₁₉	112
C ₄ C ₅ C ₁₀	120	C ₅ C ₁₀ C ₁₉	110
C ₆ C ₅ C ₁₀	117	C ₅ C ₁₀ C ₁₉	105
C ₅ C ₆ C ₇	128	C ₉ C ₁₀ C ₁₉	110
C ₅ C ₆ O _B	113	C ₉ C ₁₁ C ₁₂	103
C ₇ C ₆ O _B	118	C ₁₁ C ₁₂ C ₁₃	111
C ₆ C ₇ C ₈	109	C ₁₂ C ₁₃ C ₁₄	113
C ₆ C ₇ O _C	124	C ₁₂ C ₁₃ C ₁₇	115
C ₈ C ₇ O _C	126	C ₁₂ C ₁₃ C ₁₈	102

TABLE VI (Contd.)

$C_{14} C_{13} C_{17}$	108	$C_{13} C_{14} C_{15}$	109
$C_{14} C_{13} C_{18}$	109	$C_{13} C_{14} O_D$	106
$C_{17} C_{13} C_{18}$	111	$C_{15} C_{14} O_D$	58
$C_8 C_{14} C_{13}$	125	$C_{14} C_{15} C_{16}$	98
$C_8 C_{14} C_{15}$	125	$C_{14} C_{15} O_D$	59
$C_8 C_{14} O_D$	110	$C_{16} C_{15} O_D$	106
$C_{15} C_{16} C_{17}$	110	$C_{22} C_{23} O_B$	100
$C_{13} C_{17} C_{16}$	98	$C_{32} C_{31} O_B$	119
$C_{13} C_{17} C_{20}$	120	$C_{32} C_{31} O_F$	124
$C_{16} C_{17} C_{20}$	112	$O_B C_{31} O_F$	117
$C_{17} C_{20} C_{21}$	135	$C_{31} C_{32} I$	110
$C_{17} C_{20} C_{22}$	120	$C_6 O_B C_{31}$	115
$C_{21} C_{20} C_{22}$	93	$C_{14} O_D C_{15}$	63
$C_{20} C_{21} O_E$	110	$C_{21} O_E C_{23}$	114
$C_{20} C_{22} C_{23}$	108		

INTRAMOLECULAR NON-BONDED DISTANCES < 4 Å

C ₁ - C ₆	3.61	C ₁ - C ₈	3.92
C ₁ - C ₁₁	3.17	C ₁ - C ₂₈	3.75
C ₁ - O _A	3.44	C ₂ - C ₅	2.76
C ₂ - C ₉	3.74	C ₂ - C ₁₉	3.21
C ₂ - C ₂₈	3.22	C ₂ - C ₂₉	3.93
C ₃ - C ₆	3.83	C ₃ - C ₁₉	3.23
C ₄ - C ₉	3.91	C ₄ - C ₁₉	3.22
C ₄ - C ₃₁	3.72	C ₄ - O _B	2.82
C ₅ - C ₈	2.95	C ₅ - C ₁₁	3.90
C ₅ - C ₃₀	3.41	C ₅ - C ₃₁	3.37
C ₅ - O _A	3.61	C ₅ - O _C	3.62
C ₅ - O _F	3.53	C ₆ - C ₁₄	3.80
C ₆ - C ₁₉	3.50	C ₆ - C ₂₈	3.17
C ₆ - C ₂₉	3.23	C ₆ - C ₃₀	2.99
C ₆ - C ₃₂	3.82	C ₆ - O _F	2.47
C ₇ - C ₁₀	3.05	C ₇ - C ₁₁	3.84
C ₇ - C ₁₃	3.53	C ₇ - C ₁₅	3.33
C ₇ - C ₁₈	3.54	C ₇ - C ₃₁	3.00
C ₇ - O _D	3.66	C ₇ - O _F	2.91
C ₈ - C ₁₂	3.15	C ₈ - C ₁₆	3.84
C ₈ - C ₁₇	3.90	C ₈ - C ₁₈	3.39
C ₈ - C ₁₉	3.28	C ₈ - O _B	3.74
C ₈ - O _F	3.83	C ₉ - C ₁₅	3.93
C ₉ - C ₁₈	3.27	C ₉ - O _C	3.41
C ₉ - O _D	3.45	C ₁₀ - C ₁₂	3.81
C ₁₀ - C ₁₄	3.88	C ₁₀ - C ₂₈	3.79

TABLE VII (Contd.)

$C_{10} - C_{29}$	3.72	$C_{10} - C_{30}$	3.13
$C_{10} - O_A$	3.95	$C_{10} - O_B$	3.76
$C_{10} - O_C$	4.15	$C_{11} - C_{17}$	3.87
$C_{11} - C_{18}$	3.67	$C_{11} - C_{19}$	3.01
$C_{11} - C_{30}$	3.18	$C_{11} - O_D$	3.30
$C_{12} - C_{15}$	3.83	$C_{12} - C_{16}$	3.76
$C_{12} - C_{20}$	3.45	$C_{12} - C_{22}$	3.41
$C_{12} - O_D$	3.20	$C_{13} - C_{22}$	3.31
$C_{13} - C_{21}$	3.59	$C_{13} - C_{30}$	3.76
$C_{13} - O_C$	3.82	$C_{14} - C_{20}$	3.85
$C_{14} - O_C$	2.82	$C_{15} - C_{18}$	3.51
$C_{15} - C_{20}$	3.89	$C_{15} - C_{30}$	3.20
$C_{15} - O_C$	3.14	$C_{16} - C_{18}$	3.12
$C_{16} - C_{21}$	3.21	$C_{16} - C_{22}$	3.89
$C_{17} - C_{23}$	3.74	$C_{17} - O_B$	3.67
$C_{17} - O_D$	2.54	$C_{18} - C_{20}$	3.12
$C_{18} - C_{21}$	3.37	$C_{18} - C_{22}$	3.58
$C_{18} - O_C$	3.64	$C_{18} - O_D$	3.93
$C_{19} - C_{29}$	3.65	$C_{19} - C_{30}$	3.04
$C_{28} - C_{31}$	3.81	$C_{28} - O_A$	3.00
$C_{28} - O_B$	2.81	$C_{29} - C_{31}$	3.49
$C_{29} - O_A$	2.96	$C_{29} - O_B$	3.15
$C_{29} - O_F$	3.63	$C_{30} - O_C$	3.17
$C_{30} - O_D$	2.60	$C_{30} - O_F$	3.55
$C_{31} - O_C$	3.03	$O_B - O_C$	2.76
$O_C - O_D$	3.89	$O_C - O_F$	3.02
$I - O_B$	3.94	$I - O_F$	3.43

TABLE VIIIINTERMOLECULAR DISTANCES ($< 4 \text{ \AA}$)

$C_{32} \dots O_D^I$	3.11	$C_{15} \dots C_{19}^I$	3.76
$O_E \dots O_A^{IV}$	3.14	$C_{32} \dots C_{22}^{II}$	3.81
$C_{23} \dots O_A^{IV}$	3.23	$O_{23} \dots C_{28}^{IV}$	3.86
$O_C \dots C_1^{II}$	3.35	$C_{32} \dots O_{12}^{II}$	3.87
$C_{21} \dots O_A^{II}$	3.36	$C_{18} \dots C_2^{II}$	3.88
$C_{23} \dots C_{29}^{III}$	3.53	$O_E \dots C_{29}^{III}$	3.92
$O_F \dots C_{11}^I$	3.57	$C_{22} \dots C_{29}^{III}$	3.93
$O_C \dots C_{19}^I$	3.67	$O_B \dots C_{12}^{II}$	3.96
$O_C \dots C_2^{II}$	3.67	$C_{20} \dots C_{29}^{III}$	3.98

The superscripts refer to the following positions:

I	$\frac{1}{2} - x,$	$-y,$	$\frac{1}{2} + z$
II	$-\frac{1}{2} - x,$	$-y,$	$\frac{1}{2} + z$
III	$-x,$	$\frac{1}{2} + y,$	$\frac{1}{2} - z$
IV	$-1 - x,$	$\frac{1}{2} + y,$	$\frac{1}{2} - z$

TABLE IXSTANDARD DEVIATIONS OF THE FINAL ATOMIC CO-ORDINATES (\AA)

<u>Atom</u>	<u>$\sigma(x)$</u>	<u>$\sigma(y)$</u>	<u>$\sigma(z)$</u>
C ₁	0.059	0.042	0.046
C ₂	0.058	0.045	0.044
C ₃	0.069	0.042	0.043
C ₄	0.051	0.043	0.047
C ₅	0.049	0.038	0.044
C ₆	0.061	0.040	0.044
C ₇	0.064	0.051	0.049
C ₈	0.056	0.041	0.046
C ₉	0.047	0.035	0.048
C ₁₀	0.072	0.050	0.048
C ₁₁	0.068	0.049	0.055
C ₁₂	0.063	0.042	0.051
C ₁₃	0.054	0.047	0.044
C ₁₄	0.053	0.047	0.041
C ₁₅	0.069	0.038	0.043
C ₁₆	0.059	0.040	0.050
C ₁₇	0.055	0.041	0.049
C ₁₈	0.051	0.036	0.047
C ₁₉	0.053	0.048	0.050
C ₂₀	0.059	0.048	0.043
C ₂₁	0.069	0.058	0.055

TABLE IX (Continued)

<u>Atom</u>	<u>$\sigma(x)$</u>	<u>$\sigma(y)$</u>	<u>$\sigma(z)$</u>
C ₂₂	0.050	0.046	0.053
C ₂₃	0.084	0.046	0.063
C ₂₈	0.067	0.046	0.051
C ₂₉	0.075	0.050	0.055
C ₃₀	0.063	0.045	0.044
C ₃₁	0.052	0.045	0.056
C ₃₂	0.057	0.058	0.051
O _A	0.051	0.031	0.032
O _B	0.037	0.028	0.030
O _C	0.037	0.028	0.033
O _D	0.033	0.024	0.027
O _E	0.078	0.042	0.058
O _F	0.042	0.026	0.028
I	0.004	0.003	0.004

TABLE X.COMPARISON OF THE BOND LENGTHS IN SOME FURAN RINGS.

<u>Compound</u>	<u>Bond Lengths (Å)</u>			<u>σ (l) Å</u>	<u>Reference</u>
	C - C	C - O	C = C		
Furan	1.433	1.372	1.355	-	(44)
Cedrelone	1.46	1.32	1.34	0.09	This Thesis
Iodoacetate		1.22			
Epilimonal	1.44	1.42	1.25	0.08	(29)
Iodoacetate					
Guariganyl	1.45	1.36	1.25	0.08	(37)
Iodoacetate		1.25			

TABLE XI

Displacements (Å) of atoms from the mean plane through atoms
C20 C21 C22 C23 O_E.

C(17)	0.020
C(20)	0.180
C(21)	- 0.160
C(22)	- 0.213
C(23)	0.130
O(E)	0.044

PART III.

THE STRUCTURE OF CHIMONANTHINE: X-RAY
ANALYSIS OF CHIMONANTHINE DIHYDROBROMIDE.

3. (1) INTRODUCTION

Recently Hodson, Robinson and Smith (48) isolated a new alkaloid from the leaves of Chimonanthus fragrans (Lindley), a deciduous shrub growing naturally to about eight feet. This compact shrub was introduced to this country in 1766 from China and is closely related to the Calycanthaceae. Because its sweet-smelling flowers appear in December, it is commonly known as Winter Sweet.

These workers named the alkaloid Chimonanthine and gave its formula as $C_{22}H_{26}N_4$. Chimonanthine was shown to be a diacidic base of equivalent weight 175 and from U.V. spectral evidence to contain a Ph-N-C-N grouping. Further it was proved that the compound contained two N-methyl groups and that N-H groups were present. Reduction with zinc and hydrochloric acid gave the indoline, 3-2¹ - methylaminoethylindole, showing that like folicanthine (49) and calycanthine (50) its skeleton is composed of two tryptamine units. It was also shown that like calycanthine, chimonanthine had aromatic NH groups and aliphatic tertiary N-methyl groups. Hodson et al proposed two probable structures for chimonanthine neither of which was readily chemically distinguishable from the other.

The X-ray analysis of chimonanthine was carried with crystals of chimonanthine dihydrobromide, $C_{22}H_{26}N_4 \cdot 2HBr$,

supplied by G.F. Smith of the Department of Chemistry, the University, Manchester. The analysis to determine the molecular and crystal structure of chimonanthine was commenced shortly before the above chemical work was published.

3. (2) CRYSTAL DATA

Chimonanthine dihydrobromide	$C_{22}H_{26}N_4 \cdot 2HBr$
Molecular Weight	= 508.31
Melting Point	= 188 - 189°C
Density Calculated	= 1.311 gm/c.c.
Density Measurement	= 1.356

By flotation using benzene/carbon tetrachloride).

The crystal is tetragonal with

$$a = b = 13.95 \pm 0.02 \text{ \AA}$$

$$c = 26.67 \pm 0.02 \text{ \AA}$$

$$\text{Volume of the unit cell} = 5190 \text{ \AA}^3$$

$$\text{Number of molecules per unit cell} = 8.$$

Absent spectra; $00l$ when $l \neq 4n$

$h00$ when $h \neq 2m$

Space group $P 4_1 2_1 2$ (D_4^4) or its enantiomorph $P 4_3 2_1 2$ (D_4^8)

Linear absorption coefficient for X-rays (Copper $K\alpha$ radiation)

$$\mu = 42 \text{ cm}^{-1}$$

Total number of electrons per unit cell $F(000) = 2064$

$$\sum f^2 \text{ (light atoms)} = 1016 \text{ (} \sin \Theta = 0 \text{)}$$

$$\sum f^2 \text{ (heavy atoms)} = 2450 \text{ (")}$$

3. (3). INTENSITY DATA

Rotation, oscillation and moving-film photographs were taken with copper $K\alpha$ ($\lambda = 1.542 \text{ \AA}$) radiation. The unit cell dimensions were obtained from rotation and equatorial layer line photographs of a crystal mounted about the a - axis. The space group was determined, from the systematic halvings in the X-ray spectra, to be $P4_12_12$ (D_4^4) or its enantiomorph $P4_32_12$ (D_4^8).

Small crystals, crystallised from dry ethyl alcohol, bathed in a uniform X-ray beam were used for the intensity measurements. No absorption corrections were made. Using a Weissenberg equi-inclination camera the $0k\ell - 9k\ell$ spectra were collected photographically. Correlation of strong and weak reflections was achieved by means of the multiple film technique (24) employing a calibrated step-wedge. The intensities were estimated visually and were corrected for Lorentz, polarisation and rotation (25) factors. The values of the structure amplitudes, $|F_0|$, were obtained by the mosaic crystal formula.

As the crystal belongs to the tetragonal system most reflections have symmetrically occurring equivalent reflections

in different zones obtained by rotation about the same axis. The reflection (h,k,l) equals reflection (l,h,l) in intensity under these conditions and the occurrence of such reflection equalities was used as a basis for interzonal scaling. In general in any zone (HKL) , the data used for structure determination is of the type $(H, K \gg H, L)$ and the data used for scaling is of the type $(H, K \ll H, L)$, e.g. in the zone $(5KL)$ calculations used $(5,5,L)$, $(5,6,L)$, $(5,7,L)$ etc. and scaling used $(5,0,L)$ $(5,4,L)$. All zones were put on the same relative scale in this way and the absolute scale was found at a later stage by comparison with the calculated structure factors, $|F_c|$. In all 2093 independent structure amplitudes were measured. Apart from these, 525 structure amplitudes were found whose intensity was less than the lowest value on the step-wedge used. These reflections were not included in any stage of the structure determination.

3. (4) DETERMINATION OF THE HEAVY ATOM POSITIONS.

The Patterson function expression $P(U,V,W)$ of a crystal having point group symmetry 422 is,

$$P(U,V,W) = \frac{8}{V_c} \sum_0^{\infty} \sum_0^{\infty} \sum_0^{\infty} |F(hkl)|^2 \cos 2\pi h U \cos 2\pi k V \cos 2\pi l W.$$

The interpretation of the map of this function will be complicated by the high symmetry of the tetragonal system and the presence of two heavy atoms per asymmetric unit. Each set of N symmetrically related heavy atoms will give rise to $N(N-1)$ basic vectors.

Thus there will be 112 bromide ion - bromide ion vectors between symmetry related bromide ions, 56 per set of symmetrically related atoms. Further, there will be 128 bromide ion - bromide ion vectors between non-symmetry related bromide ions. On account of the symmetry of the Patterson function, it is only necessary to consider six peaks due to vectors between each set of symmetrically related bromide ions and eight peaks due to vectors between non-symmetrically related bromide ions.

The two dimensional Patterson projection, $P(V,W)$ was computed with 319 terms. The projection contained a great many peaks and offered no hope of providing the bromide coordinates. The three-dimensional map was accordingly computed over one eighth of the unit cell volume using 2093 terms.

The peaks to be expected on the three Harker sections of the three-dimensional Patterson synthesis, $P(U,V,\frac{1}{4})$, $P(U,V,\frac{1}{2})$ and $P(U,\frac{1}{2},W)$ are in themselves insufficient to define fully the two sets of bromide ion coordinates. The occurrence of a $Br^- - Br^-$ vector at $2x, 2y, \frac{1}{2}$ on section $P(U,V,\frac{1}{2})$ does not distinguish the following x, y - coordinates, $x, y; \frac{1}{2} - x, y; x, \frac{1}{2} + y; \bar{x}, y; x, \bar{y}$; etc. In a similar fashion the peaks on the section $P(U,\frac{1}{2},W)$ at $\frac{1}{2} - 2x, \frac{1}{2}, \frac{1}{4} - 2z$ and $\frac{1}{2} - 2y, \frac{1}{2}, \frac{1}{4} + 2z$

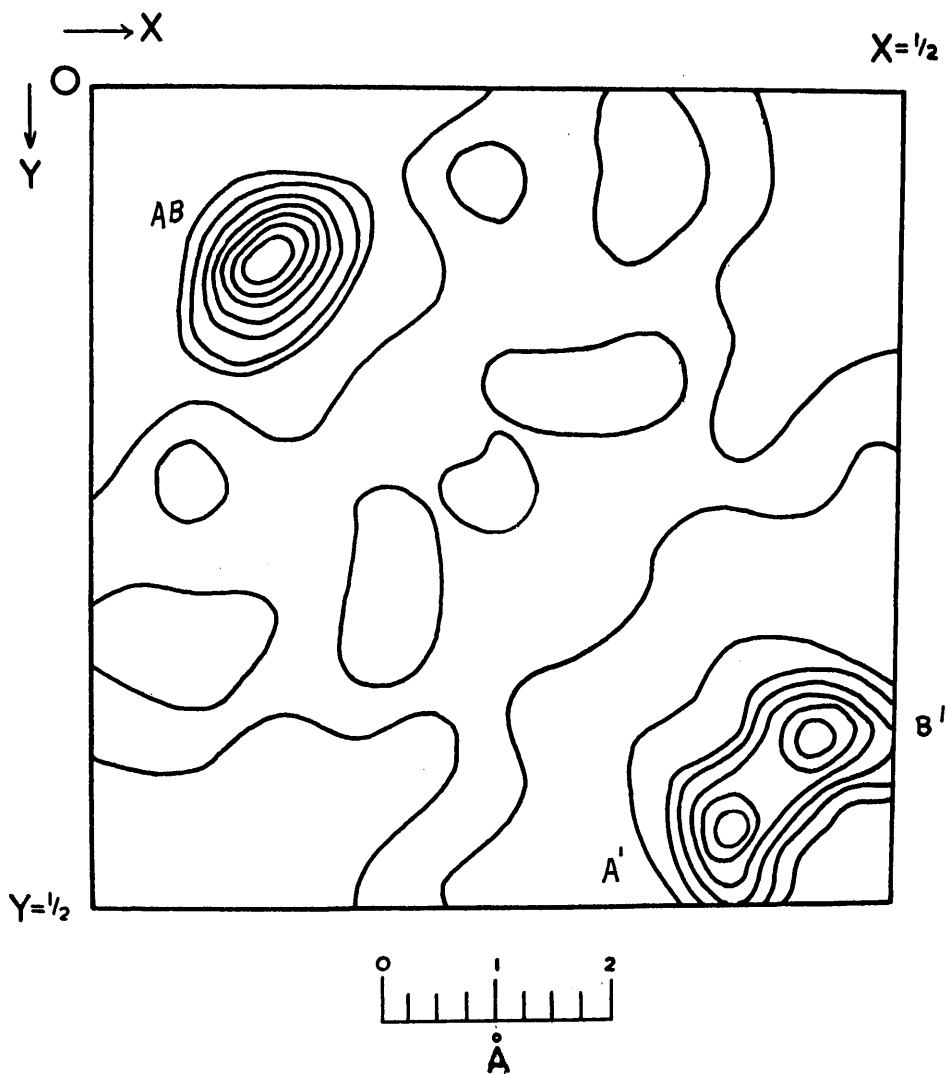


Fig. I.

The three-dimensional Patterson function section $P(U, V, \frac{1}{4})$. Contour levels are arbitrary. The peaks mentioned in the text are shown.

could be caused by bromide ions having any of the coordinates listed above. Thus the three Harker sections will provide a set of coordinates which will be consistent for all the peaks expected on these sections but they, in all probability, will not be consistent with the peaks to be expected in general positions in the body of the Patterson function. This initial set of coordinates will be referred to as the "basic set".

The section of the three-dimensional Patterson synthesis $P(U, V, \frac{1}{2})$, Fig. II, should contain peaks at $2x_1, 2y_1, \frac{1}{2}$ and $2x_2, 2y_2, \frac{1}{2}$ for bromide ions at (x_1, y_1, z_1) , Br(I), and (x_2, y_2, z_2) , Br(II), respectively. The diagonal symmetry of this section means it should contain peaks at $2y_1, 2x_1, \frac{1}{2}$ and $2y_2, 2x_2, \frac{1}{2}$ related to the first two peaks. In Fig. II the four most prominent peaks are C, C¹, D and D¹ - the first two being symmetry related to the last two. Each peak was assigned coordinates in arbitrary units. The units chosen were; the a and b - axes were divided into 40ths and the c - axis into 80ths. All peak coordinates were then expressed in these units. Peak C, Fig. II, has coordinates $(0^{40\text{ths}}, 8.6^{40\text{ths}}, 40^{80\text{ths}})$ and peak C¹ has coordinates $(3^{40\text{ths}}, 6^{40\text{ths}}, 40^{80\text{ths}})$. If we assign peak C to Br.(I), the ion then has coordinates $(0, 4.3, z_1)$ expressed in the chosen arbitrary units. Similarly if peak C¹ is assigned to Br.(II), this ion has coordinates $(1.5, 3, z_2)$. Peaks D and D¹ being related to peaks C and C¹

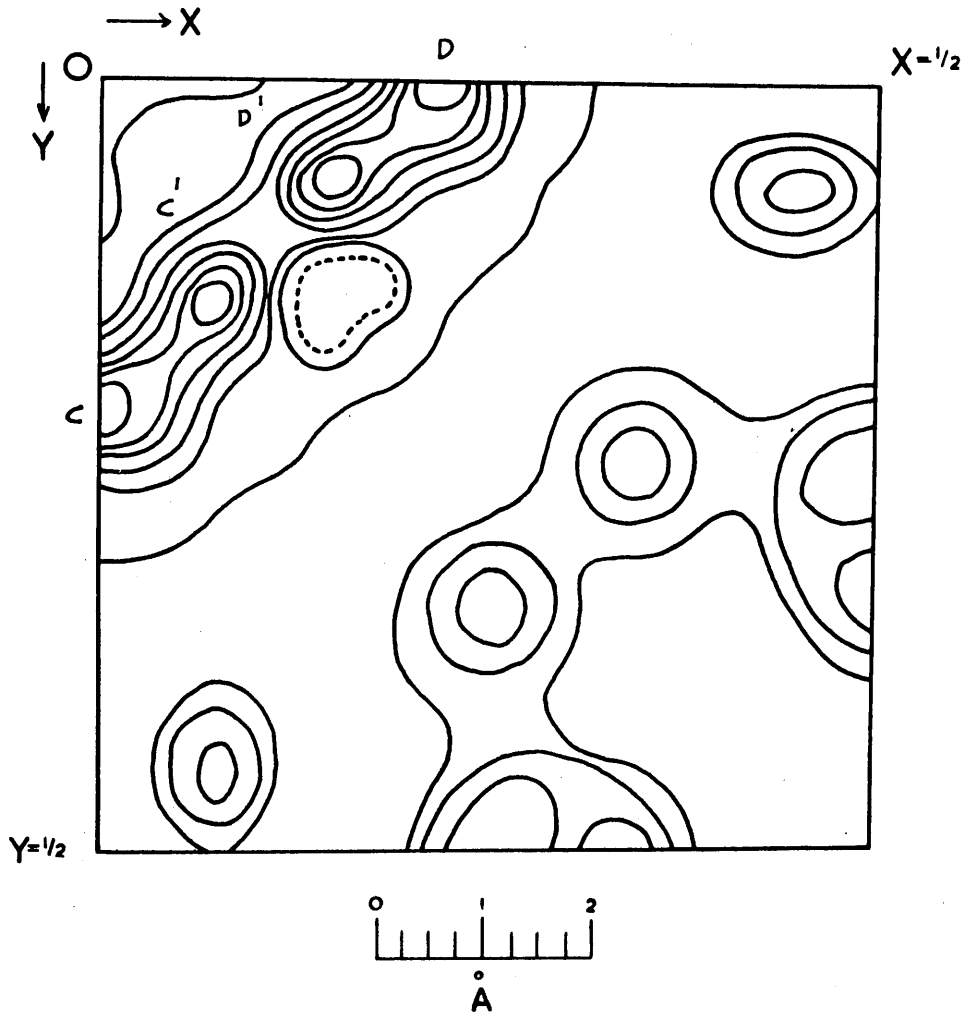


Fig. II

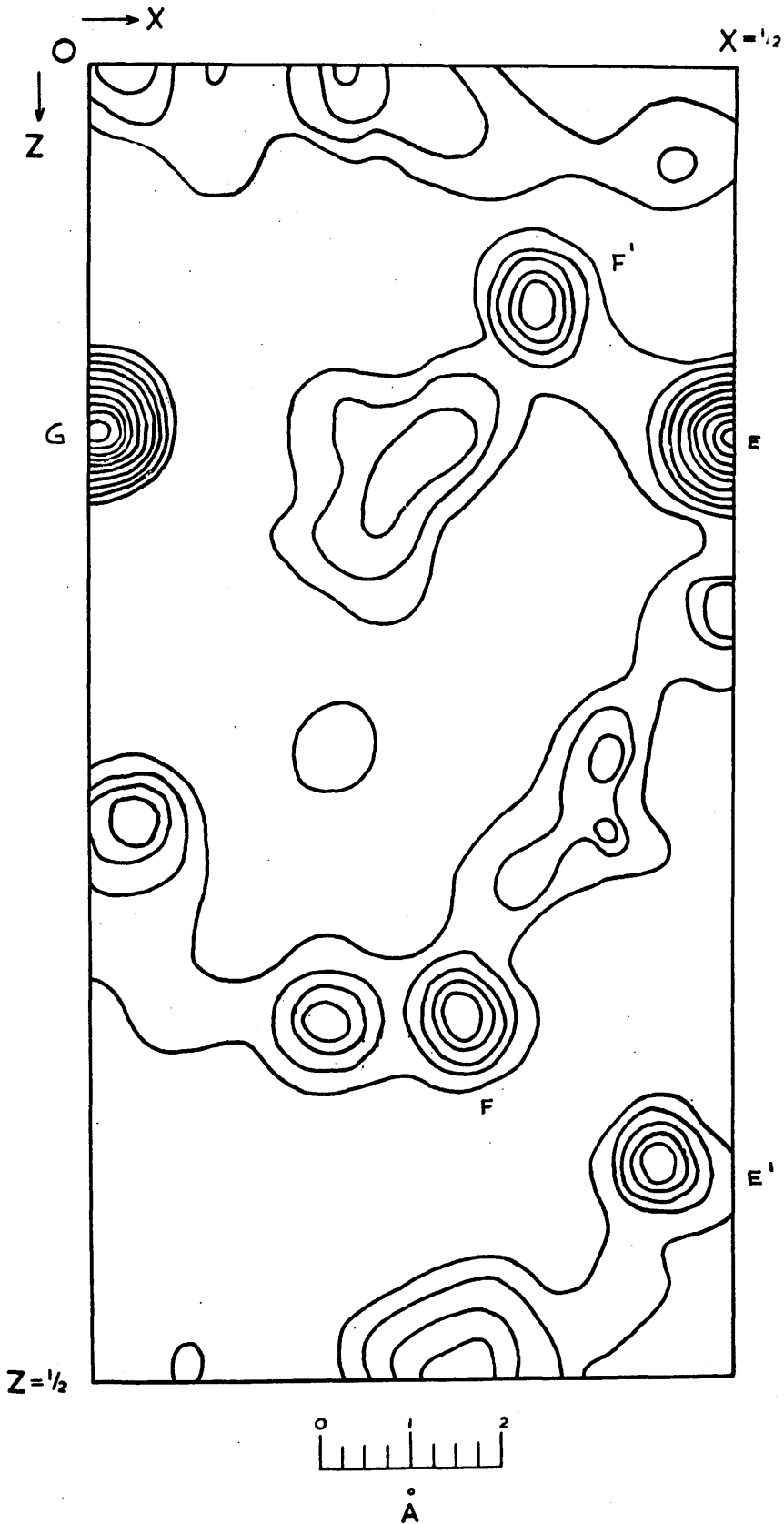
The three-dimensional Patterson function section $P(U, V, \frac{1}{2})$. Contour levels are arbitrary, the dashed contour being negative. The peaks mentioned in the text are shown.

respectively give identical x - and y - coordinates for the two Bromide ions.

The section of the three dimensional Patterson synthesis $P(U, V, \frac{1}{4})$, Fig. I. should contain four peaks at; $\frac{1}{2} + x_1 - y_1$, $\frac{1}{2} - x_1 - y_1$, $\frac{1}{4}$ and at $\frac{1}{2} + x_2 - y_2$, $\frac{1}{2} - x_2 - y_2$, $\frac{1}{4}$ and the symmetry related peaks; $\frac{1}{2} - x_1 - y_1$, $\frac{1}{2} + x_1 - y_1$, $\frac{1}{4}$ and $\frac{1}{2} - x_2 - y_2$, $\frac{1}{2} + x_2 - y_2$, $\frac{1}{4}$. The section $P(U, V, \frac{1}{4})$ only contained three prominent peaks, marked (A,B), A^1 and B^1 respectively on Fig. I. As peak (AB) is the largest peak on the section and is nearly elliptical in shape it can be assumed that the two peaks expected for one atom on this section either lie on the diagonal mirror plane or lie so close to it as to be fused into one large elliptical peak due to lack of resolution. The peak (AB) has coordinates (4.3, 4.3, 20) whilst peaks A^1 and B^1 have coordinates (15.5, 18.5, 20) and (18.5, 15.5, 20) respectively. From section $P(U, V, \frac{1}{2})$, Bromide ion I, (x_1, y_1, z_1) was assigned coordinates $x = 0$ and $y = 4.3$ units. Peak (AB) is clearly due to Bromide ion (I) and the y - coordinate for the basic set of this atom now becomes $y = 15.7$. In section $P(U, V, \frac{1}{2})$ the y - coordinate must really be $\frac{1}{2} - y$. Thus at this stage Br (I) has coordinates (0, 15.7, z_1) Calculation of the coordinates of the peaks to be expected in section $P(U, V, \frac{1}{4})$ due to Bromide ion (II), using the x , y - values obtained from $P(U, V, \frac{1}{2})$ gives peak coordinates corresponding exactly to those of peaks A^1 , and B^1 . Thus Br (II) has still coordinates (1.5, 3, z_2).

Fig. III

The three dimensional Patterson function section $P(U, \frac{1}{2}, W)$. Contour levels are arbitrary. The peaks mentioned in the text are shown.



The section of the three dimensional Patterson synthesis, $P(U, \frac{1}{2}, W)$ should contain four peaks, two per non-symmetrically related ion at; $\frac{1}{2} - 2x_1, \frac{1}{2}, \frac{1}{4} - 2z_1$; $\frac{1}{2} - 2x_2, \frac{1}{2}, \frac{1}{4} - 2z_2$; $\frac{1}{2} - 2y_1, \frac{1}{2}, \frac{1}{4} + 2z_1$; and $\frac{1}{2} - 2y_2, \frac{1}{2}, \frac{1}{4} + 2z_2$. This section is shown in Fig. III and can be seen to contain several peaks the largest of which are lettered E, F, E^1, F^1 and G respectively. Peaks E and F with respective coordinates (20, 20, 11) and (11.4, 20, 29) are due to Br (I). From these peak coordinate values, Br (I) is found to have coordinates (0, 4.3, 4.5). Clearly at this stage the y- coordinate of this ion can not be unambiguously assigned. Peak E^1 and F^1 with respective coordinates (17, 20, 33) and (14, 20, 7) belong to Br (II). From these coordinates we find that $\frac{1}{4} - 2z_2 = 33$ and $\frac{1}{4} + 2z_2 = 7$ thus making $z_2 = -6.5$. Thus these three Harker sections have given us our basic set of coordinates,

$$\text{Br I } (0, 4.3, 4.5) \quad \text{Br II } (1.5, 3, -6.5)$$

which will be used to locate $\text{Br}^+ - \text{Br}^-$ vectors in the body of the Patterson synthesis. These peaks in general positions will decide whether or not the basic set is correct.

Fig. Ref.	Vector	Coord. Found (arbitrary units)			$P(U, V, W)$ arb. units
A	$\frac{1}{2} - x_1 - y_1, \frac{1}{2} + x_1 - y_1, \frac{1}{4}$	4.3(40ths)	4.3(40ths)	20(80ths)	60
C	$2x_1, 2y_1, \frac{1}{2}$	0	8.6	40	54
E	$\frac{1}{2} - 2x_1, \frac{1}{2}, \frac{1}{4} - 2z_1$	20	20	11.0	112
F	$\frac{1}{2} - 2y_1, \frac{1}{2}, \frac{1}{4} + 2z_1$	11.4	20	29.0	44

Fig. Ref.	Vector	Coord. Found (Arbitrary Units)			P(U,V,W) Arb. units
	$y_1+x_1, x_1+y_1, \frac{1}{2}+2z_1$	15.7	15.7	31.0	35
	$y_1-x_1, -x_1+y_1, 2z_1$	15.7	15.7	9.0	39
A ¹	$\frac{1}{2}-x_2-y_2, \frac{1}{2}+x_2-y_2, \frac{1}{4}$	15.5	18.5	20	51
C ¹	$2x_2, 2y_2, \frac{1}{2}$	3.0	6.0	40	50
E ¹	$\frac{1}{2}-2x_2, \frac{1}{2}, \frac{1}{4}-2z_2$	17.0	20	33.0	41
F ¹	$\frac{1}{2}-2y_2, \frac{1}{2}, \frac{1}{4}+2z_2$	14.0	20	7.0	42
	$y_2+x_2, x_2+y_2, \frac{1}{2}+2z_2$	1.5	1.5	27.0	54
	$y_2-x_2, -x_2+y_2, 2z_2$	4.5	4.5	13.0	54
G	$x_1+x_2, y_1+y_2, \frac{1}{2}+z_1-z_2$	18.5	1.3	11.0	109
	$x_2-x_1, y_2-y_1, z_2-z_1$	18.5	7.3	29.0	47
	$y_1+x_2, x_1, +y_2, \frac{1}{2}-z_1, -z_2$	5.8	17.0	2.0	44
	$x_2-y_1, y_2-x_1, z_2+z_1$	3.0	17.0	38.0	41
	$\frac{1}{2}-x_2+y_1, \frac{1}{2}-y_2-x_1, \frac{1}{4}+z_2-z_1$	17.2	3.0	31.0	40
	$\frac{1}{2}-y_2+y_1, \frac{1}{2}-x_2-x_1, \frac{1}{4}-z_2-z_1$	12.7	1.5	18.0	69
	$\frac{1}{2}-x_2+x_1, \frac{1}{2}-y_2-y_1, \frac{1}{4}+z_2+z_1$	1.5	18.7	22.0	35
	$\frac{1}{2}-y_2+x_1, \frac{1}{2}-x_2+y_1, \frac{1}{4}-z_2+z_1$	3.0	17.2	9.0	36

The table above lists all the vectors to be expected in the three-dimensional Patterson synthesis; the coordinates found (in arbitrary units), and the peak value of P(UVW) in arbitrary units. The reference letters used in Figs. I, II and III are shown opposite

the appropriate vectors. It is seen that these are two vectors per set of symmetrically related bromide ions and eight vectors between non-symmetrically related bromide ions in the body of the map.

Using the basic set of coordinates for Br (I) and Br (II) these general peaks were assigned coordinates then looked for in the body of the Patterson map. Of the twelve vectors, only four were found in the expected positions. Clearly the basic set of coordinates was not correct. Accordingly, the whole Patterson map was searched for vector peaks with values of $P(UVW)$ greater than 30 (in arbitrary units). These peaks were assigned coordinates. In all only twenty vectors satisfying these conditions were found and of these, sixteen consisted of two symmetry related sets of eight vectors. One set of eight vectors was rejected leaving twelve vectors in all - the number expected to be found. The final sets of coordinates were found by solving the twenty simultaneous equations provided by the vectors listed above to give two sets of Bromide ion coordinates which would agree with the calculated and observed positions of any given $Br^- - Br^-$ vector. The final sets of coordinates found in this manner were;

$$Br\ I\ (20, -4.5, 4.5) \quad Br\ II\ (38.5, 3, 33.5)$$

These coordinates were related to the basic set by the symmetry of the Patterson function.

In the Harker section $P(U, \frac{1}{2}, W)$, Fig. III, there is a large vector $\{ P(U, V, W) = 109 \}$ which is marked G. This vector is caused by non-symmetrically related bromide ions and is the vector; $x_1 + x_2, y_1 + y_2, \frac{1}{2} + z_1 - z_2$. The observed and calculated positions of this vector are $(0, 20, 11)$ and $(18.5, 1.3, 11)$ respectively. The observed position has its x- and y- coordinates lying on the mirror planes $U = 0$ and $v = \frac{1}{2}$. This vector occurs twice in the map the other observed position being $(20, 0, 11)$ with x- and y- coordinates on $U = \frac{1}{2}$ and $V = 0$. Clearly this large peak arises from the fusion of four smaller peaks near the intersecting mirror planes due to lack of resolution.

3. (5) STRUCTURE DETERMINATION

The ratio $\sum f_H^2 / \sum f_L^2$ for chimonanthine dihydro-bromide is 2.41 indicating that the first set of phasing calculations based on the positions of the bromide ions alone should give a reasonable approximation to the correct phases.

The Fourier programme devised by Dr. J.S. Rollett for the DEUCE computer cannot conveniently be used for crystals belonging to the space group $P4_12_12$. The high symmetry of this space group requires very large computing time to calculate a full three-dimensional synthesis. It was therefore advisable to change the space group to one of lower symmetry. At the suggestion of

Dr. T. A. Hamor, it was observed that $P4_12_12$ could be transferred to the orthorhombic space group $P2_12_12_1$. This arises on account of $P4_12_12$ having 222 as a sub-point group to its point group 422. $P2_12_12_1$ contains four asymmetric units per unit cell whereas $P4_12_12$ contains eight per unit cell. Thus, this transformation will require two molecules of chimonanthine dihydrobromide to comprise the new asymmetric unit. It was also necessary to include symmetrically equivalent reflections in all calculations having $P2_12_12_1$ as space group. In the three dimensional Patterson synthesis, 2093 independent terms were used. The extra $|F_0|$ values for the Fourier calculations were obtained by preparing a set of $|F_0|$ values from the original 2093 by interchanging the h and k indices but leaving the value of $|F_0|$ the same. These two sets of data together make up the data to be used for all future Fourier calculations. In preparing the extra data, reflections with indices of the type $(h, k = h, l)$ were not treated in this manner. This resulted in 4003 structure amplitudes for inclusion in the Fourier calculations. If under these new conditions the origin is changed to $(\frac{1}{2}, 0, \frac{3}{8})$ the space group effectively becomes $P2_12_12_1$.

The first set of phasing calculations was carried out using the coordinates of four Bromide ions. Two of these Bromide ions had coordinates assigned to them from the Patterson synthesis. The other two were related to the first two bromide

ions by tetragonal symmetry. If (x, y, z) is a bromide ion from the Patterson synthesis, then its symmetry related bromide ion has coordinates $(y, x, -z)$. An equal isotropic temperature factor, $B_{\theta} = 4.5 \text{ \AA}^2$, was assumed for each bromide ion. The average discrepancy between observed and calculated structure factors was 39.9%. A three dimensional Fourier map was computed using the phases obtained and all 4003 $|F_o|$ values. This map was computed over one quarter of the unit cell volume and drawn out on stacked glass sheets, parallel to (001), to give a three-dimensional effect. The complete structure of the molecule could clearly be seen in this map. As expected both molecules in the asymmetric unit were identical in every respect as they were related to each other by tetragonal symmetry. The structure found was seen to be the same as one of the two structures proposed by Hodson et al (48), a fact which aided the structure determination considerably. With the exception of four atoms out of the 56 atoms (excluding hydrogen) in the asymmetric unit, all atoms had an electron density greater than $2 e \text{ \AA}^{-3}$. These 52 regions of high electron density were the only ones present reaching such a value. Thus the determination of the structure at this early stage was straight-forward.

An improved set of phases was obtained in the next cycle of structure factor calculations. This cycle had the coordinates

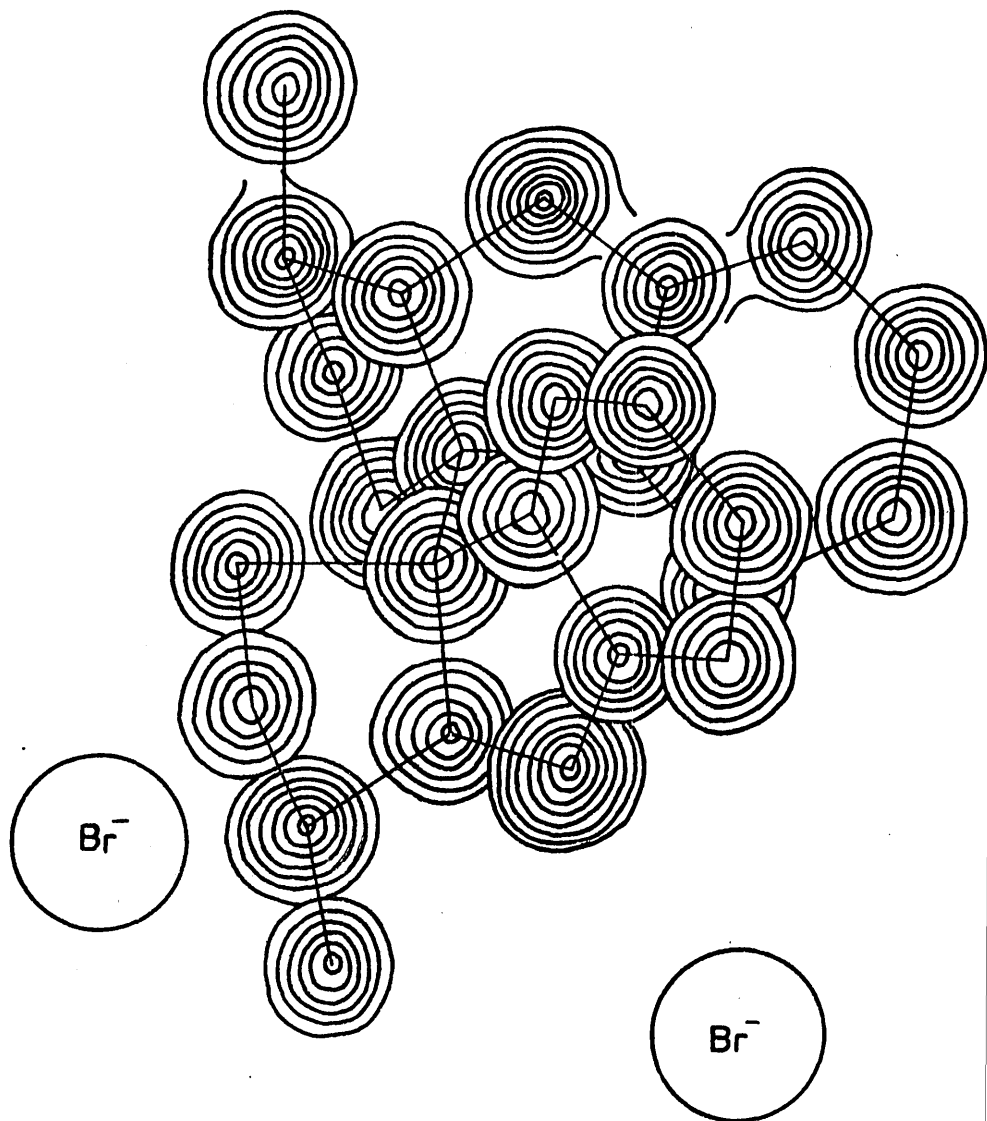
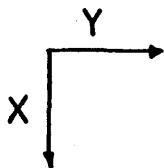


Fig. IV The third electron-density distribution for chimonanthine dihydrobromide. The superimposed contour sections are drawn parallel to (001). Contour level $1e^{-3}$ except around the bromide ions, which are shown as open circles. The first contour level has been omitted.

of all 56 atoms in the asymmetric unit included. Except for the four bromide ions, all other atoms were included as carbon atoms and each atom was assigned an isotropic temperature factor of $B_{\theta} = 4.5 \text{ \AA}^2$. The value of R, the discrepancy, fell from 39.9% in the previous cycle to 29.3%. A second Fourier synthesis was computed using the new phases and 4003 terms. On drawing up this map as before, it could be seen that both molecules in the asymmetric unit were now clearly resolved. Further, very few areas of positive electron density, other than those due to atomic locations, remained.

From a consideration of peak heights it was now possible to determine which atoms were nitrogen atoms. Accordingly a third cycle of structure factors was computed including four bromide ions, eight nitrogen and forty-four carbon atoms. Each atom was assigned an isotropic temperature factor $B_{\theta} = 4.0 \text{ \AA}^2$. The average discrepancy was lowered to 23.2%. The third Fourier synthesis based on these phases by now contained very few areas of spurious electron density. This map is shown in Figure IV. as superimposed contour sections drawn parallel to (001). The corresponding atomic arrangement is given in Figure V.

3. (6) REFINEMENT.

Using the atomic coordinates obtained from the third

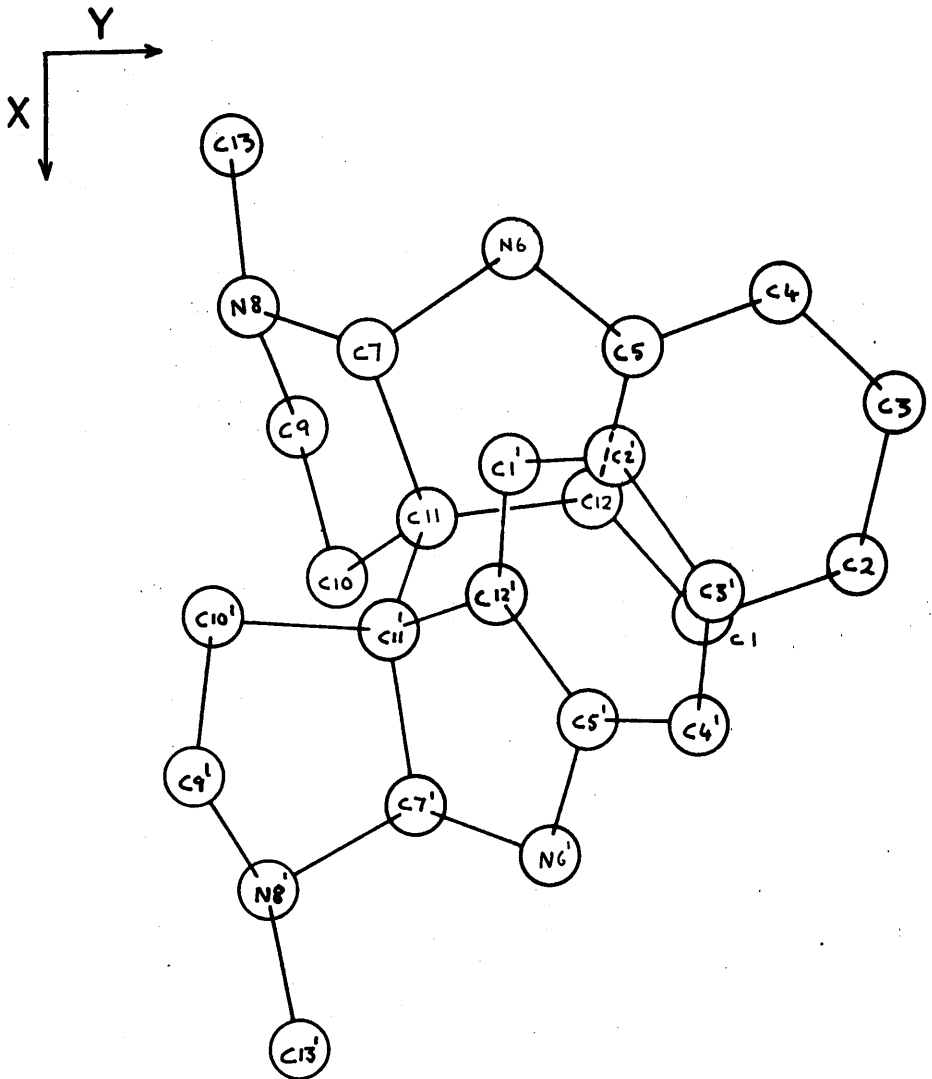


Fig. V.

The arrangement of atoms in the molecule corresponding to Fig.

electron-density distribution, a fourth cycle of structure factors was calculated. Once more each atom was assigned an isotropic temperature factor of $B_{\text{O}} = 4.0 \text{ \AA}^2$. The discrepancy, R, was lowered to 21.4%. Further refinement of the atomic coordinates was carried out by computing both $|F_{\text{O}}|$ and $|F_{\text{C}}|$ Fourier maps. The two sets of atomic coordinates obtained from these maps were used to correct the coordinates used in the fourth structure-factor cycle, for termination-of-series errors.

It was now felt that further refinement of the structure by Fourier methods would not be very effective. Accordingly, it was decided to refine the positional and thermal parameters by the method of least squares. The space group of the crystal was changed back to $P4_12_12$ by the reverse of the process outlined in section (3.5). Two cycles of least-squares calculations were carried out using the DEUCE programme of Dr. J.S. Rollett (32), which refines three positional and six thermal parameters. The first cycle used the coordinates which had been corrected for termination-of-series errors. After these two cycles, the value of R stood at 17.1%.

Refinement was completed by the calculation of a final set of structure factors, each atom having the anisotropic temperature factors calculated in the second cycle of least squares. The final value of R, calculated over 2093 observed structure factors was 14.9%.

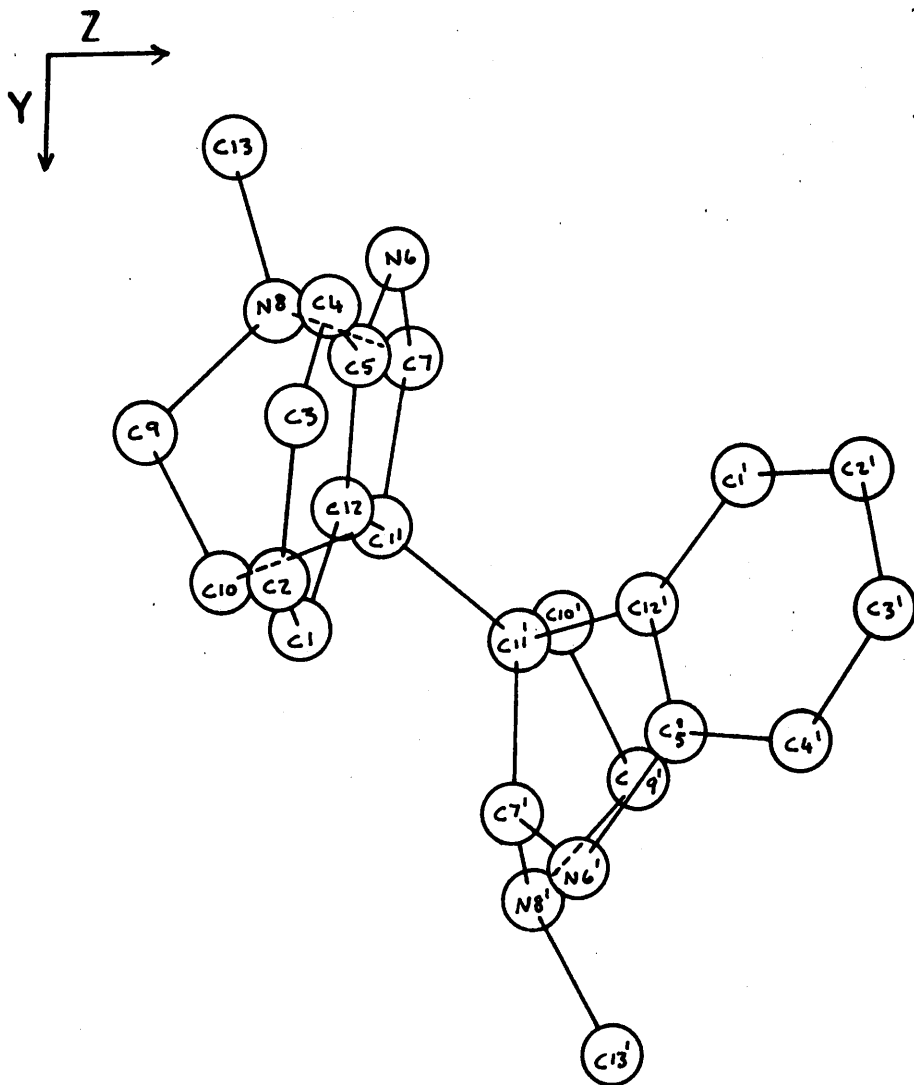


Fig. VI.

The arrangement of atoms in the molecule as viewed in projection along the *a* - axis.

The theoretical atomic scattering factors employed in the structure-factor calculations were those of Berghuis et al (30) for carbon and nitrogen, and the Thomas-Fermi (31) values for bromine (a bromide ion scattering curve was not employed). The course of the analysis is given in Table I. The weighting scheme used in the least-squares refinement was as follows; $\sqrt{w} = |F_o| / |F^*|$ if $|F_o| < |F^*|$; $\sqrt{w} = |F^*| / |F_o|$ if $|F_o| > |F^*|$ where $|F^*|$ is constant. It was taken equal to the average value of $|F_o|$ (about 20).

3. (7) RESULTS.

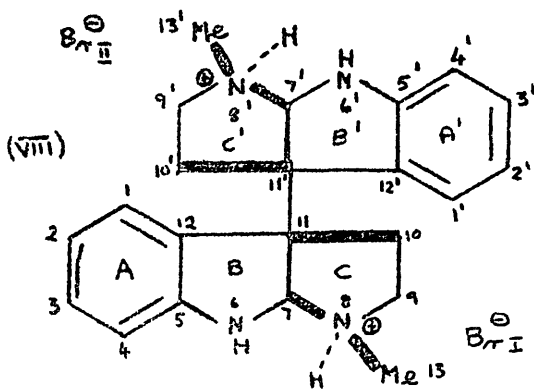
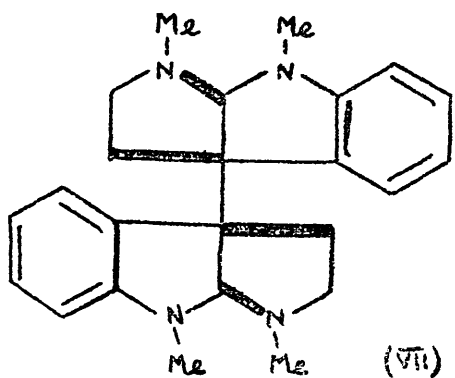
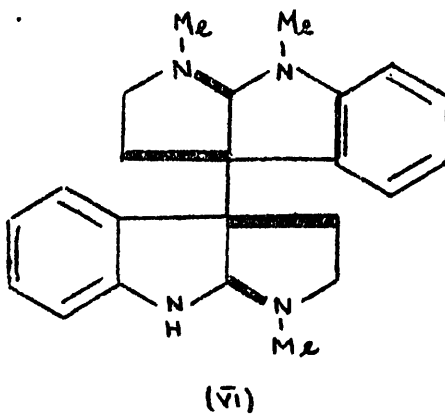
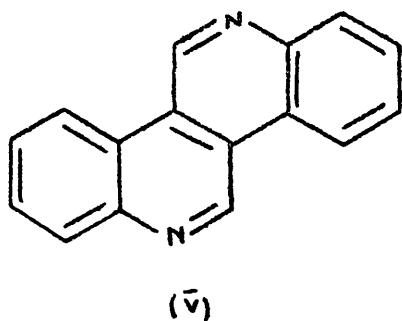
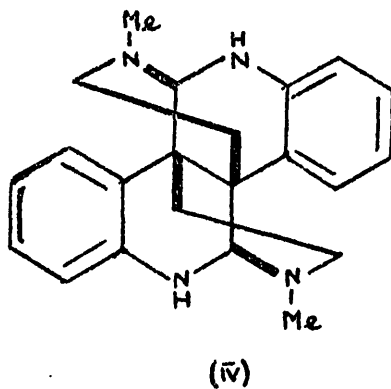
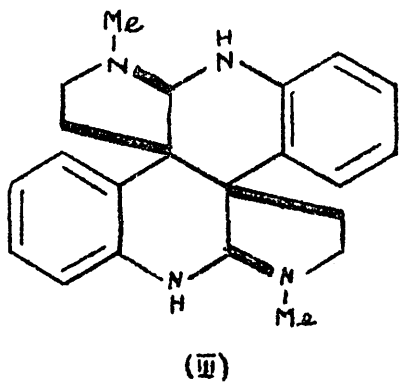
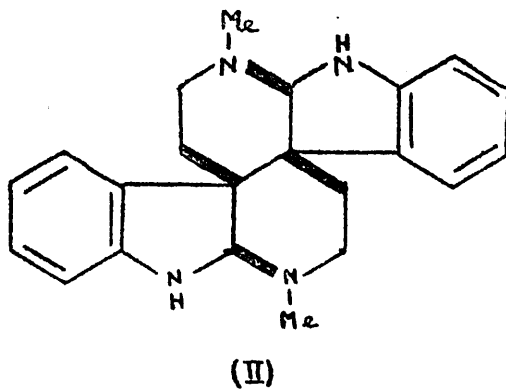
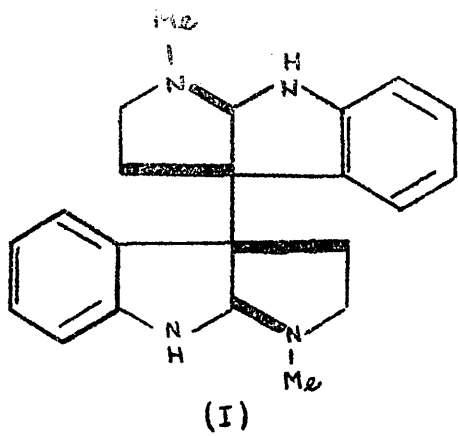
The final atomic coordinates are listed in Table II and the anisotropic temperature factors, b_{ij} , listed in Table III. Table IV contains the final values of F_o , F_c and α for the 2093 observed independent reflections. The inter-atomic distances and valency angles calculated from the final atomic coordinates are given in Tables V - VIII. The standard deviations of the final coordinates were estimated in the usual manner from the least squares residuals and are shown in Table IX. The average estimated standard deviation in the coordinate of a carbon atom is 0.06 Å, of a nitrogen atom 0.045 Å and of a bromide ion 0.006 Å. From these results the average estimated standard deviation of a carbon-carbon bond is about 0.08 Å, of a carbon-nitrogen bond is about 0.07 Å and of a nitrogen bromide ion bond of 0.045 Å. The average estimated standard deviation of

a valency angle is about 4° .

Figure VI shows the atomic arrangement as viewed in projection down the a - axis. The arrangement of the molecules in the unit cell is shown in Figure VII as seen in projection down the b - axis. The bromide ions are shown as large open circles and the nitrogen atoms as small black circles. Distances between bromide ions and nitrogen atoms are printed beside the broken line linking the atoms.

3. (8) DISCUSSION

Shortly after commencing this analysis, Hodson et al (48) on the basis of chemical evidence suggested four structures which could be taken into consideration for the structure of chimonanthine (I) - (IV). However, of these (IV) was recently assigned to calycanthine (51, 52), and Hofmann degradation indicated that (III) was also unlikely. Zinc dehydrogenation of calycanthine, which has a preformed quinoloquinoline skeleton, gives calycanine (53), (V), (52) in 8% yield. Chimonanthine on being treated similarly gave only traces of calycanine (< 0.1%) lending support to (I) or (II) being the correct structure. Hodson et al (48) also showed that the alkaloid folicanthine (49) is almost certainly bis - N(a) - methylchimonanthine. More recently (54) the alkaloid calycanthidine was proved to represent the intermediate stage in the methylation of chimonanthine to folicanthine. Chemical evidence does not



distinguish structures (I) and (II) but support for (I) as being the correct structure came from the mass-spectral observation that the molecule exhibits easy halving. Folicanthine and calycanthidine were shown to behave in a similar manner.

The final results of this structure analysis have established the constitution and stereochemistry (apart from absolute configuration) of chimonanthine to be as in (I). It follows that calycanthidine and folicanthine must be (VI) and (VII) respectively. Chimonanthine dihydrobromide is therefore (VIII) and is given with the atomic numbering system used in the text and tables of results.

The chimonanthine molecule consists of two chemically and stereochemically identical halves of formula $(C_{11} H_{13} N_2 \cdot H Br)$. Rings C and C¹ are fused cis- to rings B and B¹ respectively. The two halves of the molecule can in theory rotate freely about the single bond, C(11) - C(11¹). In the crystal the molecule adopts a cis- conformation in which the benzene rings are inclined at an angle of 60°. The mean molecular plane calculated by the method of Schomaker et al (47) through the atoms of benzene ring A has equation;

$$0.133 X + 0.156 Y + 0.972 Z - 14.105 = 0$$

where X, Y, Z are coordinates expressed in Angstrom units referred to orthogonal axes a, b and c. This ring is planar to

within 0.013 \AA . Similarly the mean plane through the atoms of benzene ring A^1 is,

$$0.352 X - 0.697 Y + 0.625 Z - 9.512 = 0$$

and the ring is planar to within 0.019 \AA . The equation of the mean plane through atoms C1, C2, C3, C4, C5, N6, C7, C11, C12 is;

$$0.131X + 0.199 Y + 0.971Z - 14.097 = 0$$

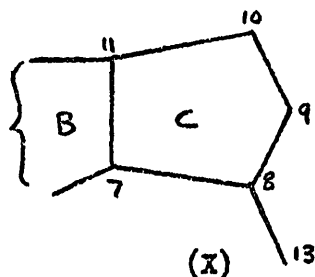
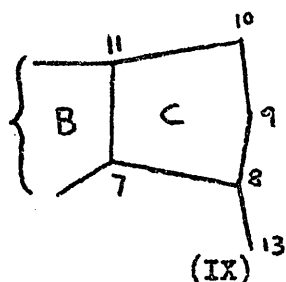
and is planar to within 0.017 \AA . The equation of the mean plane through atoms $C1^1$, $C2^1$, $C3^1$, $C4^1$, $C5^1$, $N6^1$, $C7^1$, $C11^1$, $C12^1$ is;

$$0.313 X - 0.679 Y + 0.664 Z - 9.810 = 0$$

and is planar to within 0.07\AA . The planes through the atoms of rings B and B^1 are planar to within 0.017 \AA and 0.071 \AA respectively. Thus it can be seen that rings A and B and rings A^1 and B^1 are, within experimental error planar as one would expect. Table X gives the deviations of atoms from various planes in the molecule.

However, rings C and C^1 can in no way be considered planar. The mean molecular planes through these rings are only planar to within 0.162 \AA and 0.195\AA respectively. In these rings, atoms C9 and $C9^1$ respectively lie out of the plane so that the rings adopt the so-called "envelope" configuration. In chimonanthine the adoption of this configuration is very pronounced and is probably caused by steric repulsion between atoms N6 and C13 in ring C and atoms $N6^1$ and $C13^1$ in ring C^1 .

The mean plane calculated through atoms C13, N8, C9, C10 of ring C is planar to within 0.057 \AA . This high degree of planarity of these atoms is unexpected, but is due to the ring having a folded appearance which when viewed from above resembles (IX) not the more usual appearance (X)



The angle between the mean plane through atoms C7, N8, C10, C11 and the plane through C13, N8, C9, C10 is 72° . In ring C¹ the mean plane through atoms C13¹, N8¹, C9¹, C10¹ is planar to within 0.096 \AA and is inclined at an angle of 64° to the plane through atoms C7⁸, N8¹, C10¹, C11¹. In ring C, as atom C9 does not lie in the usual configuration but is forced to lie nearer ^{the} benzene ring, the methyl group at C13 is forced further away from atom N6. Measurement of a standard Dreiding model gave a C1 - C9 distance of 4.45 \AA whereas the value found in the molecule is 4.07 \AA . The N6 - C13 distance observed is 2.91 \AA whilst the model gives a value of 2.55 \AA . Below is a list of non-bonded distances compared with the corresponding distances in a standard model, which illustrate the configurations of rings C and C¹.

Ring C	Observed	Measured	Observed	Ring C ¹
C1 - C9	4.07	4.45	3.89	C1 ¹ - C9 ¹
C5 - C9	3.49	3.90	3.44	C5 ¹ - C9 ¹
C5 - C13	3.99	3.60	3.80	C5 ¹ - C13 ¹
N6 - C9	3.19	3.40	3.16	N6 ¹ - C9 ¹
N6 - C13	2.91	2.55	2.72	N6 ¹ - C13 ¹
C9 - C12	3.19	3.45	3.04	C9 ¹ - C12 ¹
C10 - C13	3.75	3.60	3.80	C10 ¹ - C13 ¹
C11 - C13	3.77	3.60	3.77	C11 ¹ - C13

The average length of the carbon-carbon aromatic bond is 1.39 Å which agrees favourably with the length of 1.395 Å in benzene. The individual values vary from 1.34 Å to 1.44 Å, a variation which is not significant when the standard deviation of 0.03 Å of an aromatic bond length is considered. The average carbon-carbon single bond length between sp³- hybridised carbon atoms is 1.54 Å, in good agreement with the accepted value in diamond of 1.545 Å. The average carbon-carbon single bond between sp²- and sp³- hybridised atoms is 1.52 Å again in good agreement with the accepted value of 1.525 Å (55).

The carbon-nitrogen bond-lengths show a greater spread, varying from 1.36 Å to 1.57 Å. However, these are not all of the same type. Three types are present, carbon (sp²- hybridised) - nitrogen, carbon (sp³- hybridised) - nitrogen and carbon (sp³- hybridised) - N⁺. The carbon (sp²- hybridised) - nitrogen bond length has been measured in acetanilide (56) as 1.33 Å, in

2 - chloro - 4 - nitroaniline (57) as 1.37 Å, in calycanthine dihydrobromide dihydrate (51) as 1.40 Å, in echitamine bromide methanol solvate (58) as 1.38 Å and in ibogaine hydrobromide (59) as 1.40 Å. The average value found in chimonanthine of 1.43 Å agrees reasonably well with most of these values. The average carbon (sp^3) - nitrogen bond length at 1.44 does not differ significantly from, the accepted value of 1.47 Å (55), the calycanthine (51) value of 1.44 Å and the echitamine (58) value at 1.43 Å.

In chimonanthine there are six C (sp^3) - N⁺ bonds varying from 1.41 Å to 1.57 Å with an average value of 1.50 Å. This variation in length exceeds the standard deviation of 0.075 Å of this type of bond. However, wide variations in the length of this bond in molecules containing several such bonds are frequently observed. Calycanthine (51) has six such bonds which vary from 1.43 Å - 1.56 Å (average 1.50 Å). The values 1.51 Å in d 1 alphaprodine hydrochloride (60), 1.503 Å in (+) - Dos - (oxymethylene) - lycoctonine hydriodide monohydrate (61), 1.506 Å in d - methadone hydrobromide (62) suggest that the average value in chimonanthine is reasonably good.

The average bond angle of the two benzene rings in chimonanthine is 120°, equal to the expected value. Rings B and B¹ have an average value of 107.6° whilst rings C and C¹ have a value of 104°. The alkaloid echitamine (58) has a ring system

almost identical to the ring systems ABC and $A^1B^1C^1$ in chimonanthine. In echitamine, the equivalent of rings B and B^1 has an average valency angle of 108° and the equivalent of rings C and C^1 has an average valency angle of 106° . In five membered rings average valency angles consistently smaller than tetrahedral have been reported, in hydroxy - L - proline (106°), (63), isoclovene hydrochloride (105°), (64), himbacine hydrobromide (105°), (65) and clerodin bromolactone (106°), (43). These values are consistent with the non-planarity and consequent angle deformation in cyclopentane (66). When a five-membered ring is fused to an aromatic ring (as in chimonanthine) or incorporates a double bond the average valency angle is slightly larger than in the above examples. In bromogeigerin acetate (67) the average valency angle in the cyclopentenone ring is 107° , in 5 - bromogriseofulvin the equivalent angle is 108° (68). The value of 107.6° in chimonanthine is consistent with these results. The average tetrahedral bond angle in chimonanthine is 110° in favourable agreement with the accepted value of $109^\circ 28'$.

In the crystal the positively charged molecules and the bromide ions are held together both by the normal ionic forces and hydrogen bonds. The nitrogen atom-bromide ion hydrogen bonds involve the indole nitrogen atom and N^+ atom in one half of the molecule the corresponding nitrogen atoms in the other half of the molecule not being bonded in this fashion. Each of the

crystallographically independent bromide ions has two contacts

4.00\AA with two nitrogen atoms in different molecules. Bromide (I) has contacts of 4.00\AA and 3.43\AA with nitrogen atoms of the type N8 and N6^1 respectively whilst bromide (II) has contacts of 3.86\AA and 3.18\AA with nitrogen atoms of the type N6 and N8^1 respectively. These contacts are shown in Fig. VII which shows the contents of the unit cell in projection down the b - axis. The Br (I) - N6^1 distance of 3.43\AA corresponds to a weak hydrogen bond and is similar to the values of $\text{NH} - \text{Br}^-$ distances in echitamine bromide methanol solvate (58), calycanthine dihydrobromide dihydrate (51), ibogaine hydrobromide (59), and in cystine dihydrobromide (69). The Br (II) - N8^1 distance of 3.18\AA corresponds to a hydrogen bond and is in agreement with the equivalent distances in codeine hydrobromide (3.17\AA) (70), strychnine hydrobromide (3.17\AA) (71), and ibogaine hydrobromide (3.23\AA) (59). The angles $\text{C7}^1 - \text{N8}^1 - \text{Br(II)}$; $\text{C9}^1 - \text{N8}^1 - \text{Br(II)}$, $\text{C13}^1 - \text{N8}^1 - \text{Br(II)}$ are 116° , 105° , 114° respectively indicating the hydrogen bond lies tetrahedrally along the $\text{H}^+ - \text{N}$ bond. The closest carbon-bromide ion distance is 3.76\AA between C4^1 (vi) and Br (I) a value greater than the average value of 3.62\AA found in similar compounds. The closest approach between two chimonanthine

molecules is 3.26\AA between C4 of the reference molecule (x,y,z) and C4 of the molecule related to it by the tetragonal symmetry operation (y,x,-z).

TABLE I
COURSE OF ANALYSIS

<u>Operation</u>	<u>Date Used</u>	<u>Atoms Included</u>	<u>R%</u>	<u>Space Group</u>
3D Patterson Synthesis	2093	-	-	P4 ₁ 2 ₁ 2
1st 3D F _o Synthesis	4003	4 Br̄	39.9	P2 ₁ 2 ₁ 2 ₁
2nd 3D F _o	4003	4 Br̄ + 52C	29.3	"
3rd 3D F _o	4003	4 Br̄ + 8N + 44C	23.2	"
4th 3D F _o and 1st 3D F _o	4003	4 Br̄ + 8N + 44C	21.4	"
1st Least Squares Cycle	2093	2 Br̄ + 4N + 22C	19.1	P4 ₁ 2 ₁ 2
2nd " "	2093	2 Br̄ + 4N + 22C	17.1	P4 ₂ 2 ₁ 2
5th 3D F _o Synthesis	4003	4 Br̄ + 8N + 44C	14.9	P2 ₁ 2 ₁ 2 ₁

77.

TABLE IIATOMIC CO-ORDINATES(Origin of co-ordinates as in "International Tables")

<u>Atom</u>	<u>x/a</u>	<u>y/b</u>	<u>z/c</u>
C ₁	0.7967	0.4854	0.4351
C ₂	0.7670	0.5813	0.4280
C ₃	0.6668	0.6053	0.4330
C ₄	0.6007	0.5361	0.4435
C ₅	0.6302	0.4449	0.4527
C ₇	0.6303	0.2788	0.4689
C ₉	0.6774	0.2363	0.3850
C ₁₀	0.7690	0.2581	0.4115
C ₁₁	0.7340	0.3136	0.4600
C ₁₂	0.7232	0.4192	0.4479
C ₁₃	0.5073	0.1977	0.4127
C ₁ '	0.7016	0.3649	0.5779
C ₂ '	0.6986	0.4311	0.6161
C ₃ '	0.7823	0.4912	0.6248
C ₄ '	0.8641	0.4812	0.5988
C ₅ '	0.8582	0.4132	0.5578
C ₇ '	0.9096	0.3051	0.5048
C ₉ '	0.8899	0.1697	0.5449
C ₁₀ '	0.7932	0.1830	0.5187
C ₁₁ '	0.8022	0.2895	0.5057

TABLE II (Continued)

<u>Atom</u>	<u>x/a</u>	<u>y/b</u>	<u>z/c</u>
C ₁₂ '	0.7815	0.3584	0.5487
C ₁₃ '	1.0587	0.2324	0.5380
N ₆	0.5710	0.3692	0.4647
N ₈	0.6039	0.2065	0.4268
N ₆ '	0.9423	0.3873	0.5262
N ₈ '	0.9607	0.2134	0.5122
BrI	0.4868	0.1069	0.5537
BrII	0.9715	0.0758	0.4173

TABLE IIIANISOTROPIC TEMPERATURE-FACTOR PARAMETERS ($b_{ij} \times 10^5$)

	b_{11}	b_{22}	b_{33}	b_{12}	b_{23}	b_{13}
C_1	661	663	182	-17	10	-700
C_2	899	627	182	-92	- 2	-141
C_3	638	553	174	-60	-63	- 46
C_4	965	681	106	-243	- 9	229
C_5	551	705	143	-51	-101	921
C_7	453	710	174	-58	44	-299
C_9	619	324	104	85	179	- 73
C_{10}	534	457	124	-39	- 51	912
C_{11}	421	1083	217	-305	-44	-636
C_{12}	592	745	175	175	115	703
C_{13}	892	607	197	2	-4	933
C_1'	961	274	177	-11	63	82
C_2'	891	885	216	-79	-49	-507
C_3'	730	286	139	69	-172	-869
C_4'	468	422	196	-247	103	400
C_5'	886	753	85	-9	-216	287
C_7'	675	232	116	46	48	-195
C_9'	802	858	263	13	-475	434
C_{10}'	296	564	183	-199	82	256
C_{11}'	577	566	191	5	131	294
C_{12}'	536	552	178	-152	18	429

TABLE III (Contd.)

	\underline{b}_{11}	\underline{b}_{22}	\underline{b}_{33}	\underline{b}_{12}	\underline{b}_{23}	\underline{b}_{13}
C_{13}^1	266	659	123	- 26	- 18	301
N_2	415	593	182	-151	-64	155
N_8	487	736	101	-332	- 57	396
N_6^1	639	606	135	2	81	254
N_8^1	541	505	128	180	-80	119
Br_I	681	735	209	-74	-6	-89
Br_{II}	694	667	192	-131	-49	418

Table IV.

Measured and calculated valves of the structure factors.

Table with multiple columns (h, k, l, |Fp|, |Fc|, etc.) containing numerical data for various crystallographic reflections. The table is organized into several groups, each with its own set of column headers. The data includes measured values and calculated values for structure factors, often with associated error bars or standard deviations.

MOLECULAR DIMENSIONSInteratomic Distances (Å) and AnglesTABLE V.Intramolecular bonded Distances

$C_1 - C_2$	1.41	$C_1' - C_2'$	1.38
$C_2 - C_3$	1.44	$C_2' - C_3'$	1.44
$C_3 - C_4$	1.36	$C_3' - C_4'$	1.34
$C_4 - C_5$	1.35	$C_4' - C_5'$	1.45
$C_5 - C_{12}$	1.35	$C_5' - C_{12}'$	1.34
$C_{12} - C_1$	1.42	$C_{12}' - C_1'$	1.36
$C_5 - N_6$	1.38	$C_5' - N_6'$	1.49
$N_6 - C_7$	1.51	$N_6' - C_7'$	1.36
$C_7 - C_{11}$	1.54	$C_7' - C_{11}'$	1.51
$C_{11} - C_{12}$	1.52	$C_{11}' - C_{12}'$	1.52
$C_7 - N_8$	1.55	$C_7' - N_8'$	1.48
$N_8 - C_9$	1.57	$N_8' - C_9'$	1.45
$C_9 - C_{10}$	1.49	$C_9' - C_{10}'$	1.53
$C_{10} - C_{11}$	1.58	$C_{10}' - C_{11}'$	1.53
$N_8 - C_{13}$	1.41	$N_8' - C_{13}'$	1.55
	$C_{11} - C_{11}'$	1.58	

TABLE VIINTERBOND ANGLES.

$C_{12} - C_1 - C_2$	116°	$C_{12}' - C_1' - C_2'$	120°
$C_1 - C_2 - C_3$	119	$C_1' - C_2' - C_3'$	119
$C_2 - C_3 - C_4$	121	$C_2' - C_3' - C_4'$	123
$C_3 - C_4 - C_5$	120	$C_3' - C_4' - C_5'$	114
$C_4 - C_5 - C_{12}$	121	$C_4' - C_5' - C_{12}'$	124
$C_5 - C_{12} - C_1$	123	$C_5' - C_{12}' - C_1'$	121
$C_{12} - C_{11} - C_7$	104	$C_{12}' - C_{11}' - C_7'$	96
$C_{11} - C_7 - N_6$	104	$C_{11}' - C_7' - N_6'$	117
$C_7 - N_6 - C_5$	109	$C_7' - N_6' - C_5'$	100
$N_6 - C_5 - C_{12}$	113	$N_6' - C_5' - C_{12}'$	113
$C_5 - C_{12} - C_{11}$	109	$C_5' - C_{12}' - C_{11}'$	110
$C_{11} - C_{10} - C_9$	103	$C_{11}' - C_{10}' - C_9'$	99
$C_{10} - C_9 - N_8$	106	$C_{10}' - C_9' - N_8'$	106
$C_9 - N_8 - C_7$	101	$C_9' - N_8' - C_7'$	97
$N_8 - C_7 - C_{11}$	108	$N_8' - C_7' - C_{11}'$	111
$C_7 - C_{11} - C_{10}$	105	$C_7' - C_{11}' - C_{10}'$	103
$C_9 - N_8 - C_{13}$	117	$C_9' - N_8' - C_{13}'$	114
$C_7 - N_8 - C_{13}$	119	$C_7' - N_8' - C_{13}'$	110
$C_1 - C_{12} - C_{11}$	128	$C_1' - C_{12}' - C_{11}'$	129

TABLE VI (Contd.)

$C_4 - C_5 - N_6$	125	$C_4' - C_5' - N_6'$	123
$N_6 - C_7 - N_8$	111	$N_6' - C_7' - N_8'$	121
$C_{12} - C_{11} - C_{11}'$	116	$C_{12}' - C_{11}' - C_{11}$	109
$C_{10} - C_{11} - C_{11}'$	110	$C_{10}' - C_{11}' - C_{11}$	109
$C_7 - C_{11} - C_{11}'$	112	$C_7' - C_{11}' - C_{11}$	124
$C_{12} - C_{11} - C_{10}$	109	$C_{12}' - C_{11}' - C_{10}'$	115

TABLE VIIINTRAMOLECULAR NON - BONDED DISTANCES < 4.0 Å

O1 - N6	3.62	O1 ¹ - N6 ¹	3.64
O1 - O7	3.81	O1 ¹ - O7 ¹	3.59
O1 - O9	4.07	O1 ¹ - O9 ¹	3.89
O1 - O10	3.26	O1 ¹ - O10 ¹	3.25
O2 - O11	3.85	O2 ¹ - O11 ¹	3.83
O3 - N6	3.65	O3 ¹ - N6 ¹	3.74
O4 - O7	3.68	O4 ¹ - O7 ¹	3.57
O4 - O11	3.64	O4 ¹ - O11 ¹	3.75
O5 - N8	3.42	O5 ¹ - N8 ¹	3.36
O5 - O9	3.49	O5 ¹ - O9 ¹	3.44
O5 - O10	3.43	O5 ¹ - O10 ¹	3.49
O5 - O13	3.99	O5 ¹ - O13 ¹	3.80
N6 - O9	3.19	N6 ¹ - O9 ¹	3.16
N6 - O10	3.47	N6 ¹ - O10 ¹	3.53
N6 - O13	2.91	N6 ¹ - O13 ¹	2.72
N8 - O12	3.45	N8 ¹ - O12 ¹	3.36
O9 - O12	3.12	O9 ¹ - O12 ¹	3.04
O10 - O13	3.75	O10 ¹ - O13 ¹	3.80
O11 - O13	3.77	O11 ¹ - O13 ¹	3.77
O1 - O5 ¹	3.53	O9 - O11 ¹	3.74
O1 - N6 ¹	3.45	O10 - N8 ¹	3.84
O1 - O7 ¹	3.50	O10 - O7 ¹	3.24

TABLE VII (Contd.)

C1 - C11 ¹	3.32	C10 - C10 ¹	3.06
C1 - C12 ¹	3.51	C10 - C12 ¹	3.92
C5 - C1 ¹	3.66	C11 - C1 ¹	3.26
C5 - C11 ¹	3.53	C11 - C5 ¹	3.42
C5 - C12 ¹	3.53	C11 - N6 ¹	3.55
N6 - C1 ¹	3.53	C11 - N8 ¹	3.73
N6 - C11 ¹	3.58	C11 - C9 ¹	3.73
N6 - C12 ¹	3.70	C12 - C1 ¹	3.56
C7 - C1 ¹	3.30	C12 - C5 ¹	3.48
C7 - C10 ¹	2.95	C12 - N6 ¹	3.73
C7 - C12 ¹	3.19	C12 - C7 ¹	3.41
N8 - C10 ¹	3.62	C12 - C10 ¹	3.92
N8 - C11 ¹	3.66	C12 - C12 ¹	2.93
C9 - C10 ¹	3.99		

TABLE VIII
INTERMOLECULAR DISTANCES 4.0 Å

C3 - C3 (i)	3.77	C7 - BrI	3.86
C3 - C4 (i)	3.76	N8 - BrI	4.00
C3 - C2 ¹ (i)	3.77	C10 - BrII	3.80
C3 - C3 ¹ (i)	3.80	C13 - BrI	3.98
C4 - C4 (i)	3.27	N8 ¹ - BrII	3.18
C4 - C5 (i)	3.76	C9 ¹ - BrII	3.82
C4 - C2 ¹ (i)	3.64	C10 ¹ - BrII	3.97
C13 - C13 ¹ (ii)	3.98	N6 ¹ - BrI (ii)	3.43
C9 - C13 ¹ (iii)	3.93	BrII - C13 ¹ (ii)	3.84
C10 - C13 (iii)	3.92	C9 - BrI (iii)	3.92
C2 - C3 ¹ (v)	3.92	BrII - C4 (iii)	3.80
C2 - C4 ¹ (v)	3.73	BrII - C5 (iii)	3.90
C2 - C5 ¹ (v)	3.89	BrII - N6 (iii)	3.86
C2 - C9 ¹ (v)	3.82	BrII - C13 (iii)	3.84
C3 - C9 ¹ (v)	3.68	BrI - C4 ¹ (iv)	3.76
C9 - C13 (vi)	3.93		

The figures in parentheses refer to the following equivalent positions.

- | | |
|--|---|
| (i) $y, x, -z.$ | (ii) $y + 1, x, -z.$ |
| (iii) $\frac{1}{2} + y, \frac{1}{2} - x, \frac{3}{2} + z.$ | (iv) $1\frac{1}{2} - y, -\frac{1}{2} - x, \frac{1}{2} + z.$ |
| (v) $\frac{1}{2} + y, 1\frac{1}{2} - x, \frac{3}{2} + z$ | (vi) $1\frac{1}{2} - y, \frac{1}{2} - x, \frac{1}{2} + z.$ |

TABLE IXSTANDARD DEVIATIONS OF THE FINAL ATOMIC CO-ORDINATES (Å)

<u>Atom</u>	<u>σ (x)</u>	<u>σ (y)</u>	<u>σ (z)</u>
C ₁	0.053	0.057	0.067
C ₂	0.060	0.059	0.061
C ₃	0.053	0.052	0.057
C ₄	0.058	0.053	0.059
C ₅	0.052	0.056	0.067
C ₇	0.054	0.053	0.062
C ₉	0.056	0.061	0.066
C ₁₀	0.052	0.052	0.054
C ₁₁	0.049	0.046	0.056
C ₁₂	0.043	0.042	0.059
C ₁₃	0.053	0.056	0.070
C ₁ '	0.048	0.050	0.064
C ₂ '	0.055	0.056	0.066
C ₃ '	0.059	0.057	0.071
C ₄ '	0.056	0.064	0.065
C ₅ '	0.044	0.041	0.053
C ₇ '	0.049	0.047	0.060
C ₉ '	0.059	0.058	0.060
C ₁₀ '	0.053	0.054	0.061
C ₁₁ '	0.050	0.043	0.057

TABLE IX (Continued)STANDARD DEVIATIONS OF THE FINAL ATOMIC CO-ORDINATES (\AA)

<u>Atom</u>	<u>σ (x)</u>	<u>σ (y)</u>	<u>σ (z)</u>
C ₁₂ '	0.052	0.051	0.057
C ₁₃ '	0.061	0.063	0.077
N ₆	0.039	0.040	0.049
N ₈	0.047	0.044	0.052
N ₆ '	0.040	0.044	0.055
N ₈ '	0.041	0.041	0.051
BrI	0.006	0.006	0.007
BrII	0.006	0.006	0.007

TABLE X.DEVIATIONS (A) OF THE ATOMS FROM VARIOUS PLANES.

- a Plane through benzene ring atoms C1, C2, C3, C4, C5, C12
b Plane through benzene ring atoms C1¹, C2¹, C3¹, C4¹, C5¹, C12¹.
c Plane through atoms C1, C2, C3, C4, C5, N6, C7, C11, C12.
d Plane through atoms C1¹, C2¹, C3¹, C4¹, C5¹, N6¹, C7¹, C11¹, C12¹.

<u>Atom</u>	<u>a</u>	<u>b</u>	<u>c</u>	<u>d</u>
C1 (1 ¹)	-0.013	0.021	-0.022	0.030
C2 (2 ¹)	0.006	-0.003	0.005	0.065
C3 (3 ¹)	0.013	-0.028	0.017	0.015
C4 (4 ¹)	-0.026	0.036	-0.022	0.006
C5 (5 ¹)	0.020	-0.016	0.017	-0.102
N6 (6 ¹)	-	-	0.009	-0.048
C7 (7 ¹)	-	-	-0.024	0.208
N8 (8 ¹)	-	-	-	-
C9 (9 ¹)	-	-	-	-
C10 (10 ¹)	-	-	-	-
C11 (11 ¹)	-	-	0.031	-0.096
C12 (12 ¹)	0.000	-0.011	-0.010	-0.078
C13 (13 ¹)	-	-	-	-

REFERENCES PART I, II AND III

- (1) W.L. Bragg, Proc. Camb.Phil.Soc., 17, 43 (1913)
- (2) James and Brindley, Phil. Mag., 12, 81 (1931)
- (3) Thomas, L.H., Proc.Camb. Phil.Soc., 23, 542 (1927)
- (4) Fermi, E., Z.Physik, 48, 73 (1928)
- (5) McWeeny, R., Acta Cryst., 4, 513 (1951)
- (6) Tomile and Stam, Acta Cryst., 11, 126 (1958)
- (7) Berghuis, Hsanappel, Potters, Loopstra, MacGillavry, and Veenendaal, Acta Cryst., 8, 478 (1955)
- (8) Debye, P., Ann. Physik, 43, 49 (1914)
- (9) Wilson, A.J.C., Nature, 150, 151 (1942)
- (10) Cruickshank, D.W.J., Acta Cryst., 2, 747 (1956)
- (11) Patterson, A.L., Phys. Rev., 46, 372 (1934)
- (12) Patterson, A.L., Z.Krist., 90, 517 (1935)
- (13) Robertson and Woodward; J. Chem. Soc., 36, 207 (1940)
- (14) Lipson and Cochran; 1953 "The Determination of Crystal Structures", p.207, G. Bell and Sons, Ltd., London.
- (15) Sim, G.A., Acta Cryst., 10, 177 (1957)
- (16) Booth, A.D., Proc. Roy. Soc., (1946) A, 188, 77
- (17) Hughes, E.W., J. Amer. Chem. Soc., 63, 1737 (1941)
- (18) Cruickshank and Robertson, Acta Cryst., 6, 698 (1953)
- (19) Fisher and Yates, Statistical Tables, 1957, Oliver and Boyd, Edinburgh.
- (20) Parihar and Dutt, J. Indian Chem. Soc., 27, 77 (1950)
- (21) Grant, Hamilton, Hamor, Hodges, McGeachin, Raphael, Robertson and Sim, Proc. Chem. Soc., (1961), 444.

- (22) Gopinath, Govindachari, Parthasarathy, Veswanathan, Arigoni and Wildman, Proc. Chem. Soc., 1961, 446.
- (23) Barton, Pradhan, Sternhell and Templeton, J. Chem. Soc., 1961, 225.
- Barton, Corey, and Jeger in collaboration with Cagliotti, Dev, Ferini, Glazier, Melera, Pradhan, Schaffner, Sternhell, Templeton and Tobinaga, *Experientia*, (1960), 16, 41
- (24) Robertson, J. Sci. Instr., 20, 175, (1943)
- (25) Tunell, Amer. Min., 24, 448, (1939)
- (26) Burns, D.M., Acta Cryst., 8, 516 (1955)
- (27) Ladell and Katz, Acta Cryst., 7, 460 (1954)
- (28) Booth, A.D., "Fourier Technique in X-ray Organic Crystal Analysis". p.64 Cambridge University Press.
- (29) Arnott, Davie, Robertson, Sim and Watson, J. Chem. Soc., 1961, 4183; *Experientia*, 16, 49, (1960)
- (30) Berghuis, Haanappel, Potters, Loopstra, MacGillavry and Veenerdaal; Acta Cryst., 8, 478, (1955)
- (31) "Internationale Tabellen zur Bestimmung von Kristallstrukturen", Bomtrager, Berlin, 1935, Vol.II, p.572.
- (32) Rollettin, "Computing Methods and the Phase Problem in X-ray Crystal Analysis", ed. Pepinsky, Robertson and Speakman, Pergamon Press, Oxford, 1961, p.87
- (33) Hodges, MacGeachin and Raphael, (unpublished results)
- (34) Barton, McChie, Pradhan and Knight, Chem. and Ind., 1954, 1325; J. Chem. Soc., 1955, 876
- (35) Barton, Pradhan, Sternhell and Templeton; J. Chem. Soc., 1961, 255.
- (36) Laurie, Hamilton, Spring and Watson; J. Chem. Soc., 1956, 3272.
- (37) S.A. Sutherland (unpublished results)
- (38) Bartell and Bonham; J. Chem. Phys., 27, 1414, (1957)

- (39) Davies and Blum; *Acta Cryst.*, 8, 129, (1955)
- (40) Trotter; *Acta Cryst.*, 13, 86, (1960)
- (41) Cunningham, Boyd, Myers, Gwinn and Le Van, *J. Chem. Phys.*, 19, 676, (1951)
- (42) Erlandsson; *Arkiv. Fysik.*, 2, 341, (1955)
- (43) Paul, Sim, Hamor and Robertson, (unpublished results).
- (44) Bak, Hansen, and Rastrup-Andersen; *Discuss. Far. Soc.*, 19, 30, (1955)
- (45) Miller, Aamodt, Dousmanis, Townes, and Kraitchman, *J. Chem. Phys.*, 20, 1112, (1952)
- (46) Lister and Sutton; *Trans. Far. Soc.*, 37, 393, (1941)
- (47) Shomaker, Waser, Marsh and Bergman; *Acta Cryst.*, 12, 600 (1959).
- (48) Hodson, Robinson and Smith; *Proc. Chem. Soc.*, 1961, 465.
- (49) Hodson and Smith; *J. Chem. Soc.*, 1957, 1877
- (50) Robinson, R. and Teuber, *Chem. and Ind.*, 1954, 783
- (51) Hamor, Robertson, Shrivastava and Silvertown; *Proc. Chem. Soc.*, 1960, 78.
Hamor and Robertson, *J. Chem. Soc.*, 1960, 76.
- (52) Woodward, Yang, Katz, Clark, Harley-Mason, Ingleby and Sheppard, *Proc. Chem. Soc.*, 1960, 76.
- (53) Manske, R.H.F., *Canad. J. Res.*, 1938, 16, B, 432. Barger, Madineveitia and Streuli; *J. Chem. Soc.*, 1939, 510.
- (54) Saxton, Bardsley and Smith; *Proc. Chem. Soc.*, 1962, 148
- (55) "Tables of Interatomic Distances and Configuration in Molecules and Ions", 1958. The Chemical Society, Burlington House, London.
- (56) Brown and Corbridge; *Acta Cryst.*, 7, 711 (1954)
- (57) McPhail and Sim, (unpublished results).

- (58) Hamilton, Hamor, Robertson and Sim, (unpublished results)
- (59) Arai, Coppola and Jeffrey; *Acta Cryst.*, 13, 553 (1960)
- (60) Kartha, Ahmed and Barnes, ^{*Acta Cryst.*} 7, 460, (1954)
- (61) Przybylska, M., *Acta Cryst.*, 14, 424, (1961)
- (62) Hanson and Ahmed; *Acta Cryst.*, 11, 724, (1958)
- (63) Donahue and Trueblood, *Acta Cryst.*, 5, 419, (1952)
- (64) Clunie and Robertson; *J. Chem., Soc.*, 1961, 4382.
- (65) Fridrichsons and Mathieson, *Acta Cryst.*, 15, 119 (1962)
- (66) Fitzer and Donath, *J. Amer. Chem. Soc.*, 81, 3213, (1959)
- (67) Hamilton, MacPhail and Sim, *J. Chem. Soc.*, 1962, 708.
- (68) Brown and Sim, (unpublished results).
- (69) Peterson, Steinrauf and Jensen, *Acta Cryst.*, 13, 104 (1960)
- (70) Kartha, Ahmed and Barnes, *Acta Cryst.*, 15, 326 (1962)
- (71) Robertson, J.H., and Beavers, *Acta Cryst.*, 4, 270 (1951)

PART IV.

THE CUPRIC ION CATALYSED
HYDROLYSIS OF GLYCYLGLYCINE.

4. (1) INTRODUCTION

In biological systems, metal ions play a significant role in many processes. Appreciation of the variety of biological reactions which depend upon the presence of a metal ion in greater or lesser amount has grown steadily in recent years. The part played by metal ions in enzymatic processes depends on the ability of such ions to form chelate compounds with a wide variety of organic materials. The metal ion can apparently act in one of two rather different ways. Firstly the enzyme or protein molecule etc. may be so tightly bound to the metal ion that it is only removed by vigorous chemical attack and examples of such strong binding are chlorophyll and the blood proteins. Secondly, the metal ion can act in a manner similar to that in which it catalyses a non-enzymatic reaction in which case it is readily split from the enzyme or substrate. Generally the ion is not specific and different metal ions will be associated with different degrees of reactivity. Enzymes included in this group include the phosphatases and peptidases.

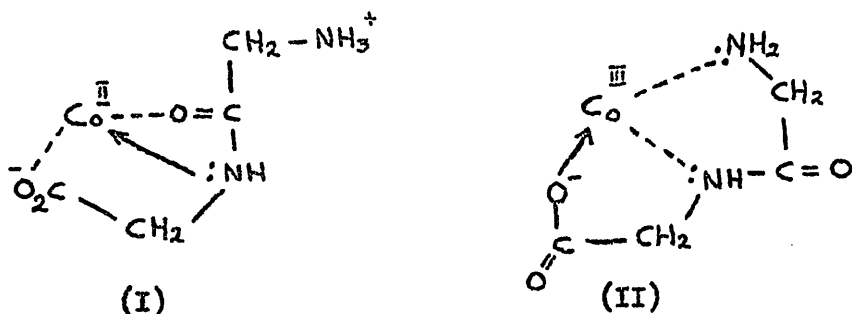
The peptidases are enzymes of low metal ion specificity but although several metal ions assist their catalytic effects, individual ions have very different efficiencies. To explain catalysis by this form of loose association between enzyme and metal ion Hellerman (1) has postulated interaction between enzyme, substrate and metal ion forming a species in which the substrate will undergo some type of chemical change. This theory has had wide acceptance but little work has been done to correlate enzymatic

reaction rates with the formation of the suggested complexes.

The dipeptidase of glycyglycine is apparently catalysed by several metal ions including cobaltous (Co^{II}). Smith (2) from spectroscopic work decided that cobaltous ions formed exceptionally stable complexes with glycyglycine. The order of stabilities of the glycyglycine chelates follows the normal Irving and Williams (3) series,

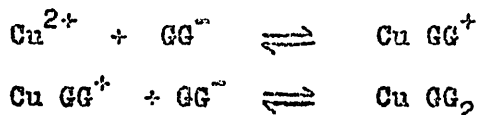


Williams (4) suggested that Smith's complex was cobaltic (Co^{III}) which did not hydrolyse in the presence or absence of an enzyme. On this basis Williams postulated structures (I) and (II) for the cobaltous and cobaltic complexes respectively;



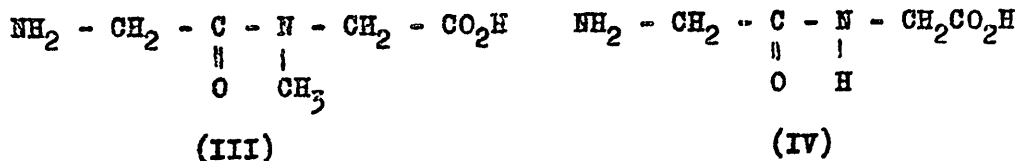
Although the stabilities of many amino acid metal ion complexes have been determined only a few peptide complexes, notably dipeptides such as glycyglycine or glycylysarcosine have been closely studied (5) - (14). Bjerrums method based on the theory of stepwise complex formation has usually been used for the calculation of stability constants. Datta and Rabin (10) have shown that cobaltous (Co^{II}) and manganous (Mn^{II}) complexes

of dipeptides form in a manner similar to that for amino acids and that a stepwise formation process appears to occur but peptide complexes with copper, however, appear to be more complicated. Datta and Rabin (10) also Dobbie and Kermack (13) discovered that if an equimolar mixture of cupric chloride and glycylglycine was titrated with alkali three equivalents of base were required to neutralise all acid species produced. If stepwise complex formation occurred;



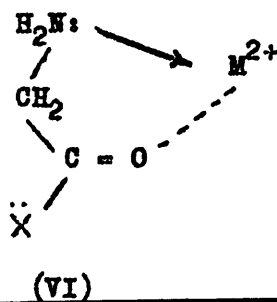
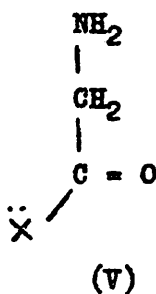
where GG^- represents the anionic form of glycylglycine. Therefore, for an equimolar mixture only one equivalent of alkali should be required for complete titration. Rabin (11) and Dobbie and Kermack (13) offered similar explanations to account for the two additional acid dissociations from this 1 : 1 dipeptide - metal complex.

The first ionisation with $\text{pK} \doteq 4.5$ is absent in glycylsarcosine - copper 1:1 - complexes. In glycylsarcosine (III) itself the peptide hydrogen atom of glycylglycine (IV) is replaced by a methyl group,



and it is reasonable to assume that this dissociation is probably

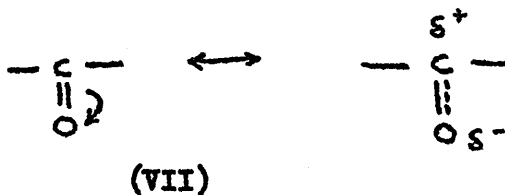
due to ionisation of the peptide hydrogen. The second dissociation, $pK \doteq 9$, can equally well be ascribed to ionisation of a hydrogen ion from a water molecule co-ordinated to the complex or to uptake of a hydroxyl ion. The ionisation of this peptide has only been definitely shown to occur from copper chelates. Thus, extremely powerful interactions must occur between the copper ion and the peptide bond. Whether the peptide carbonyl or nitrogen is involved is not immediately apparent. Rabin considers that oxygen atoms rather than nitrogen atoms are involved, at least prior to the occurrence of any additional acid dissociations. Interaction with the peptide nitrogen would lead to abolition of the resonance in the peptide bond since any interaction would have to take place with the lone pair of electrons on the nitrogen, which is energetically unfavourable. Examination of several similar compounds, including glycindimide, glycylglycine, triglycine and glycine ethyl ester shows that a linear relationship exists between the stability constant of the complex and the pK of the amino group. If such a relationship holds, only features common to all the compounds can be involved in complexing with metal ions. All the compounds possess the structure (V),



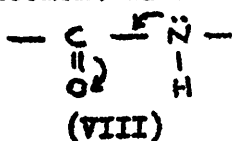
and therefore (VI) is the most likely structure for the complex. If co-ordination to the carbonyl group took place then such a linear relationship would not be anticipated. The evidence suggests that no interaction occurs with the peptide nitrogen in the initial complex but this does not preclude such interaction following on the ionisation of the peptide hydrogen. Indeed Rabin supports just such a change in co-ordination site since, according to Martell (15), copper has a great preference for nitrogen rather than oxygen co-ordination.

To summarise, Rabin (11) represents complex formation for the copper-glycylglycine system as shown in Figure I (canonical forms of complexes A and B are shown to indicate that resonance stabilisation occurs) and it is interesting to compare these structures with those proposed by Williams for the cobaltous and cobaltic complexes, (III) and (IV) respectively.

The hydrolysis of peptides depends upon the reactivity of the carbonyl group at the peptide bond and if this can be polarised, susceptibility of the carbon atom to attack by nucleophilic species occurs (VII).



Carbonyl reactivity is almost absent in peptides due to compensating electron displacement from the peptide nitrogen (VIII).



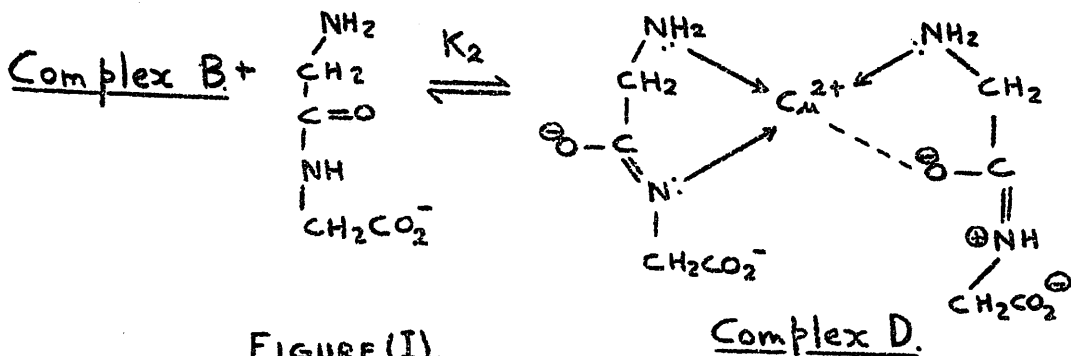
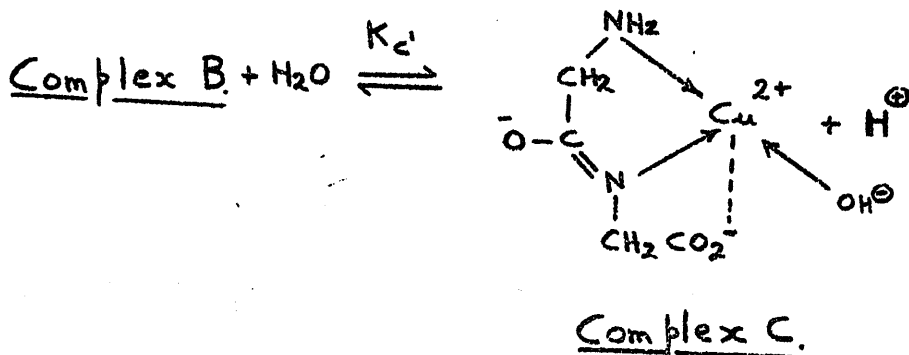
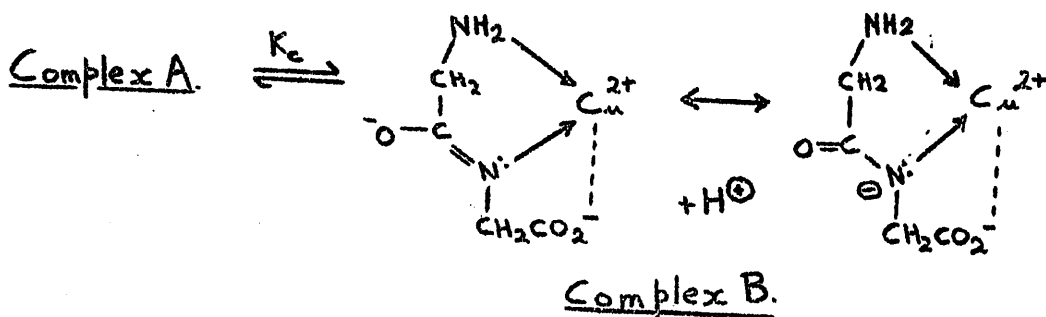
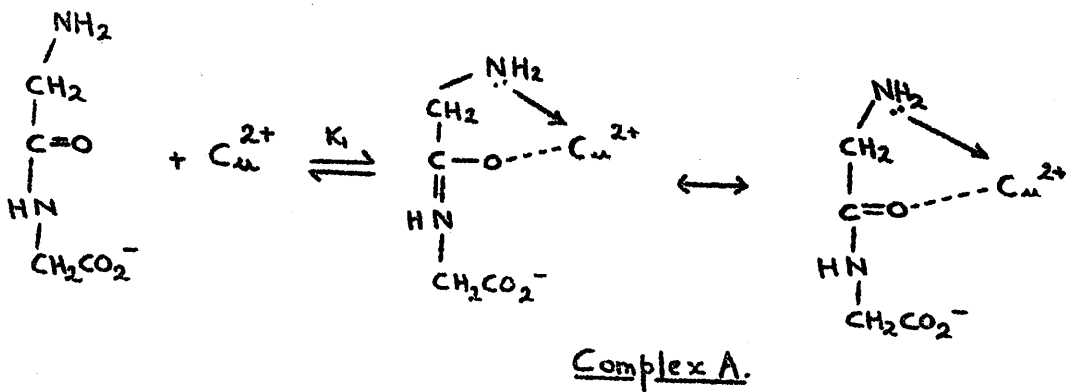
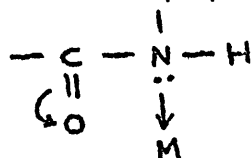


FIGURE (I).

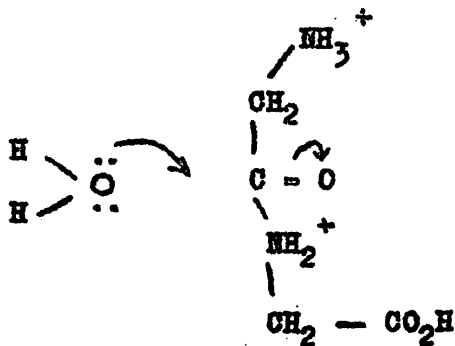
Co-ordination of the peptide nitrogen to an electrophilic species however, such as a metal atom, M, will induce carbonyl activity towards nucleophilic attack (IX).



(IX)

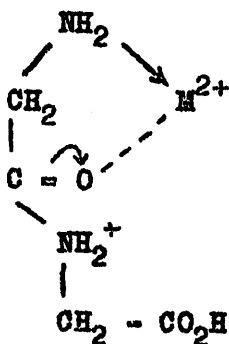
Further, such co-ordination will favour scission of the peptide bond and departure of the residue containing the peptide nitrogen following nucleophilic attack at the carbonyl group. Co-ordination to the peptide nitrogen will favour hydrolysis but if electron withdrawal at this nitrogen leads to ionisation of the peptide hydrogen, then the resulting complex will, according to Rabin (11), be inactive.

Kinetic studies of the hydrolysis of glycylglycine have usually been conducted at low pH Lawrence and Moore (16) have carried out rate measurements in concentrated hydrochloric acid and Martin (17) has studied the reaction in perchloric - acetic acid mixtures. It is generally considered that these reactions involve the protonated intermediate (X)



(X)

Lawrence and Moore (16) observed an increase in the rate of hydrolysis on the addition of cobaltous ion but they did not attempt to identify any complex species formed. Rabin, however, has suggested a possible structure (XI).



(XI)

At the low pH used by these workers only traces of such a complex could exist but Rabin believes that sufficient will form to catalyse hydrolysis.

More recently Baman, Haas and Trapman (18) have studied the metal ion catalysed hydrolysis of peptides in alkaline solution. A large number of metal ions were studied principal among which were transition and lanthanide metal ions, further, these workers noted that cupric ions in alkaline solution at 70°C gave a detectable catalytic effect. The main part of this work was devoted to a study of how that the catalysed hydrolysis of the peptide bond varied with the structure of the amino acids constituting the dipeptide.

In conclusion, we have attempted to show how the results

of Dobbie and Kermaek (13) and Rabin (11) have suggested that of the first two 1:1 copper-glycylglycine complexes only one will be hydrolysable. Rabin suggested that the first complex formed between cupric ions and glycylglycine prior to ionisation of the peptide hydrogen should undergo hydrolysis whilst the second complex should be unreactive. Therefore, at pH values significantly greater than 4.5 hydrolysis of the peptide should be inhibited. It was therefore decided to study the reaction of copper-glycylglycine complexes over a wide range of pH values and a range of cupric ion concentration.

4. (2) EXPERIMENTAL

Although it was hoped to study the reaction at 50°C it became obvious that it was too slow at this temperature. Accordingly it was decided to use a temperature of 85°C at which reactions in sealed pyrex tubes indicated appreciably faster reactions than those at 50°C. Temperature of the oil-filled thermostat was initially achieved by means of a 'Variac' bimetallic strip (85 ± 0.5°C) latterly a mercury regulator and 'Sunvic' circuit relay switch were used giving 85 ± 0.1°C.

Reactions were carried out in sealed pyrex tubes and each kinetic run consisted of about eight such tubes containing approximately 4 to 5 m.l. of reaction mixture. The tubes were supported in copper racks fitted with lids and were then suspended in the thermostat. At suitable time intervals they were removed

and their contents analysed. The pH was maintained constant by the use of buffered reaction mixtures, chloroacetic acid buffers between pH = 3.0 and 3.75, acetic acid buffers between pH = 3.75 and 5.5 and 0.1 molar hydrochloric acid used to maintain a pH = 1.0. One experiment was made at pH = 6.7 in which the solution was unbuffered and was adjusted to the required pH by addition of alkali. All reaction mixtures were 0.2 molar in the buffer acid anion since separate experiments established that was sufficient to give the required pH control. Since metal ions were present, it was impossible to use thermodynamic means to calculate the buffer ratios, and these were determined empirically by measuring the pH of trial solutions with a Cambridge pH meter and glass and calomel electrodes. The pH meter was standardised daily with two buffer solutions made from Burroughs and Wellcome pH = 4.01 and 6.99 buffer tablets.

It was first necessary to devise an analytical process for the analysis of glycylglycine/glycine solution mixtures. The complexes of ninhydrin with peptides and amino acids have long been known as colourimetric tests for such materials. Lately Yemm and Cocking (19) have succeeded in making the reaction quantitative thus giving a useful method for estimating amino acids and peptides. The method depends upon the formation of colour when ninhydrin (triketo hydrindene hydrate) is treated with a substance containing a primary amino group. Glycylglycine

contains one such group and the hydrolysis products (two molecules of glycine) give rise to two such groups. Therefore, the course of the reaction can be followed by measuring the increase in optical density of samples of the reaction mixture.

Hydrolysis reactions were followed in presence of copper ions of concentrations 0.01, 0.02, 0.033, 0.066, 0.1, 0.3 and 0.0 molar and the reaction mixtures were prepared in 50 m.l. graduated flasks in the following manner. The correct weight of glycyglycine to give a concentration of 0.01 Molar was added then, the required quantities of acetic acid and sodium acetate solutions to give the chosen pH and finally an accurately measured volume of a concentrated standard CuCl_2 solution to give the chosen copper ion concentration. The flask was then filled with distilled water, shaken, and then checked for pH to ensure the chosen value had been obtained. About 5 m.l. of the reaction mixture was then placed in the eight tubes comprising the experiment and the tubes then drawn out and sealed. The remainder of the reaction mixture was analysed to give the zero time optical density. In order to make an analysis the mixture had first to be freed of cupric ions by precipitating as copper sulphide with hydrogen sulphide under pressure and then filtering under slight suction through a hard filter paper (Whatman's No.48). Two m.l. of the copper free solution were made up to 20 m.l. in a

graduated flask with an 0.2M citrate buffer (pH = 5.5) and one m.l. of this diluted mixture was then analysed by the method of Yemm and Cocking (19) in the following manner. The one m.l. of diluted reaction mixture was placed in a test tube and to it were added 0.5 m.l. of citrate buffer (pH = 5.5), 0.2 m.l. of a 5% W/V ninhydrin - methyl cellosolve solution and then 1 m.l. of a potassium cyanide - methyl cellosolve solution. The test tube was then placed in a boiling water bath for 40 minutes to develop the complex (excessive evaporational losses were prevented by placing glass marbles on top of the test tubes). When the now deep purple solution had cooled to room temperature, 10 m.l. of a 60% by volume ethanol - water solution was added and the mixture stirred thoroughly. The optical density of this solution was determined by a Hilger and Watts Uvispek spectrophotometer at wavelength 570 m μ using 1 c.m. matched, quartz, stoppered cells. Calibration curves using 0.001 molar glycine and glycyglycine solutions revealed that the ratio of optical densities of glycine to glycyglycine for a given concentration was about 1.25. All future calculations of degree of hydrolysis had to allow for this.

The cupric chloride, sodium acetate, chloroacetic acid, potassium cyanide, citric acid and ninhydrin used were Analaar reagents and the glycine and glycyglycine (B.D.H. "Laboratory Reagent") were found to be chromatographically pure. The purity

of the glycyglycine was confirmed by formal titration (20).

Throughout only grade 'A' volumetric apparatus was used.

4. (3) RESULTS.

Thirty kinetic runs were made and many of these had to be repeated because of precipitation of copper acetate and irregularities in the analyses (reproducibility was only 15%). Table I gives a summary of all the experiments and each one is given a number under which it is listed in Tables II - IX. Each run is defined by its pH and cupric ion concentration and Tables II - IX list the experimental quantities; time in hours, corrected optical density, and percentage reaction. The ninhydrin reagent was found to deteriorate through time giving progressively lower results and as a result a check solution of 0.001 molar glycine was employed. If we let the optical density of this solution measured at $t = 0$ be D_G^0 and optical density measured after a time t , be D_G^t . Then if the optical density of the reaction mixture at time t is multiplied by D_G^0 / D_G^t it will be scaled to allow for any variations in the reagent which may exist at time t .

The values of percentage reaction quoted for each reaction were calculated as follows;

If x = fraction of glycyglycine reacted after time t giving an optical density D_t and D_0 = optical density when $t = 0$;

$$D_t = D_o - x D_o + 2x D_G^o$$

$$\therefore D_t - D_o = x (2 D_G^o - D_o)$$

$$\therefore x = \frac{(D_t - D_o)}{(2 D_G^o - D_o)}$$

$$\text{and Percentage Reaction} = \frac{100 (D_t - D_o)}{\alpha} \dots \dots \dots (a)$$

$$\text{where } \alpha = (2 D_G^o - D_o)$$

For 100% reaction, all the glycylglycine will be converted to glycine which should result in a doubling of the optical density. However, the optical density of an 0.001 M glycine solution is about 1.25 times that of an 0.001 M glycylglycine solution and the final optical density should be 2.5 D_o . If instead of this numerical factor of 1.25 we used D_G^o then at complete reaction $D_t = 2 D_G^o$ substituting in equation (a),

$$\text{Percentage Reaction} = \frac{100 (2 D_G^o - D_o)}{(2 D_G^o - D_o)} = 100\%$$

α is a constant for each reaction as D_G^o and D_o themselves are constants for any given reaction and these values of α are given for each reaction in Table I. The runs marked (x) in Table I are due to J.M. Wilson sometime of this Department and of these; runs 1, 2, 3, 4, 5, 6, 26 and 28 have no α value. In the calculation of the extent of reaction of these experiments no reagent correction was employed and the equation,

$$\text{Percentage Reaction} = \frac{100 (D_t - D_o)}{2.5 D_o - D_o}$$

TABLE ISUMMARY OF EXPERIMENTS IN TABLES II - IX.

No.	pH	Cu ²⁺	M.	α	No.	pH	Cu ²⁺	M.	α
1 *	1.0	0	-	-	16	4.0	0.01	-	2.02
2 *	3.0	0	-	-	17 *	4.3	0.033	-	2.01
3 *	3.5	0	-	-	18	4.3	0.02	-	2.02
4 *	1.0	0.033	-	-	19	4.3	0.01	-	1.90
5 *	1.0	0.30	-	-	20 *	4.6	0.033	-	1.97
6 *	3.0	0.30	-	-	21	4.6	0.02	-	2.03
7	3.5	0.10	-	1.99	22	4.6	0.01	-	1.91
8	3.75	0.033	-	1.91	23	5.0	0.02	-	1.96
9	3.75	0.033	-	1.90	24	5.0	0.01	-	1.96
10	3.75	0.02	-	1.95	25	6.0	0.01	-	2.04
11	3.75	0.02	-	1.95	26 *	6.67	0.01	-	-
12	4.0	0.10	-	1.98	27 *	5.5	0.033	-	2.03
13	4.0	0.066	-	2.01	28 *	5.5	0.1 (Zn ²⁺)	-	-
14	4.0	0.033	-	2.02	29	5.5	0.02	-	1.96
15	4.0	0.02	-	1.96	30	5.5	0.01	-	1.95

* These runs due to J.M. Wilson.

FIG. II

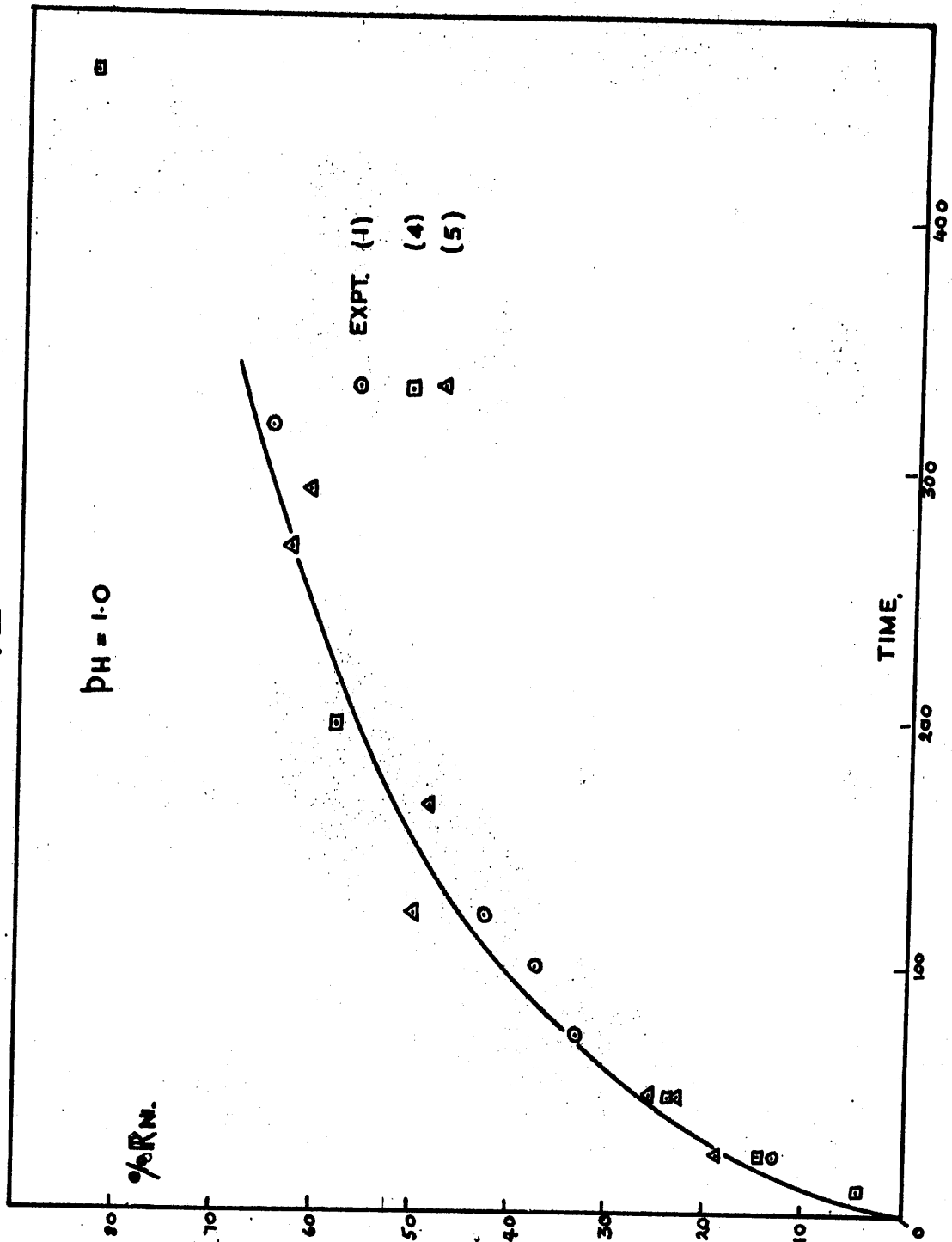


TABLE IIExperiment 1.

<u>Time</u>	<u>Dt</u>	<u>% Rn</u>
0	1.39	0
24	1.67	13.0
72	2.09	33.3
100	2.18	37.3
120	2.29	42.6
316	2.76	65.0
744	3.52	100.0

Experiment 2.

<u>Time</u>	<u>Dt</u>	<u>% Rn</u>
0	1.39	0
24	1.46	3.0
72	1.62	10.5
120	1.73	16.5
310	2.36	46.0
408	2.56	55.5
840	3.18	85.0

Experiment 3.

<u>Time</u>	<u>Dt</u>	<u>% Rn</u>
0	1.41	0
32	1.37	0
408	2.10	33
864	2.58	56.5
1392	3.10	82

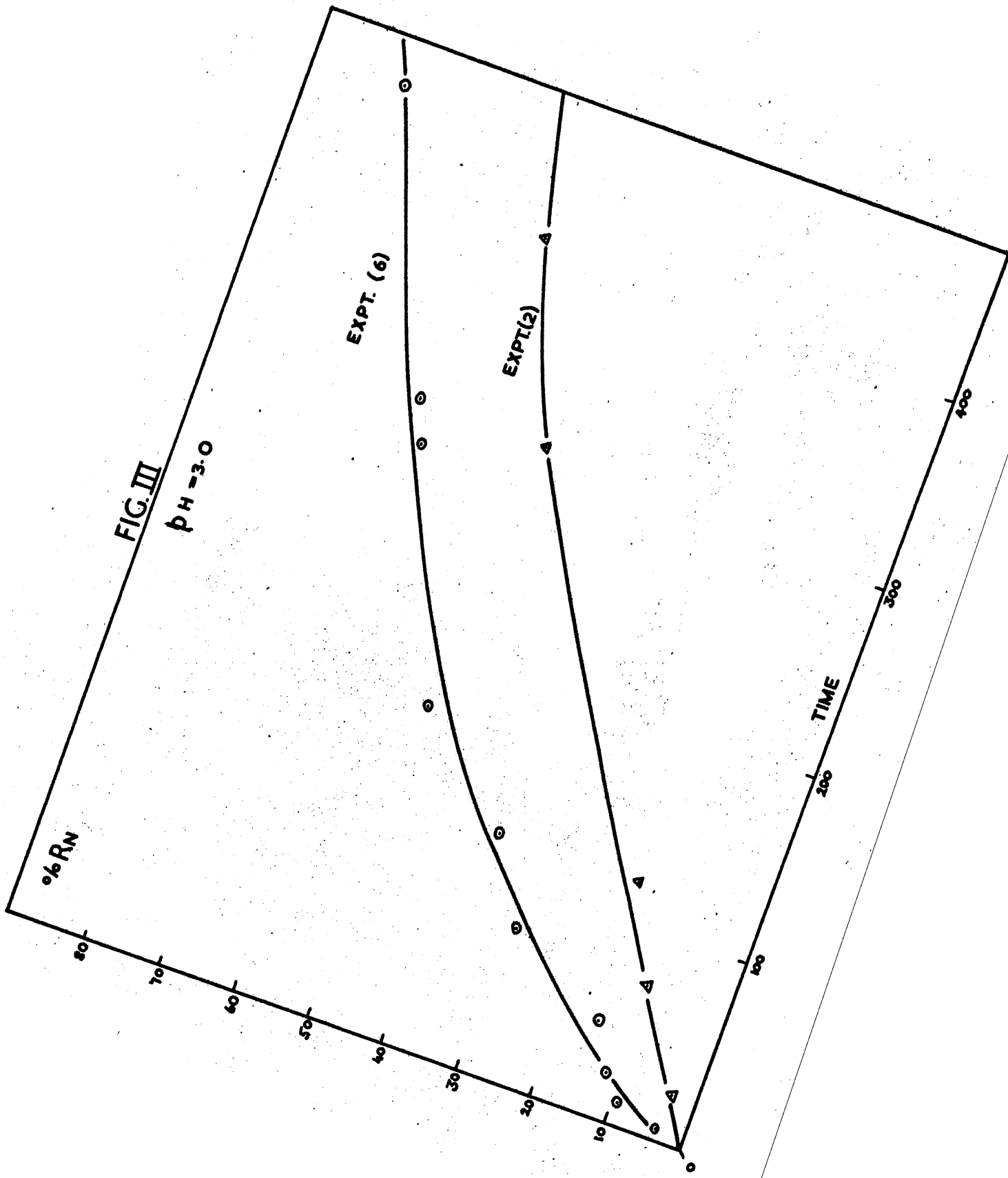


TABLE IIIEXPERIMENT 4.

<u>Time</u>	<u>Dt</u>	<u>% Rn</u>
0	1.39	0
5	1.48	4.0
24	1.69	14.0
48	1.89	23.3
196	2.62	58.0
456	3.14	83.3

EXPERIMENT 5

<u>Time</u>	<u>Dt</u>	<u>% Rn</u>
0	1.25	0
24	1.62	19.0
48	1.73	26.7
68	2.04	30.6
120	2.20	50.0
164	2.19	48.4
290	2.42	62.0
729	3.08	97.0

EXPERIMENT 6.

<u>Time</u>	<u>Dt</u>	<u>% Rn</u>
0	1.25	0
5	1.35	4.0
10	1.44	9.5
24	1.48	12.0
48	1.55	15.2
77	1.76	28.0
120	1.92	35.0
168	2.13	48.0
290	2.41	61.0
312	2.39	63.0
456	2.66	78.0

EXPERIMENT 7.

<u>Time</u>	<u>Dt</u>	<u>% Rn</u>
0	1.37	0
14	1.54	8.5
24	1.59	11.0
38	1.68	15.6
63	1.74	21.9
96	1.93	27.5
143	2.21	41.0
244	2.61	60.5
355	2.91	77.3
455	2.98	79.6
1238	3.13	88.2

FIG. IV

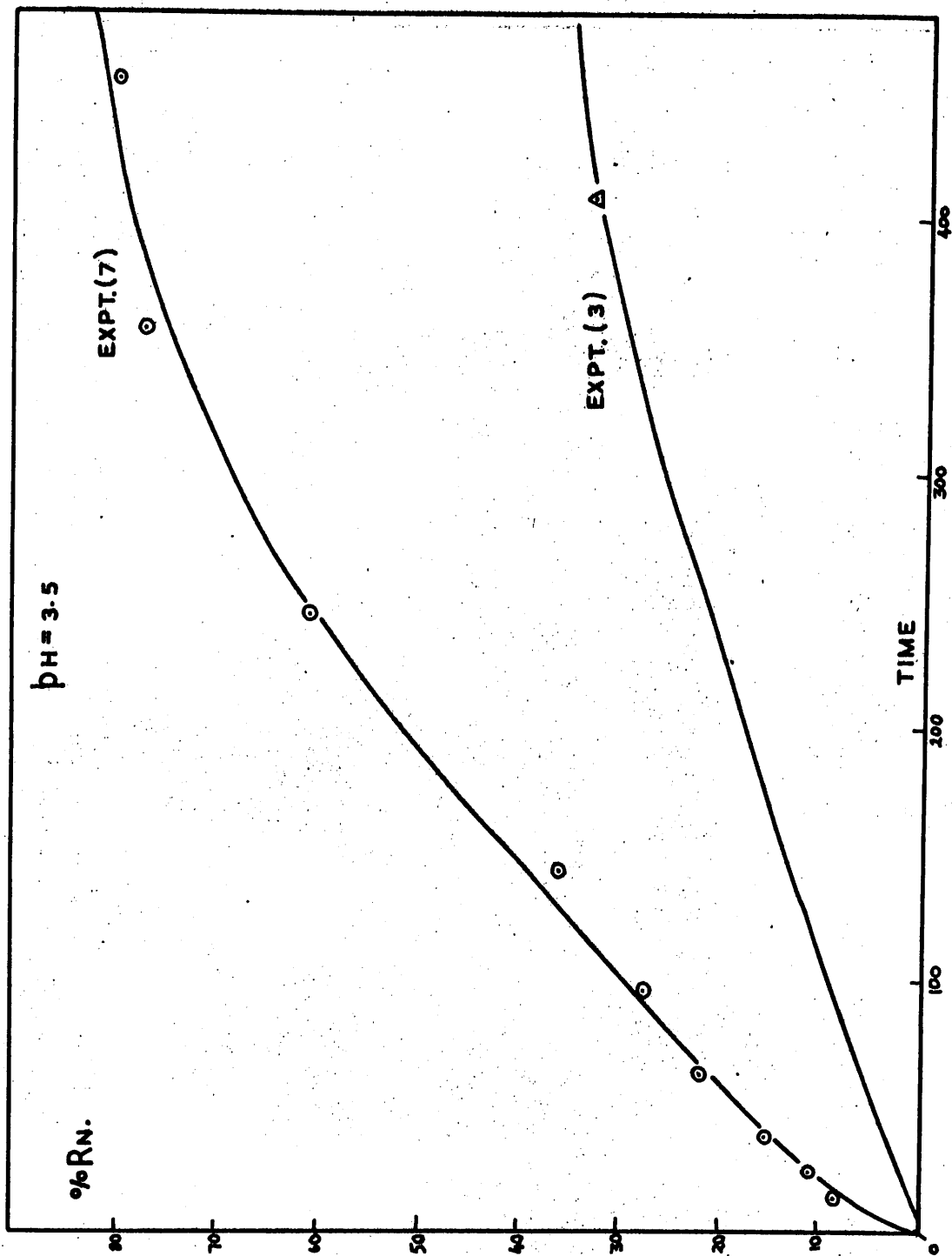


TABLE IVEXPERIMENT 8
ACETATE BUFFER

<u>Time</u>	<u>Dt</u>	<u>% Rn</u>
0	1.43	0
12	1.57	7.3
18	1.65	11.3
24	1.68	13.2
37	1.69	13.6
48	1.73	15.9
61	1.75	17.0
90	1.86	23.7
115	1.92	26.6

EXPERIMENT 9
CHLORACETATE BUFFER

<u>Time</u>	<u>Dt</u>	<u>% Rn</u>
0	1.44	0
12	1.58	7.3
18	1.66	11.5
24	1.69	13.4
37	1.71	14.0
48	1.81	19.8
61	1.83	20.9
90	1.97	29.2
115	2.02	31.8

EXPERIMENT 10
ACETATE BUFFER

<u>Time</u>	<u>Dt</u>	<u>% Rn</u>
0	1.41	0
6	1.47	2.9
24	1.56	7.3
30	1.58	8.4
43	1.60	9.4
75	1.65	12.1
98	1.69	14.3
115	1.74	16.7

EXPERIMENT 11
CHLORACETATE BUFFER

<u>Time</u>	<u>Dt</u>	<u>% Rn</u>
0	1.41	0
6	1.47	2.9
24	1.58	8.4
30	1.64	11.5
43	1.66	12.9
75	1.70	14.9
98	1.75	17.4
115	1.80	20.2

FIG. V

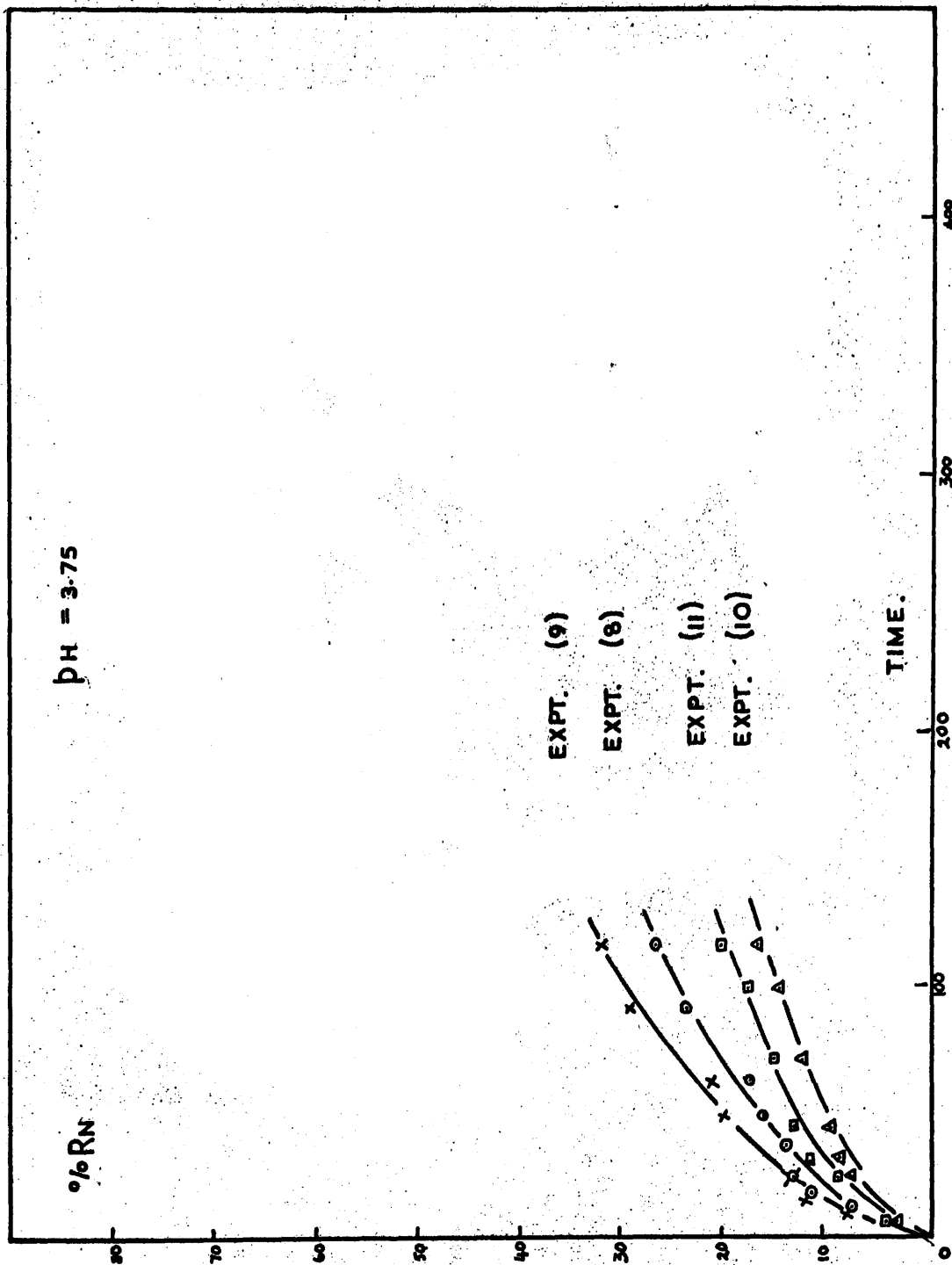


TABLE V.EXPERIMENT 12

<u>Time</u>	<u>Dt</u>	<u>% Rn</u>
0	1.42	0
15	1.86	22
23.5	1.99	29
38	2.23	41
47	2.28	46
95	2.89	78
168	3.01	84.5
240	3.14	87

EXPERIMENT 14.

<u>Time</u>	<u>Dt</u>	<u>% Rn</u>
0	1.425	0.
14	1.63	10.0
24	1.80	18.5
37	1.91	24.0
85	2.24	42.5
122	2.32	47.5
190	2.81	68.5
215.5	2.74	65.0
291	2.91	74.5
528	3.07	81.0

EXPERIMENT 13

<u>Time</u>	<u>Dt</u>	<u>% Rn</u>
0	1.425	0
14	1.74	15.5
24	1.95	21.0
40	2.23	35.0
65.5	2.52	54.5
134	2.96	75.5

EXPERIMENT 15.

<u>Time</u>	<u>Dt</u>	<u>% Rn</u>
0	1.435	0
5	1.54	5.5
23	1.66	11.5
63	1.90	24.0
100	2.01	29.0
133	2.13	35.0

EXPERIMENT 16

<u>Time</u>	<u>Dt</u>	<u>% Rn</u>
0	1.42	0
14	1.54	5.60
38	1.70	13.80
65	1.82	19.50
134	1.99	28.0

FIG. VI

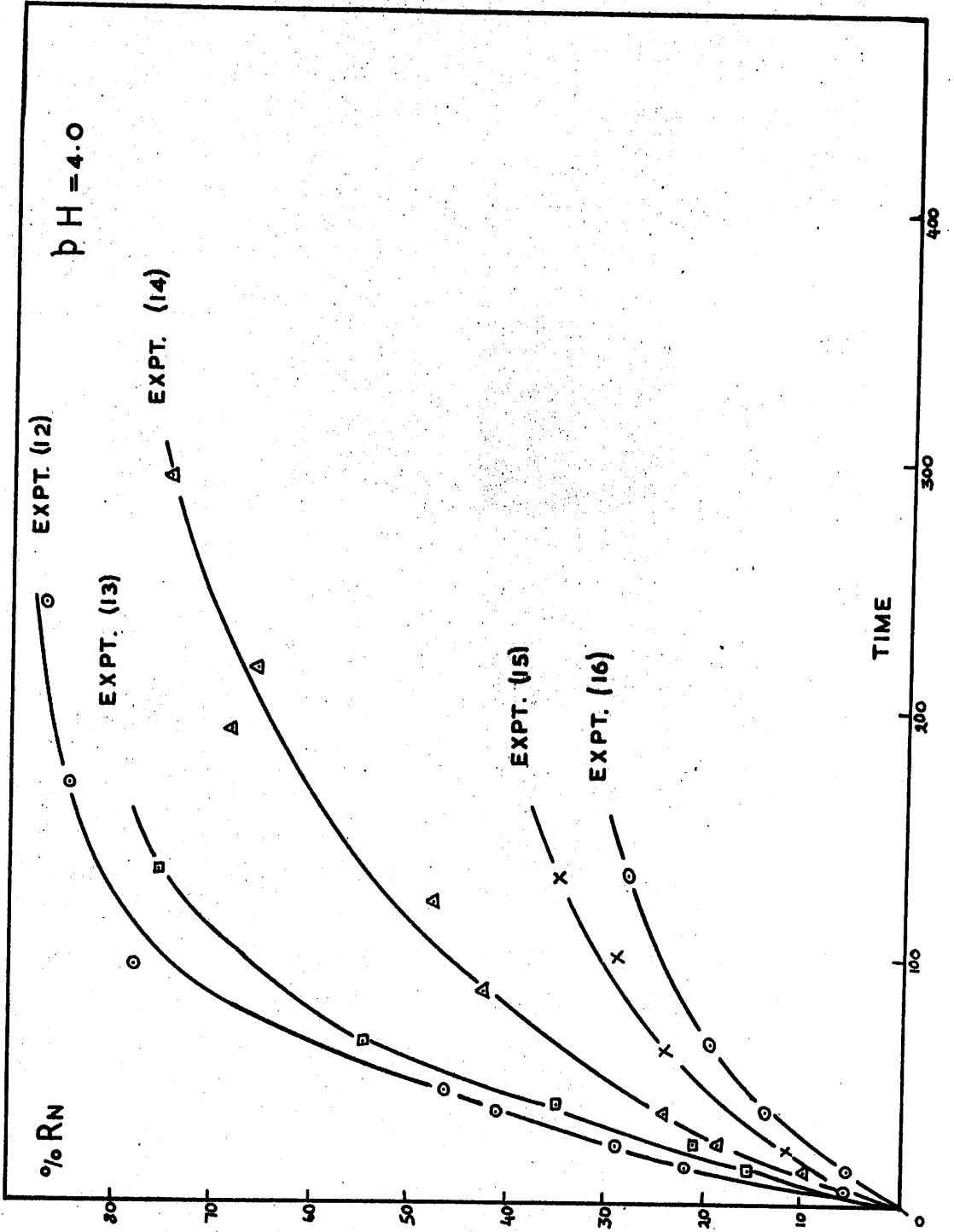


TABLE VIEXPERIMENT 17

<u>Time</u>	<u>Dt</u>	<u>% Rn</u>
0	1.44	0
14	1.72	14
22	1.78	17
31	1.86	21
44.5	2.16	36
86	2.35	45
91.5	2.45	51
162	2.64	60
163	2.80	68
408	3.12	83

EXPERIMENT 19

<u>Time</u>	<u>Dt</u>	<u>% Rn</u>
0	1.46	0
5	1.54	4.3
12	1.68	11.2
24	1.79	17.0
29	1.84	19.8
60	2.00	30.5
77	2.13	35.0
101	2.18	40.5
172	2.43	51.0

EXPERIMENT 18

<u>Time</u>	<u>Dt</u>	<u>% Rn</u>
0	1.425	0
21	1.75	16
31.5	1.86	22
44.5	1.97	27
103	2.32	44
117	2.39	48
143	2.47	52
309	2.82	70
622	3.08	83

FIG. VII

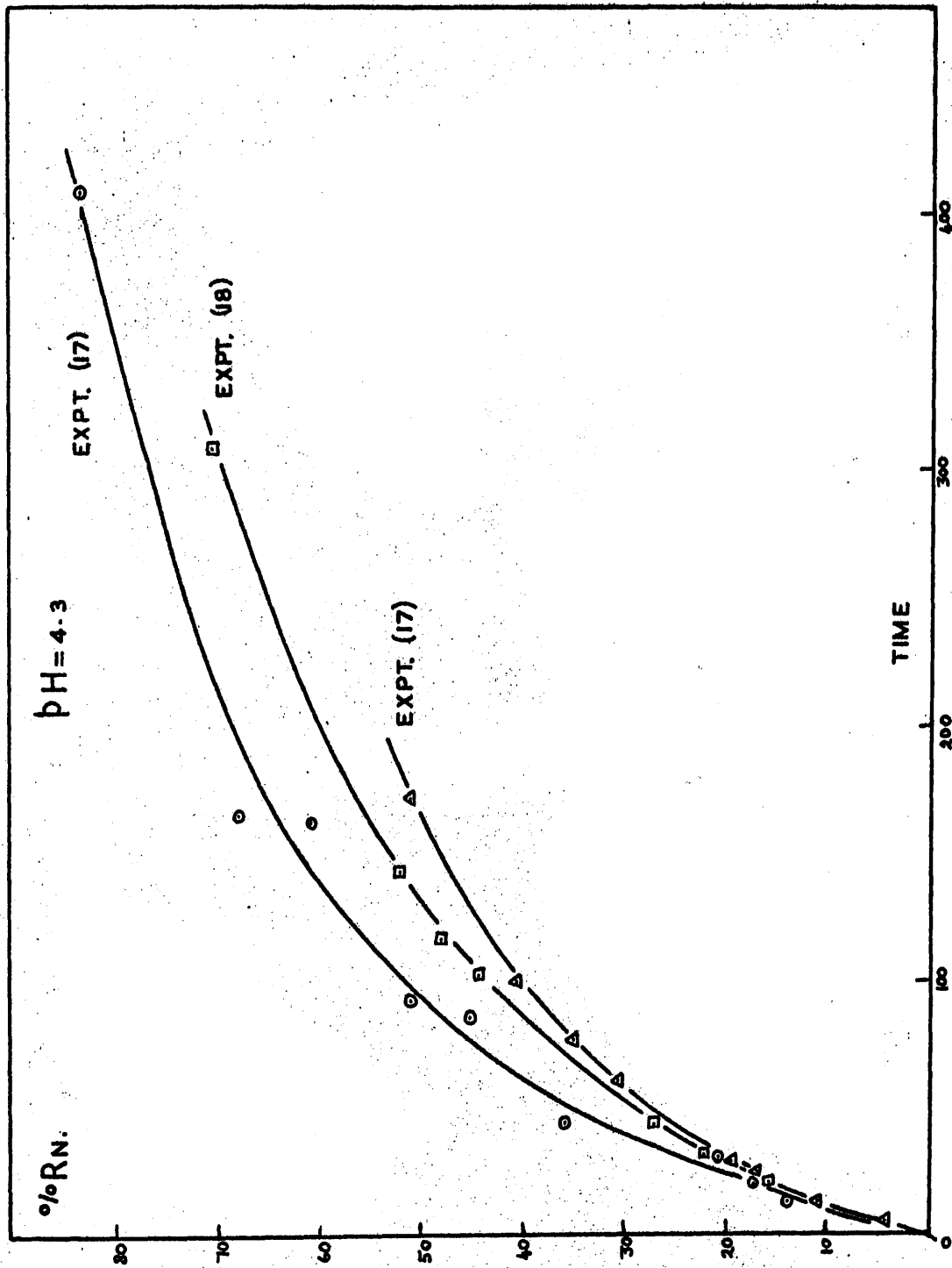


TABLE VIIEXPERIMENT 20

<u>Time</u>	<u>Dt</u>	<u>% Rn</u>
0	1.41	0
14	1.64	11
24	1.76	18
42	1.92	26
86.5	2.26	44
122	2.52	61
190	2.98	73
288	3.06	77
528	3.24	87

EXPERIMENT 21

<u>Time</u>	<u>Dt</u>	<u>% Rn</u>
0	1.42	0
21	1.67	12
31.5	1.82	20
44.5	1.86	22
103	2.17	37
117	2.26	41
143	2.33	45
309	2.59	58
622	2.79	69

EXPERIMENT 22.

<u>Time</u>	<u>Dt</u>	<u>% Rn</u>
0	1.45	0
5	1.51	3.0
12	1.64	9.5
24	1.69	12.5
29	1.73	14.5
60	1.91	25.0
77	2.04	30.5
101	2.09	35.0
172	2.27	43.0

FIG. VIII

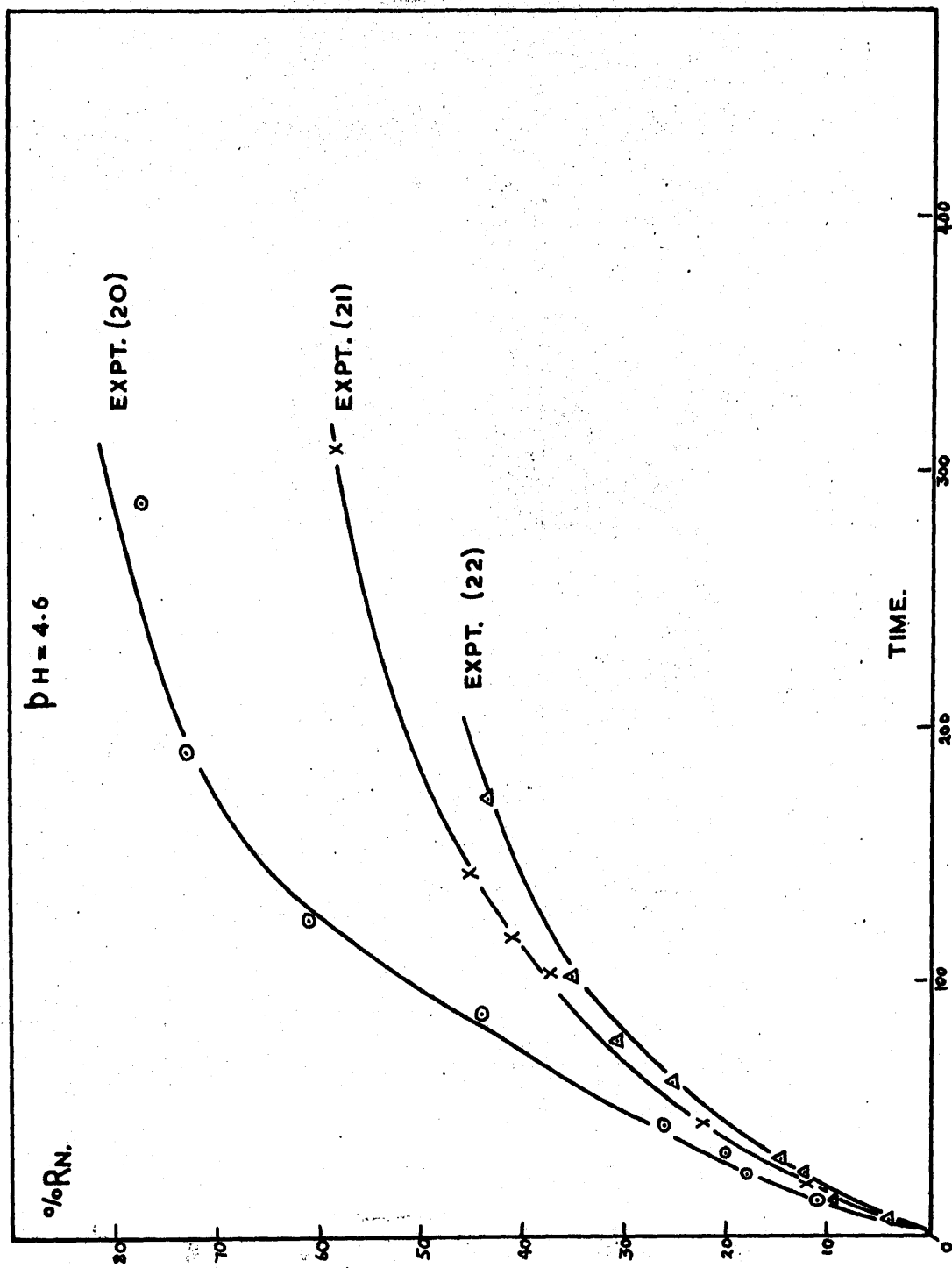


TABLE VIIIEXPERIMENT 23

<u>Time</u>	<u>Dt</u>	<u>% Rn</u>
0	1.46	0
12	1.70	12
20	1.76	15
32	1.79	17
44	1.83	20
49	1.88	22
67	1.99	28
146	2.22	39

EXPERIMENT 24

<u>Time</u>	<u>Dt</u>	<u>% Rn</u>
0	1.44	0
9	1.56	6
21	1.65	10
45	1.77	16
50	1.82	18.5
55	1.84	20
69	1.88	22

EXPERIMENT 25

<u>Time</u>	<u>Dt</u>	<u>% Rn</u>
0	1.46	0
4.5	1.53	3.5
11	1.55	4.5
27	1.61	7.5
35	1.67	11.0
54	1.73	14.0
72	1.79	16.5
168	1.92	24.0
192	1.94	24.5

EXPERIMENT 26

<u>Time</u>	<u>Dt</u>	<u>% Rn</u>
0	1.44	0
19	1.44	0
68	1.54	4.4
143	1.63	8.5
337	1.94	22.7
1340	2.34	41.2

FIG. IX

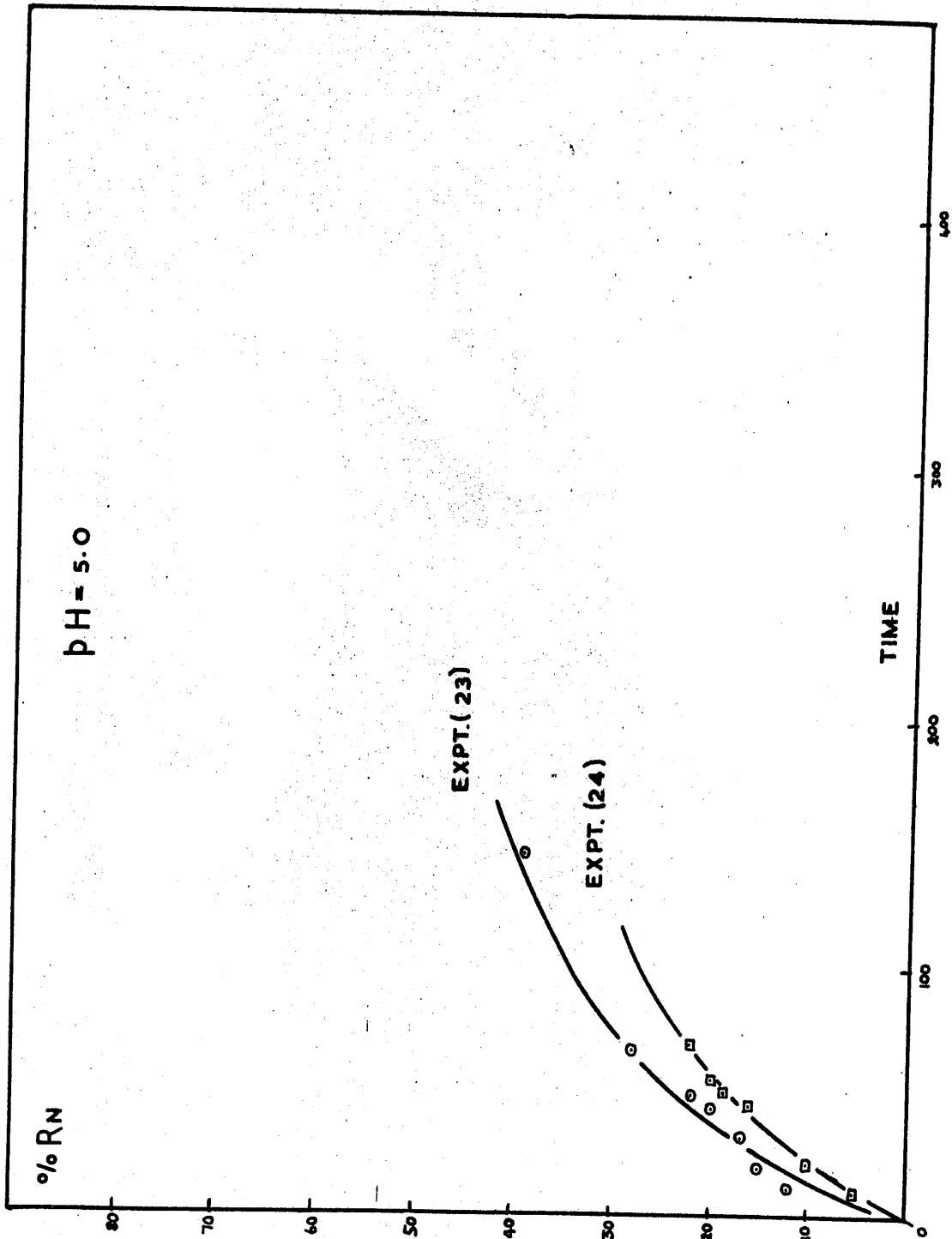


TABLE IXEXPERIMENT 27

<u>Time</u>	<u>Dt</u>	<u>% Rn</u>
0	1.40	0
5	1.40	0
24	1.51	5.6
52	1.68	14.2
96	1.84	21.8
216	1.94	26.1
1560	3.05	81.2

EXPERIMENT 28

<u>Time</u>	<u>Dt</u>	<u>% Rn</u>
0	1.40	0
5	1.48	4
10	1.57	8
24	1.77	18
52	2.06	33
96	2.62	59
840	3.29	92

EXPERIMENT 29

<u>Time</u>	<u>Dt</u>	<u>% Rn</u>
0	1.44	0
25	1.62	9.1
48	1.74	15.7
72	1.83	20.0
96	1.91	24.3
144	1.98	28.5
168	2.01	30.4

EXPERIMENT 30

<u>Time</u>	<u>Dt</u>	<u>% Rn</u>
0	1.47	0
12	1.51	2.4
22	1.55	4.3
36	1.63	8.3
49	1.68	12.2
61	1.70	13.2
67	1.76	15.4
85	1.80	17.0

FIG. X

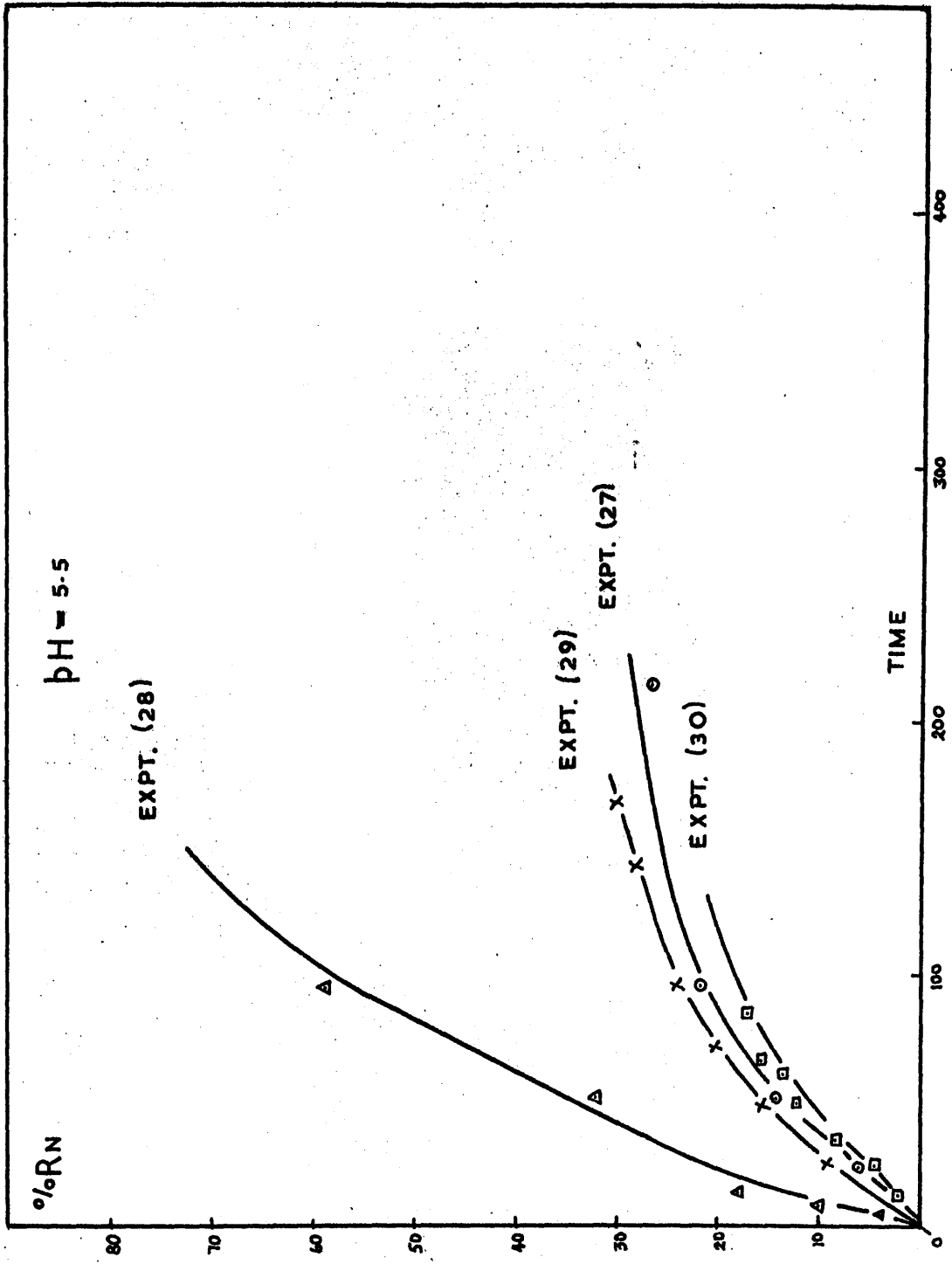
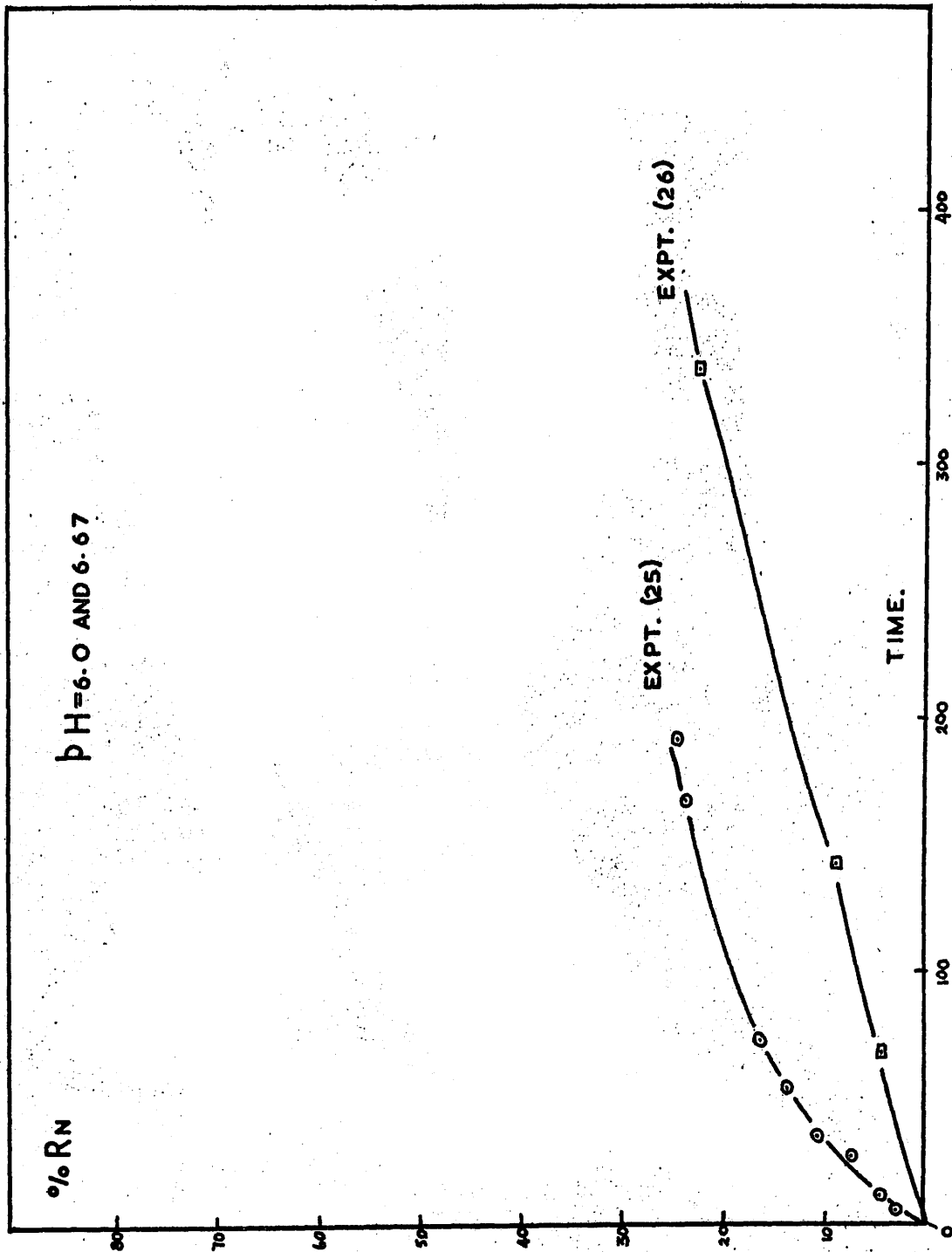


FIG. XI



$$\therefore \% R_n = \frac{100 (D_t - D_o)}{1.5 D_o} \dots \dots \dots (b)$$

was used,

Plots of percentage reaction versus time for each kinetic run are given in Figures II - XI and each run is referred to by its Table I number. Where possible all experiments made at one pH are given in the same figure. Experiments 1, 2 and 3 were carried out with no copper ion present and all others had copper present except run 28 which had 0.1 M zinc ions instead. Runs 9 and 11 were carried with chloracetic acid buffer at the same pH and metal ion concentrations as 8 and 10 respectively.

(4) DISCUSSION

Although errors in the analyses lead to the experiments being semi-quantitative, several interesting features emerge. From Fig. II it is seen that the presence of copper ions in the concentration range 0 - 0.3 molar has no effect on the reaction rate at pH = 1.0. These experiments have (within experimental error) the same rate and are all acid catalysed. At this low pH value very little complexing takes place between copper ions and glycylglycine. As the pH is raised the rate of the purely acid catalysed reaction decreases until at pH = 4.0 no reaction was observed after 1,300 hours. This observation of decreasing rate with decreasing hydrogen ion concentration is in accord with other examples of this type of catalysis,

e.g. esters. After 100 hours the extent of reaction (interpolated from Fig. II, III and IV) for the uncatalysed reactions at pH values 1.0, 3.0 and 3.5 are 39, 15 and 10% respectively.

The increase in catalytic effect in the presence of copper ions as the pH is increased from 3.0 to 3.5 is most readily seen in Figs. III and IV when it is clear that the catalytic effect is greater at the higher pH. The extent of reaction after 100 hours is the same for each run (within experimental error) despite the concentration of copper ions being one third of that at the lower pH (= 3.0). At this stage, copper-glycylglycine complexing has commenced and it would appear that that catalysis proceeds via a complex.

Rabin (11), believes that Complex A (Fig. I) will undergo hydrolysis and that Complex B will be inactive. The formation constant of Complex A is defined as:

$$K_1 = \frac{[CuGG^+]}{[Cu^{2+}].[GG^-]}$$

where $[CuGG^+]$ and $[GG^-]$ are the concentrations of Complex A and the anionic form of glycylglycine respectively. Loss of the peptide hydrogen from $CuGG^+$ gives Complex B whose stability constant is defined as;

$$K_c = \frac{[CuGG].[H^+]}{[CuGG^+]}$$

where $[CuGG]$ is the concentration of Complex B. Clearly the formation and subsequent decomposition of Complex B will depend-upon the pH

of the solution. In order to determine which complexes are effective in increasing the rate of reaction it is necessary to calculate the relative concentrations of complexes A and B in solution.

In the pH range 3.0 - 6.0, the total concentration of glycylglycine, $[GG_0]$ is given by

$$[GG_0] = [CuGG^+] + [CuGG] + 2[CuGG_2^-] + [GG^+] + [GG^\pm] + [GG^-] \quad - \quad (i)$$

where $[CuGG_2^-]$ is the concentration of Complex D (Fig. I) and $[GG^+]$ and $[GG^\pm]$ are the cationic and zwitterionic forms of glycylglycine respectively. Similarly, the total concentration of cupric ions, $[Cu_0^{2+}]$, is given by,

$$[Cu_0^{2+}] = [Cu^{2+}] + [CuGG^+] + [CuGG] + [CuGG_2^-] \quad - \quad (ii)$$

The formation constant of Complex D is defined as;

$$K_2 = \frac{[CuGG_2^-]}{[CuGG] \cdot [GG^-]}$$

also for glycylglycine,

$$K_a = \frac{[GG^-][H^+]}{[GG^\pm]}$$

and

$$K_b = \frac{[GG^\pm][H^+]}{[GG^+]}$$

Substituting these constants in equation (i) we get;

$$[GG_0] = [CuGG^+] + \frac{[CuGG^+].K_c}{[H^+]} + \frac{[CuGG^+].[H^+]}{K_a.K_1.[Cu^{2+}]} \left(\frac{[H^+]}{K_b} + 1 \right) + \frac{[CuGG^+]}{K_1.[Cu^{2+}]} + \frac{2.K_2.K_c.[CuGG^+]^2}{K_1.[H^+].[Cu^{2+}]}$$

and on rearrangement equation (i) becomes;

$$[CuGG^+] = \frac{[GG_0]}{1 + \frac{K_c}{[H^+]} + \frac{2.K_2.K_c.[GG^-]}{[H^+]} + \frac{[H^+]}{K_a.K_1.[Cu^{2+}]} \left(\frac{[H^+]}{K_b} + 1 \right) + \frac{1}{K_1.[Cu^{2+}]}} \quad \text{--- (iii)}$$

Similarly equation (i) can be expressed in terms of $[CuGG_0]$ giving;

$$[CuGG] = \frac{[GG_0]}{1 + \frac{[H^+]}{K_c} + 2.K_2.[GG^-] + \frac{[H^+]}{K_1.K_c.[Cu^{2+}]} \left(1 + \frac{[H^+]}{K_a} + \frac{[H^+]^2}{K_b} \right)} \quad \text{--- (iv)}$$

Equations (iii) and (iv) assume constant ionic strength, and activity coefficients were assumed constant, further copper - buffer acid complexing was omitted.

If we define \bar{n} as the average number of ligand molecules bound by each copper at any stage in the process of complex formation (J.Bjerrum (21)) then using the equations of Dobbie and Kermack (13) for the value \bar{n} at any pH at which it is expected to be less than one, we have;

$$\frac{(1 - \bar{n})(X - \bar{n})}{\bar{n}} = \frac{\alpha}{K_1.[Cu^{2+}](1 + K_c/[H^+])} \quad \text{--- (v)}$$

where $X = [GG_0] / [Cu_0^{2+}]$ and

$$\alpha = 1 + \frac{[H^+]}{K_a} + \frac{[H^+]^2}{K_a K_b}$$

Having obtained \bar{n} , $[GG^-]$ may be obtained from,

$$[GG^-] = \frac{[GG_0] - \bar{n} \cdot [Cu_0^{2+}]}{\alpha} \quad - \quad (vi)$$

Rewriting equation (ii) in terms of $[Cu^{2+}]$,

$$[Cu^{2+}] = \frac{[Cu_0^{2+}]}{1 + K_1 [GG^-] + \frac{K_1 K_c [GG^-]}{[H^+]} + \frac{K_1 K_2 K_c [GG^-]^2}{[H^+]}}$$

Thus by consecutive use of equations (v), (vi) and (vii) we can find the values of $[GG^-]$ and $[Cu^{2+}]$ the unknown quantities in equations (iii) and (iv).

Using constant values; $K_1 = 10^{5.88}$, $K_2 = 10^{3.26}$, $K_c = 10^{-4.25}$, $K_a = 10^{-8.37}$ and $K_b = 10^{-3.12}$, (13), and taking values of $[GG_0] = 0.01$ molar and $[Cu^{2+}] = 0.01$ and 0.02 molar, values of $[Cu GG^+]$ and $[Cu GG]$ were calculated in the pH range 3 to 7 and are shown in Table X.

Figure XII shows $[Cu GG^+]$ versus pH the upper curve corresponding to $[Cu_0^{2+}] = 0.02$ molar and the lower to $[Cu_0^{2+}] = 0.01$ molar. As can be seen, both curves have a maximum at pH = 4.2. For a comparison of Fig. XII, the extent of reaction after 100 hours for experiments with $[Cu^{2+}] = 0.01$ molar is plotted against pH, Fig. XIII, and the results given in Table XI. It is seen that as the pH is varied from 4.0 to 7.0 the extent of reaction passes through a maximum at pH = 4.2. Experiments with $[Cu^{2+}] = 0.02$ molar and 0.033 molar treated similarly give the other two curves on Fig. XIII. Maxima again occur at about pH = 4.2. It is clear that these curves are

TABLE X.

pH	$GG^0 = 0.01M, Cu^{2+}_0 = 0.01M$		$GG_0 = 0.01M$ $Cu^{2+}_0 = 0.02M$
	$CuGG^+ \times 10^5 M$	$CuGG \times 10^5 M$	$CuGG^+ \times 10^5 M$
3.0	23.3	1.3	43.9
3.5	97.1	-	154.1
4.0	215.0	105.0	301.0
4.3	241.9	-	311.0
4.5	226.6	-	276.0
5.0	125.7	556.0	145.0
5.5	44.7	-	45.3
6.0	17.0	161.0	17.4
7.0	1.8	53.3	1.8
8.0	0.2	5.6	0.2

TABLE XIEXTENT OF REACTION AFTER 100 HOURS.

pH	$Cu^{2+} = 0.01M$	$Cu^{2+} = 0.02M$	$Cu^{2+} = 0.033M$
3.75	-	15.0	25.0
4.0	19.5	31.0	46.5
4.3	40.5	46.5	52.0
4.6	34.5	37.5	50.5
5.0	27.0	34.0	-
5.5	19.0	22.0	24.5
6.0	18.5	-	-
6.67	11.5	-	-

FIG. XII

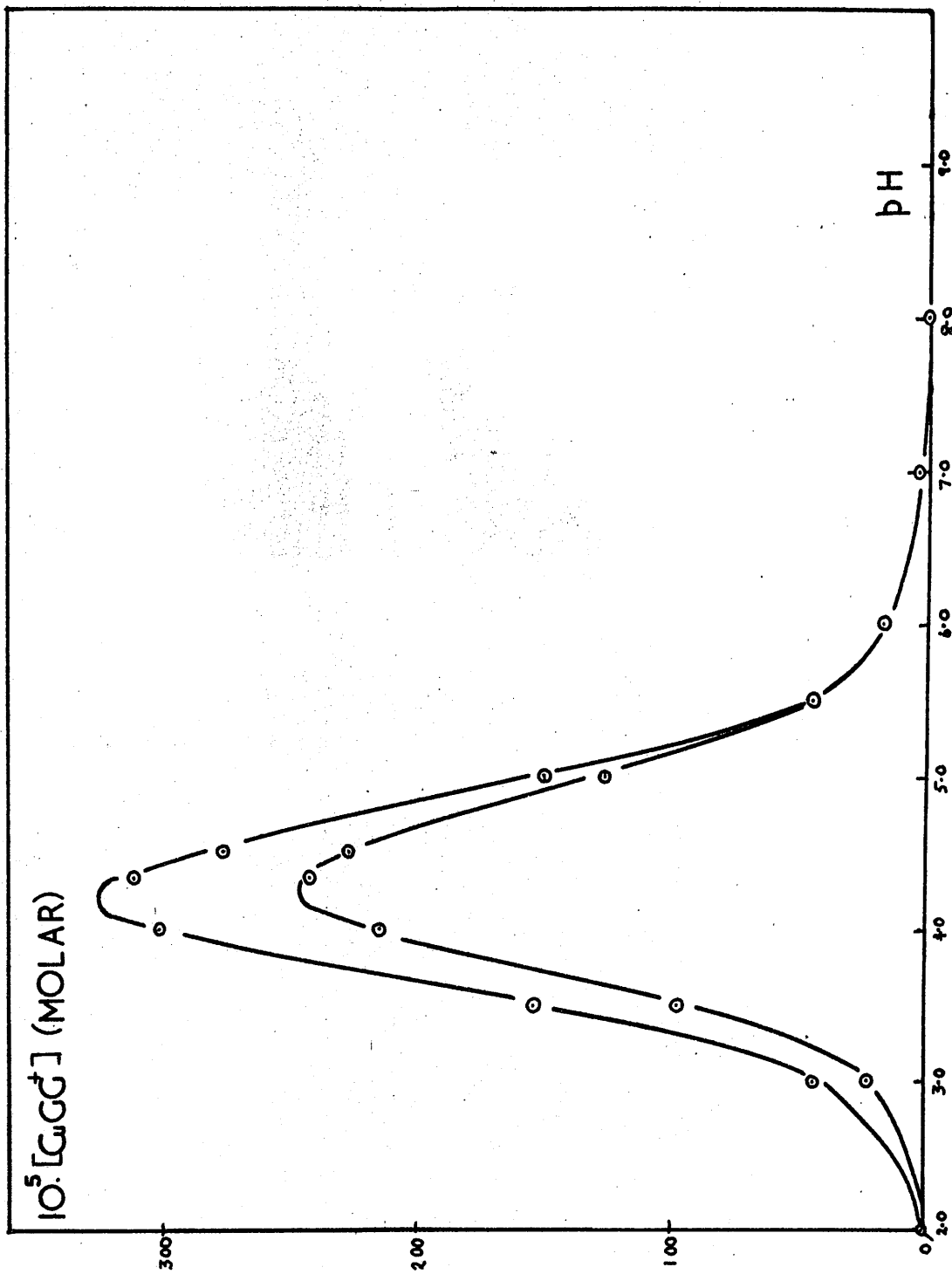
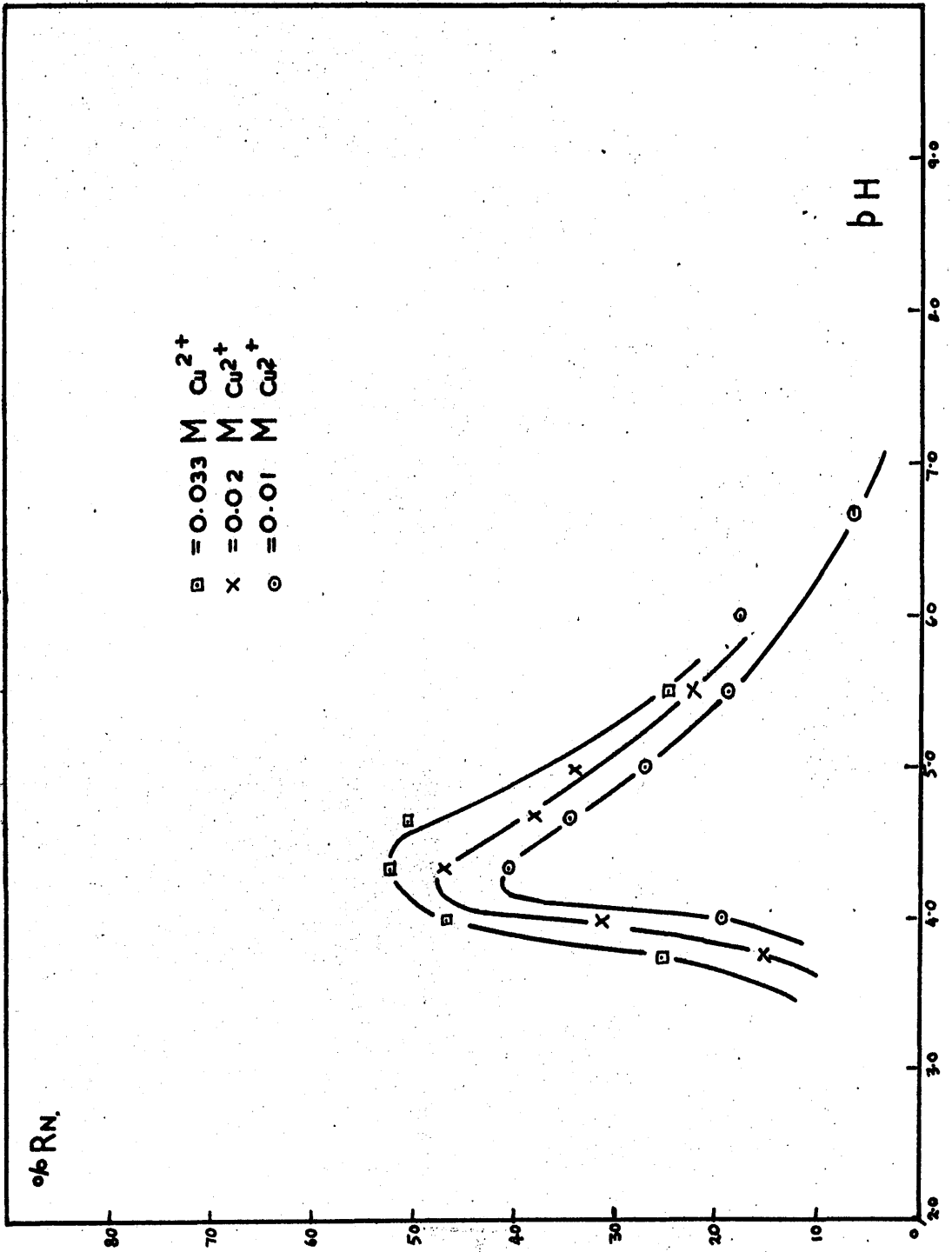
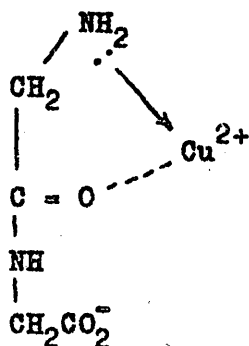


FIG. XIII



closely parallel and that the maxima correspond closely to the maximum in concentration of CuGG^+ (Fig. XII). It is likely therefore that at physiological pH's, hydrolysis of glycyglycine proceeds via Complex A. (XII).



(XII)

This result is in complete agreement with Rabin's (11) postulate that, the first complex formed between cupric ions and glycyglycine should undergo hydrolysis. He further stated that ionisation of the peptide hydrogen from the first complex shall result in a complex resistant to hydrolysis. It is seen in Table X that CuGG has a concentration maximum at $\text{pH} \approx 5.25$ (in reasonable agreement with Dobbie and Kermack's (13) value of $\text{pH} = 5.5$) and that at physiological pH's CuGG is present in greater quantities than CuGG^+ .

It has been observed that the loss of the glycyglycine peptide hydrogen to form the inactive complex occurs only when cupric ions are present. With no hydrolysis-inhibiting complex present therefore, one would expect with metal ions such as Ni^{2+} , Zn^{2+} , etc. that appreciable hydrolysis could be achieved even

at pH = 7.0. One experiment to test this hypothesis was made at pH = 5.0 and $Zn^{2+} = 0.10$ molar (experiment 28). After 100 hours the extent of reaction was 59% compared with 24.5% at the same pH but a cupric ion concentration of 0.02 molar (experiment 29). Making the reasonable assumption, zinc does not complex so strongly to glycylglycine as copper, this result lends support for Rabin's (11) conclusions.

In calculating the extent of complexing in solution, no account was taken of copper-buffer complexing. It is clear that this is present and influences the reaction rate directly. Experiments 8 and 10 in acetate buffer were exactly similar to experiments 9 and 11 in chloracetate buffer. It can be seen (Fig.V) that in the presence of chloroacetic acid the hydrolysis rate is faster. Percentages of reaction after 100 hours are as follows:

Experiment 8; 30.5%	Experiment 10; 18.5%
Experiment 9; 25.0%	Experiment 11; 15.0%

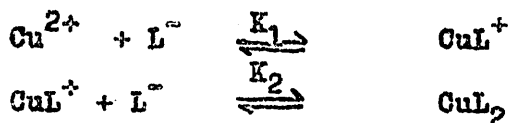
The corresponding stability constants for copper-acetate copper chloracetate complexes at 25°C are;

acetic acid; $\text{Log } K_1 = 2.24$

Chloroacetic acid; $\text{Log } K_1 = 1.61$ (Lloyd et al (22))

respectively. The stronger complex of cupric ions with acetate ion results in less copper being available for copper - glycylglycine complex formation. Thus experiments 8 and 10 are slower than the corresponding chloracetate buffered experiments 9 and 11.

Since the results are only semi-quantitative in nature it is not possible to formulate the kinetics of this reaction. From pH = 3.5 - 6.67 in presence of cupric ion the reactions were only first order for about 5 hours and linearity of first order plots only occurred during this period. Increasing deviation took place as the reaction proceeded and is probably due to the copper complexing with the reaction product, glycine. Two complexes are formed in copper-glycine solution, CuL^+ and CuL_2 , whose formation can be represented as:



where L^- is, $\text{NH}_2\text{-CH}_2\text{-CO}_2^-$. For CuL^+ , $\text{p}K_1 = 8.5$ (12) and the corresponding glycyglycine complex has $\text{p}K_1 = 5.88$ (13). Thus glycine by complex formation removes increasing quantities of cupric ions in the solution. This results in a complicated system, where the active complex, CuGG^+ , at any given pH will decrease in concentration as hydrolysis proceeds causing the reaction rate to fall and the reaction to deviate from first order kinetics.

Although the results are necessarily semi-quantitative in nature, the work has led to some interesting conclusions. It has not been possible to study the correlation between rate of hydrolysis and cupric ion concentration, although a non-linear relationship would appear to hold. Nuclear magnetic resonance studies over a wider range of pH and Cu^{2+} values would probably complete the study of this reaction.

4. (5) REFERENCES

- (1) Hellerman et al: J. Biol. Chem., 112, 179, (1935)
125, 771, (1938)
- (2) EL,Smith; J. Biol. Chem., 173, 571, (1948)
Proc. Nat. Acad. Sci. Wash., 35, 80, (1949)
- (3) Irving and Williams; J.C.S., 1953, 3192.
- (4) R.J.P. Williams; Biol. Rev., 28, (1953)
- (5) Li and Doody; J.A.C.S., 76, 221, (1954)
- (6) Li, Doody and White; J.A.C.S., 79, 5859, (1957)
- (7) Li and Chen; J.A.C.S., 80, 5678, (1958)
- (8) C.B. Monk; Trans. Far. Soc., 47, 285, (1951)
- (9) Monk and Evans; Trans. Far. Soc., 51, 1244, (1955)
- (10) Datta and Rabin; Trans. Far. Soc., 52, 1117, (1956)
- (11) B.R. Rabin; Trans. Far. Soc., 52, ⁵²1123, (1956)
52, 1130, (1956)
- (12) Dobbie, Kermack and Lees; Bioch. J. 59, 240 (1955)
- (13) Dobbie and Kermack; Bioch. J., 59, 246, (1955)
- (14) Datta and Rabin; Nature, 183, 745, (1959)
- (15) Martell, Maryak and Murphy; Arch. Biochem., 59, 373 (1955)
- (16) Larence and Moore; J.A.C.S., 73, 3973, (1951)
- (17) R.J. Martin; Nature, 175, 771, (1955)
- (18) Baman, Haas and Trapmann; Arch. Pharm., 294, 569, (1961)
- (19) Yemm and Cocking; Analyst, 80, 209, (1955)
- (20) Dunn and Loshakoff; J. Biol. Chem., 113, 359, (1936)
- (21) J. Bjerrum; "Metal Amine Formation in Aqueous Solution",
Copenhagen; Hasse and Son.
- (22) Lloyd, Wycherley and Monk; J.C.S., 1951, 1786.

THE STRUCTURE OF CEDRELONE

BY

I. G. GRANT, Miss J. A. HAMILTON, T. A. HAMOR, R. HODGES,
S. G. McGEACHIN, R. A. RAPHAEL, J. MONTEATH ROBERTSON,
and G. A. SIM

*Reprinted from Proceedings of the Chemical Society
December, 1961, page 444*

LONDON:
THE CHEMICAL SOCIETY
BURLINGTON HOUSE, W.1

The Structure of Cedrelone

By I. G. GRANT, Miss J. A. HAMILTON, T. A. HAMOR, R. HODGES, S. G. MCGEACHIN,
R. A. RAPHAEL, J. MONTEATH ROBERTSON, and G. A. SIM
(CHEMISTRY DEPARTMENT, THE UNIVERSITY, GLASGOW, W.2)

THE molecular structure of cedrelone,¹ the principal constituent of *Cedrela toona*, Roxb., has been elucidated by both detailed X-ray analysis and chemical investigation. Our results define the constitution and stereochemistry (apart from absolute configuration) of cedrelone as (I; R = H).

Elemental analysis and an accurate mass-spectrometric determination of the molecular weight of cedrelone gave the formula $C_{26}H_{30}O_5$. Cedrelone has the following spectral properties, ν_{\max} . 3400 (OH), 1674 ($\alpha\beta$ -unsaturated C=O), 3100, 1505, 878 (furan ring) cm^{-1} , λ_{\max} . 217 (ϵ 11,800), 279 (ϵ 9100), and in base λ_{\max} . 327 $m\mu$ (ϵ 5530). Acetylation under mild conditions afforded a monoacetate, the spectral properties of which [ν_{\max} . 1770 (enol OAc), 1702 ($\alpha\beta$ -unsaturated C=O) cm^{-1} ; λ_{\max} . 222 (ϵ 16,400), shoulder at 245 (ϵ ca. 8000), 320 $m\mu$ (ϵ 170)], combined with those of cedrelone, suggested the presence of an enolised α -diketone function similar in environment to that of diosphenols in the limonin series.² That cedrelone possessed a second enone function in a six-membered ring was suggested by the appearance, on mild catalytic hydrogenation, of a band at 1705 cm^{-1} (cyclohexanone) in addition to

the diosphenol carbonyl band at 1670 cm^{-1} . This was confirmed by epoxidation of cedrelone, which gave a monoepoxide $C_{26}H_{30}O_6$, ν_{\max} . 1720 (α -oxygenated cyclohexanone), 1680 (diosphenol) cm^{-1} , λ_{\max} . 201 (ϵ 7200), 276 $m\mu$ (ϵ 10,700), whose ultraviolet absorption curve on subtraction from that of cedrelone gave λ_{\max} . 225 $m\mu$ (ϵ 7300). Cedrelone, recovered from base-catalysed deuteration, showed no C-D absorption in the infrared region, which is in agreement with structure (I).

The nature of the remaining oxygen atom was indicated by the ready conversion of cedrelone acetate by the boron trifluoride-ether complex into an isomer, isocedrelone acetate, ν_{\max} . 3400 (OH), 1765 (enol OAc), 1695 (diosphenol), 1665 (cyclohexanone), 1060 (C-O stretch of hydroxyl) cm^{-1} , λ_{\max} . 210 (ϵ 23,100), 238 $m\mu$ (ϵ 26,300). Subtraction of the ultraviolet absorption curve of the acetate (I; R = Ac) from that of isocedrelone acetate gave λ_{\max} . 242 $m\mu$ (ϵ 13,200). By analogy with similar rearrangements in the limonin series,² the structure (II) is postulated for isocedrelone acetate.

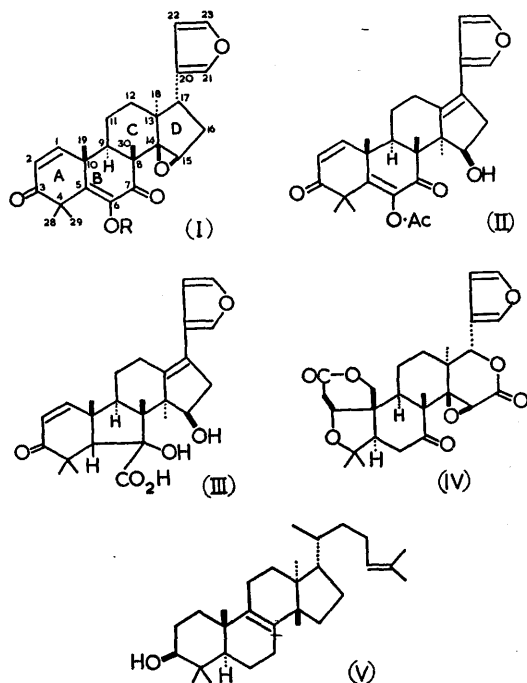
Prolonged treatment of either cedrelone or isocedrelone acetate with hot aqueous-methanolic

¹ Dutt and Parihar, *J. Indian Chem. Soc.*, 1950, 27, 77.

² Barton, Pradhan, Sternhell, and Templeton, *J.*, 1961, 255; Arigoni, Barton, Corey, and Jeger, in collaboration with Cagliotti, Dev, Ferini, Glazier, Melera, Pradhan, Schaffner, Sternhell, Templeton, and Tobinaga, *Experientia*, 1960, 16, 41.

potassium hydroxide gave a carboxylic acid, $C_{26}H_{32}O_6$, ν_{\max} . 3450, 3250 (OH), 1705 (CO_2H), 1670 (cyclohexenone), λ_{\max} . 235 $m\mu$ (ϵ 20,000), which readily gave a monomethyl ester. Since the acid no longer possessed the diosphenol function the most probable structure is (III), formed by benzilic acid rearrangement. The ultraviolet absorption is consistent with the presence of both the enone in ring A and the vinylfuran chromophore.

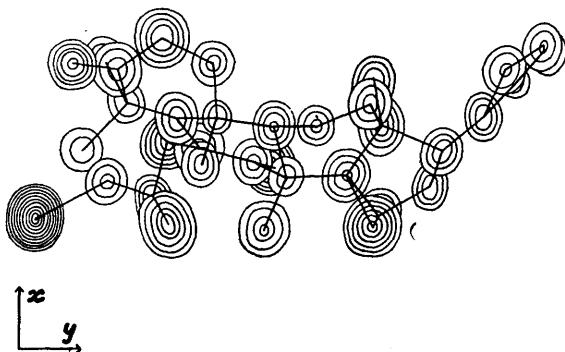
The X-ray study was carried out with cedrelone iodoacetate, the crystals of which belong to the



orthorhombic system with cell dimensions $a = 6.97$, $b = 27.44$, $c = 13.74$ Å. There are four molecules in the unit cell and the space group is $P2_12_12_1$. Three-dimensional intensity data were recorded on Weissenberg photographs and were estimated visually; in all, 1285 structure amplitudes were evaluated.

The co-ordinates of the iodine atom were obtained initially from Patterson syntheses. The z -co-ordinate is close to zero, so that spurious symmetry in the early stages of the analysis made the location of atomic sites rather more difficult than usual. After three rounds of structure-factor calculation and Fourier synthesis, the carbocyclic rings B, C, and D and the epoxide group were firmly established and

the biogenetic relationship to limonin^{2,3} (IV) was evident. Thereafter the elucidation of the structure of cedrelone iodoacetate as (I; R = $CO-CH_2I$) was straightforward.



The sixth three-dimensional electron-density distribution over the molecule of cedrelone iodoacetate shown by means of superimposed contour sections parallel to (001).

The average discrepancy between measured and calculated structure amplitudes at the present stage is 21%. Further refinement is proceeding. Superimposed contour sections illustrating the sixth three-dimensional electron-density distribution over the molecule are shown in the Figure.

Cedrelone, like limonin, is clearly a triterpenoid of the euphol (V) type⁴ from which four carbon atoms of the side chain have been lost and carbons $C_{(20)}$ to $C_{(23)}$ converted into a furan ring. Ring C adopts a boat conformation and ring A a half-boat conformation. The latter stereochemical feature is presumably partly due to steric interaction between the 28- and 29-methyl groups and the oxygen substituent at position 6.

The calculations were carried out on the Glasgow University DEUCE computer, by using programmes devised by Drs. J. S. Rollett and J. G. Sime. We thank the Department of Scientific and Industrial Research for maintenance grants (to I.G.G., J.A.H., and S.G.McG.), the University of Glasgow for an I.C.I. Research Fellowship (to T.A.H.), the Tropical Products Institute for supplies of *Cedrela toona*, and Mr. J. H. Beynon (Imperial Chemical Industries Limited) for the mass-spectrometric measurement.

(Received, August 8th, 1961.)

³ Arnott, Davie, Robertson, Sim, and Watson, *Experientia*, 1960, 16, 49; *J.*, 1961, 4183.

⁴ Barton, McGie, Pradhan, and Knight, *Chem. and Ind.*, 1954, 1325; *J.*, 1955, 876.

THE STRUCTURE OF CHIMONANTHINE

BY

I. J. GRANT, T. A. HAMOR, J. MONTEATH ROBERTSON,
and G. A. SIM

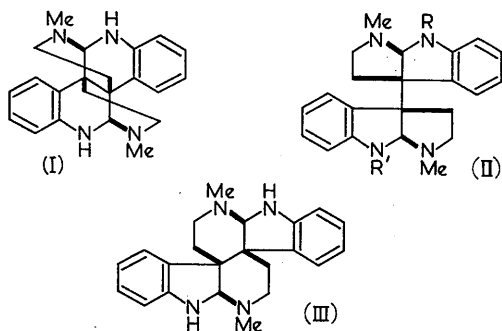
*Reprinted from Proceedings of the Chemical Society
April 1962, page 148*

LONDON:
THE CHEMICAL SOCIETY
BURLINGTON HOUSE, W.1

The Structure of Chimonanthine

By I. J. GRANT, T. A. HAMOR, J. MONTEATH ROBERTSON, and G. A. SIM
(CHEMISTRY DEPARTMENT, THE UNIVERSITY, GLASGOW, W.2)

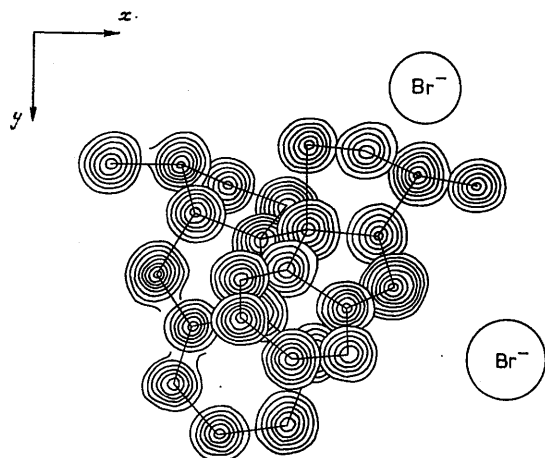
HODSON, ROBINSON, and SMITH recently reported¹ the isolation from *Chimonanthus fragrans* of a new alkaloid, chimonanthine, $C_{22}H_{26}N_4$, isomeric with calycanthine (I).² By considering chemical and spectroscopic evidence they narrowed the structural possibilities to two formulæ (II; R = R' = H) and (III). We have now carried out a detailed X-ray analysis of chimonanthine dihydrobromide, which was kindly supplied by Dr. G. F. Smith, and find that the correct structure for this alkaloid is (II; R = R' = H).



Two other naturally occurring alkaloids, calycanthidine and folicanthine, have now been shown³ to represent successive further stages of methylation of chimonanthine; it follows that calycanthidine must be formulated as (II; R = H, R' = Me) and folicanthine as (II; R = R' = Me).

Crystals of chimonanthine dihydrobromide (from dry ethanol) belong to the tetragonal system with cell dimensions $a = b = 13.95$, $c = 26.67$ Å. There are eight molecules in the unit cell and the space group is $P4_12_12$ (or the enantiomorphous $P4_32_12$). 2083 independent structure amplitudes were evaluated.

Fourier methods were used for the structure



The third three-dimensional electron-density distribution for chimonanthine dihydrobromide shown by means of superimposed contour sections drawn parallel to (001).

analysis. The third electron-density synthesis is shown in the Figure by means of superimposed contour sections drawn parallel to (001) and covering the region of one molecule. It will be seen that in the crystal the molecule adopts the *cis*-conformation.

The average discrepancy between measured and calculated structure amplitudes at the present stage is 21%. Refinement is continuing.

The extensive calculations were carried out on the Glasgow University DEUCE computer with programmes devised by Dr. J. S. Rollett and Dr. J. G. Sime. We thank the University of Glasgow for an I.C.I. Fellowship (to T.A.H.), and the Department of Scientific and Industrial Research for a maintenance grant (to I.J.G.).

(Received, March 7th, 1962.)

¹ Hodson, B. Robinson, and Smith, *Proc. Chem. Soc.*, 1961, 465.

² Sir R. Robinson and Teuber, *Chem. and Ind.*, 1954, 783; Hamor, Robertson, Shrivastava, and Silvertown, *Proc. Chem. Soc.*, 1960, 78; Woodward, Yang, Katz, Clark, Harley-Mason, Ingleby, and Sheppard, *Proc. Chem. Soc.*, 1960, 76.

³ Saxton, Bardsley, and Smith, *Proc. Chem. Soc.*, 1962, preceding communication.

S U M M A R Y

X-ray studies have been carried out on crystals of heavy atom derivatives of naturally -occurring organic compounds. Two structures have been successfully determined in this fashion; the triterpene cedrelone ($C_{26} H_{30} O_5$) and the alkaloid chimonanthine ($C_{22} H_{26} N_4$).

Information on the structure of cedrelone was limited to spectral considerations alone, when a crystalline sample of the iodoacetate derivative was provided by Mr. S.G. McGeachin of Glasgow. The structure analysis was hindered initially by the iodine atom being close to a special position in the unit cell which gave rise to false symmetry in the initial Fourier syntheses. The fourth Fourier synthesis, however, resulted in most of the structure being determined and thereafter the complete structure was obtained and refined to give a discrepancy of, $R = 17.5\%$. The crystal and molecular dimensions were in agreement with accepted values although no attempt was made to locate atomic positions accurately.

Dr. G.F. Smith of Manchester University provided crystals of the dihydrobromide derivative of chimonanthine an alkaloid of the calycanthaceous variety. Chemical and spectral evidence had progressed to the stage where the structure was probably one of two possibilities. The first major problem in this

structure analysis was the determination of the position of the bromide ions in the unit cell of the crystal. There were two bromide ions per asymmetric unit and the derivative crystallised in the tetragonal system; these two facts resulted in a very complex Patterson map which required much study before a solution was found. Thereafter the major problem was minimising the extremely large amounts of computer time required for this analysis. The structure and relative stereochemistry of chimonanthine have been determined and the structure was in fact one of the two structures proposed by the organic chemists. The crystal and molecular dimensions agree with accepted values within the limits of experimental accuracy and refinement of this structure has been carried out to give an average discrepancy between observed and calculated structure amplitudes of 14.9%.

The final section of this thesis describes the work carried out under the supervision of Dr. E. Gelles lately of this Department. The copper ion catalysed hydrolysis of glycylglycine has been studied over a range of pH values and cupric ion concentrations. It has been established that the first complex formed between glycylglycine and cupric ions (Cu GG^+) is the one responsible for catalysed hydrolysis and that subsequently formed complexes inhibit hydrolysis. These results are in agreement with other workers theoretical predictions.

(iv)

The structure analysis of cedrelone was carried in conjunction with Dr. J.A. Hamilton of this department and the kinetic studies were a continuation of experiments first started by Mr. J.M. Wilson lately of this department.